

**Correlation of Permeability, Hydration, and Crosslink
Density in Polyelectrolyte Hydrogel Membranes**

by

Karen P. Adler

S.B., Boston University, 1985

Submitted in Partial Fulfillment of the
Requirements for the Degree of
Master of Science

at the

Massachusetts Institute of Technology
May, 1988

© Massachusetts Institute of Technology, 1988

Signature of Author *Karen P. Adler*
Department of Electrical Engineering and Computer Science
May, 1988

Certified by *[Signature]* Thesis Supervisor

Accepted by *[Signature]* Chair, Department Committee

MASSACHUSETTS INSTITUTE
OF TECHNOLOGY

JUL 26 1988

LIBRARIES
ARCHIVES

Correlation of Permeability, Hydration, and Crosslink Density in Polyelectrolyte Hydrogel Membranes

by

Karen P. Adler

Submitted to the Department of Electrical Engineering and Computer Science in partial fulfillment of the requirements for the Degree of Master of Science, May, 1988.

Abstract

This thesis investigates the effects of membrane swelling and composition on the diffusion of two neutral solutes— one on the order of the membrane mesh size (Lis-dex), the other much smaller (NSPA). Hydration and transport experiments were performed on a series of polyelectrolyte PMAA membranes differing only in the volume fraction of crosslinker added at the time of polymerization.

At a given pH, permeability to Lis-dex increases as the crosslinker concentration increases. Membrane permeability to Lis-dex differs by as much as three and a half orders of magnitude for the two membranes having the least and greatest percentage of crosslinker. If the membranes are ordered, at a given pH, in terms of increasing permeability (or increasing hydration), the ordering is essentially from the heaviest to the lightest crosslinked membrane. In sharp contrast to the Lis-dex data, the NSPA data reveals modest differences in permeability from membrane to membrane, with no apparent ordering of the membrane formulations.

In these experiments, two factors affect transport— hydration and crosslink density. In order to correlate diffusion data to crosslink density, the permeability is compared to crosslinker concentration, *at constant hydration*. This is accomplished by interpolating from the hydration data. It is found that the crosslinker content, alone, has an enormous effect on the diffusion of Lis-dex. At constant hydration, Lis-dex permeability differs by more than a factor of 18 for the two membranes having the least and greatest percentage of crosslinker.

The free volume theory of diffusion is used to model the diffusion of both Lis-dex and NSPA. In both cases, the data are accurately described by the model. The sieve term in the free volume expression plays an important role in fitting the Lis-dex data; it is insignificant in fitting the NSPA data. These results suggest that chain mobility affects the diffusion of Lis-dex, but not the diffusion of NSPA.

Thesis Supervisor: Alan J. Grodzinsky

Title: Professor of Electrical Engineering and Bioengineering

Acknowledgements

I thank Prof. Al Grodzinsky for the advice and supervision he has given to this project. I couldn't have wished for a better thesis advisor. I also enjoyed having Al as a teacher for 6.561; the in-class breakfasts of bagels and coffee were especially memorable.

Special thanks go to Paul Grimshaw, who so many times dropped his own work to help me with mine. I appreciate the time and expert advice that Paul has given to this project.

Thanks to all my friends and colleagues in the lab, especially Aryeh Weiss, Eliot Frank, Bob Sah, Ann Morgenthaler, John Kenny, Jeremy Nussbaum, David Huang, Zeke Gluzband, and the Pres. of Slime Inc.—Linda Bragman.

Most of all, I thank my parents and grandmother for the encouragement they've given me. This thesis is dedicated to them.

The author gratefully acknowledges the support of a National Science Foundation Fellowship. This research was also supported in part by NSF ERC Grant CDR-8500003 and NSF Grant CBT-8512814.

Karen P. Adler
May 1988

Contents

Abstract	2
Acknowledgements	4
List of Symbols	11
I Introduction	14
1.1 Goals of Thesis	14
1.2 Previous Studies	15
1.2.1 Effects of pH and Ionic Strength on Membrane Permeability	15
1.2.2 Effects of Crosslinks on Membrane Permeability	17
1.3 Diffusion Models	20
1.3.1 Porous Membrane Models	20
1.3.2 Nonporous Membrane Models	22
1.3.3 Free Volume Diffusion Models	22
II Background	27
2.1 Membrane Chemical Structure	27
2.2 Swelling Controls-Ionic Strength and pH	27
2.2.1 pH	29
2.2.2 Ionic Strength	29
2.2.3 Slab Swelling Model	37
2.3 Crosslink Density	37
2.4 Solutes	40
III Methods and Materials	41
3.1 Membrane Preparation	41
3.2 Hydration Experiments	42
3.3 Transport Experiments	48
3.3.1 Equipment	48
3.3.2 Protocol for Transport Experiments	52
IV Results	57
4.1 Hydration vs. pH	57
4.2 Errors and Membrane Homogeneity	57
4.3 Transport Results	63
V Theory	82
5.1 One-Component System	82
5.2 Two-Component System	83
5.3 Three-Component System	85

VI	Discussion	94
6.1	Membrane Homogeneity	94
6.2	Membrane Formulation Trends	94
6.3	Swelling Model	95
6.4	Hydration vs. Crosslinker Concentration and Solvent Volume	96
6.5	Lis-dex Permeability vs. Crosslinker Concentration and Solvent Volume	98
6.5.1	Constant pH	98
6.5.2	Constant Hydration	98
6.6	NSPA Permeability vs. Crosslink Density	108
6.7	Interpretation of Data in Terms of Free Volume Theory	109
6.7.1	Lis-dex Data	109
6.7.2	NSPA Data	117
A	One step recipe for PMAA membranes	122
B	Linear Least Squares Fit to Multiple Lines	123
	References	125

List of Figures

1.1	Theoretical free volume theory plot of D/D_0 vs. H [Yasuda (1969 Part III:Equation7)].	21
2.1	Membrane chemical structure, showing formation of PMAA chains and crosslinking of chains.	28
2.2	PMAA titration curve, showing increase in negative fixed charge groups with increase in pH [Nussbaum(1986)].	30
2.3	Charged polymer chain with surrounding ion cloud. The potential decays to $1/e$ of its value at $x=0$ in one Debye length.	31
2.4	Membrane with double layer of charge on each face. A debye length away from the membrane surfaces, charge neutrality holds.	35
2.5	Slab swelling model	38
2.6	Effects of crosslink density on swelling and diffusion.	39
3.1	S.2/1, S.4/1, and S.6/1 membranes, showing locations of discs.	44
3.2	Transport Cell	51
3.3	Transport Experiment Setup [Grimshaw et al.(1988)]	53
4.1	Hydration vs. pH for each membrane, without error bars. At a given pH, hydration increases with decreasing crosslink density.	58
4.2	Hydration vs. pH for each membrane, with error bars.	59
4.3	Hydration vs. pH for intermembrane discs (S.2/1), with error bars	62
4.4	Diameter vs. pH for intramembrane discs. See Chapter III for definition of A, B, C, D, L, M, R.	64
4.5	Hydration vs. pH for intramembrane discs, with error bars. See Chapter III for definition of A, B, C, D, L, M, R.	65
4.6	Weight at ascending pH vs. weight at descending pH for 3 discs, with error bars.	66
4.7	Diameter at ascending pH vs. diameter at descending pH for 3 discs.	67
4.8	W/W_0 vs. $(d/d_0)^3$, showing isotropic swelling.	68
4.9	Raw transport data for Lis-dex and NSPA from chart recorder, showing downstream normalized concentration of both solutes. Prior to $t=0$, the membrane had been preconditioned by cycling from low pH to high pH and back to low pH, following which the solutes were added. 70	
4.10	Results from transport experiment on S.4/.5 membrane, comparing Lis-dex and NSPA permeabilities. The change in Lis-dex permeability with pH is significant. The higher Lis-dex pH3 bar is the permeability using the upper error bar ($P=8.65e-9$ cm/sec); the shorter bar is the mean permeability ($P=2.25e-9$ cm/sec).	73

4.11	Results from transport experiment on S.05/1 membrane, comparing Lis-dex and NSPA permeabilities. The membrane is essentially open to both solutes.	74
4.12	Permeability vs. pH for Lis-dex (log scale). At a given pH, permeability increases with decreasing crosslink density.	75
4.13	Permeability vs. pH for Lis-dex, with standard deviation error bars.	76
4.14	Permeability vs. pH for Lis-dex, up to pH6.7 and pH7. These were the only experiments in which the pH was raised beyond pH5.5.	77
4.15	Permeability vs. pH for NSPA (log scale). There is no ordering of the membranes with respect to crosslinker.	80
5.1	Theoretical free volume theory plot of D/D_0 vs. H [Yasuda (1969 Part III:Equation 7)].	92
6.1	Swelling model function, $H = H_o + H_1(\bar{c}_m^s)^2 \exp \left[-H \frac{H}{i_d} \right]$, fit to hydration data for S.2/2 membrane. This plot is typical of the other membrane hydration fits.	97
6.2	Hydration vs. volume of crosslinker for S.X/1 (top) and S.X/2 (bottom) membranes at 4 different pH values. The volume of crosslinker added at the time of polymerization has a significant effect on hydration.	99
6.3	Hydration vs. volume of D.I. water for S.4/Y (bottom), S.1/Y (top left), and S.2/Y (top right) membranes at 4 different pH values. The volume of water added at the time of polymerization has less of an effect on hydration than does the volume of crosslinker.	100
6.4	Lis-dex permeability vs. volume of crosslinker for S.X/1 (top) and S.X/2 (bottom) membranes at 4 different pH values.	101
6.5	Lis-dex permeability vs. volume of water for S.4/Y (bottom), S.1/Y (top left), and S.2/Y (top right) membranes at 4 different pH values. The water added at the time of polymerization has a substantial effect on the permeability.	102
6.6	Lis-dex permeability vs. hydration.	104
6.7	$\ln(P)$ vs. hydration for Lis-dex, showing that, at low hydrations, a small change in hydration can cause a tremendous change in permeability.	105
6.8	Lis-dex permeability vs. volume of crosslinker for S.X/1 (top) and S.X/2 (bottom) membranes, at <i>constant hydration</i> . Strands are more easily "pushed aside" by the diffusing solute in the more lightly crosslinked membranes.	106
6.9	Lis-dex permeability vs. volume of water for S.4/Y (bottom), S.1/Y (top left), and S.2/Y (top right) membranes at <i>constant hydration</i>	107

- 6.10 Normalized diffusion D/D_0 vs. hydration from free volume theory equation: $\frac{D}{D_0} = \Phi \exp -\frac{\beta}{H}$. Small changes in hydration can cause great changes in diffusion. 110
- 6.11 $P \frac{\delta_0}{D_0}$ vs. H from free volume theory equation: $P \frac{\delta_0}{D_0} = \Phi \frac{H}{(1+H)^{4/3}} \exp -\frac{\beta}{H}$. $\Phi = 1$ and $\beta=0.5, 5, 10, 100$ 112
- 6.12 Plot of $P \frac{(1+H)^{4/3}}{H}$ vs. $1/H$ using Lis-dex data. Free volume theory expression is: $P \frac{(1+H)^{4/3}}{H} = \frac{D_0}{\delta_0} \Phi \exp -\frac{\beta}{H}$ 113
- 6.13 Plot of $\ln [P(1+H)^{4/3}H^{-1}]$ vs. $1/H$ using Lis-dex data. Free volume theory expression is: $\ln [P(1+H)^{4/3}H^{-1}] = \ln \left(\frac{D_0}{\delta_0} \Phi \right) - \frac{\beta}{H}$. According to the free volume theory, each membrane data set should fit a line. The slope, $-\beta$, should be the same for each data set while the intercept, $\ln \left(\frac{D_0}{\delta_0} \right)$, should be different. 115
- 6.14 Plot of $\ln [P(1+H)^{4/3}H^{-1}] + \ln \left(\frac{D_0}{\delta_0} \Phi \right)$ vs. $1/H$ for Lis-dex for each membrane data set. Also shown is a line with slope $-\beta$ and zero intercept. β and the 8 intercepts were obtained using a linear least squares fit on each data set, simultaneously. 116
- 6.15 Comparison of free volume theory P vs. H (from expression $P = \frac{D_0}{\delta_0} \Phi \frac{H}{(1+H)^{4/3}} \exp -\frac{\beta}{H}$) to Lis-dex transport data. $\Phi \frac{D_0}{\delta_0}$ and β were obtained using a simultaneous linear least squares fit. Membranes: S.05/1, S.1/1, S.2/2, S.4/1 118
- 6.16 Comparison of NSPA and Lis-dex plots of $\ln [P(1+H)^{4/3}H^{-1}]$ vs. $1/H$. The NSPA data could be convincingly fit to a single line. . . . 119
- 6.17 NSPA data points, $y = \ln [P(1+H)^{4/3}H^{-1}]$ and $x = 1/H$, fit to multiple lines (bottom), as was done for the Lis-dex data, and a single line (top). For the lower plot, the data points were offset by the appropriate intercept. For the upper plot, the data points were offset by the intercept -8.215 121

List of Tables

3.1	Membranes used in experiments, differing in crosslinker and water content. SX/Y: X=volume crosslinker; Y=half volume water	42
3.2	Mean weights for every disc at each pH. For the S.2/1, S.4/1, and S.6/1 weights, all intra and intermembrane discs were used in calculating the mean and s.d. for that membrane.	46
3.3	Mean thicknesses for every disc at each pH. For the S.2/1, S.4/1, and S.6/1 thicknesses, all intra and intermembrane discs were used in calculating the mean for that membrane.	47
3.4	Diameters for every disc at each pH. For the S.2/1, S.4/1, and S.6/1 diameters, all intra and intermembrane discs were used in calculating the diameter for that membrane.	49
3.5	Dyes: Their molecular weight, excitation λ , emission λ	54
4.1	Mean hydrations for each disc. For the S.2/1, S.4/1, S.6/1 hydrations, all intra and intermembrane discs were used in calculating mean hydration and standard deviation.	60
4.2	Lis-dex and NSPA permeabilities for each membrane formulation at each pH. pH's are given in the same order in which they occurred in the corresponding transport experiment. *No transport-concentration curve looked horizontal to the eye.	71
4.3	Percent changes in hydration and permeability compared to percentage crosslinker. % crosslinker = (vol TEGDMA /total vol)*100. % change in permeability = (perm@pH5.5-perm@ pH3)/(perm@pH3). % change in hydration = (hyd@pH5.5-hyd@pH3)/ (hyd@pH3). *Using upper error bar (P=8.65e-9 cm/sec). If the mean permeability (2.25e-9) is used, then % change in perm=22,789.	78
6.1	Swelling Model Parameters	96
6.2	Crosslinker concentration for each membrane. % crosslinker = (vol TEGDMA/total vol)*100.	108
6.3	Intercepts obtained from simultaneous linear least squares fit of all eight data sets. Slope= $-\beta = -5.11933$	114

List of Symbols

P	permeability
H	hydration=ratio of fluid volume to solid volume in hydrated membrane ($H = \frac{v_w}{v_s}$)
v_w	volume of hydrated membrane
v_s	volume of dry membrane
D	solute diffusion coefficient
D_o	solute diffusivity in pure water
W	weight of hydrated membrane
W_o	weight of membrane at pH3
d	diameter of hydrated membrane
d_o	diameter of membrane at pH3
W_t	total weight of hydrated membrane
W_s	dry weight of membrane
ρ_p	polymer density
ρ_f	fluid density
δ	thickness of hydrated membrane
δ_o	thickness of membrane at zero hydration (dry)
H_v	volume fraction of solvent in membrane ($H_v = \frac{v_w}{v_w + v_s}$)
Φ	sieve term in free volume theory expression
V_f	total free volume in membrane (used in free volume theory)
$V_{f,13}$	free volume of solvent-polymer mixture
$V_{f,1}$	free volume of pure solvent
$V_{f,3}$	free volume of pure polymer
$V_{f,eff}$	effective free volume available to solute in membrane

B	proportionality constant, from free volume theory expression, which includes diffusional jump length
r_s	effective solute radius
β	$= \frac{B\pi r_s^2}{V_{f,1}}$
Ψ	electric potential
$\Delta\Psi_D$	Donnan potential drop
E	electric field
Γ	net flux of ion species
μ	ionic mobility
ϵ	dielectric constant
F	Faraday constant (96,500 C/mol)
R	ideal gas constant (8.314 J/mol-K)
T	absolute temperature (Kelvin)
ρ_u	volume charge density in fluid phase
σ_d	surface fixed charge
$\frac{1}{\kappa}$	Debye length $= \sqrt{\frac{\epsilon RT}{2c_o F^2}}$
\bar{c}_{mo}	total concentration, in moles/wet liter, of carboxyl groups (fixed charge density)
\bar{c}_{mos}	total concentration, in moles/dry liter, of carboxyl groups
\bar{c}_m^s	$= \frac{K_m \bar{c}_{mos}}{\bar{c}_H + K_m}$
$c_H(x)$	local concentration of hydrogen ions at point x
\bar{c}_H	concentration of H within the membrane
pH	$= -\log_{10} c_H$
K_m	dissociation constant for membrane carboxyl group ($K_m = 10^{-pK_{COOH}}$)
σ_m	surface fixed charge density
π_{rep}	electrostatic double layer repulsive force

H_o, H_1, l_r swelling model parameters

l_d Debye length = $\frac{1}{\kappa}$

ϕ porosity factor = fraction of surface area consisting of solvent

t time [sec]

c_d downstream dye concentration [moles/liter]

c_u upstream dye concentration [moles/liter]

A area of membrane gasket

Chapter I

Introduction

1.1 Goals of Thesis

Various electrical, mechanical, and chemical mechanisms can be used to control the transport of solutes across polyelectrolyte membranes. There are numerous industrial and medical applications, including protein separation and purification and drug delivery systems. What is needed for these applications is a membrane which can be selectively opened or closed to the diffusion of various solutes.

Mechanisms for controlling solute transport can be divided into two categories— those that act upon the solute and those that alter the membrane. Donnan exclusion, electrophoresis, and electroosmosis are transport effects that fall into the first category. Membrane swelling and crosslink density fall into the second category; these are the effects investigated in this thesis. By altering these two parameters alone, the membrane can be size tuned to the solute. Solute controlling effects can then be superimposed on the membrane controlling effects to further refine solute separation.

Other studies have focused on the effects of membrane swelling and crosslink density on solute diffusivity, but have not separated these two effects. This thesis first studies the relationship between hydration and crosslinker concentration, then, using these results, studies the relationship between solute diffusivity and crosslinker concentration alone, independent of membrane hydration.

1.2 Previous Studies

1.2.1 Effects of pH and Ionic Strength on Membrane Permeability

Large changes in solute transport across charged polymer membranes can be induced by altering the chemistry of the surrounding bath. The degree of ionization of the fixed charge groups in the membrane is modified by the pH of the surrounding bath. As more charge groups become ionized, the double layer electrostatic repulsive force between the charge groups causes the membrane to swell. The spaces within the mesh of polymer chains and crosslinks enlarge, allowing the solute to diffuse through more easily. The membrane swells until the mechanical restoring force produced by the crosslinks balances the double layer electrostatic repulsive force. The more heavily crosslinked the membrane is, the less it can swell.

Kirstein et al.(1985) investigated the diffusion of small solutes through poly(2-hydroxyethyl methacrylate)(PHEMA) membranes copolymerized with weakly acidic/basic groups. They found that membrane swelling was greatly altered by changes in bath pH. As the bath pH was increased from pH6.5 to pH8, the diffusivity of urea increased by a factor of ≈ 20 for the HME-2B membrane. Similar results were reported in several studies on various solutes diffusing through crosslinked polyelectrolyte hydrogel membranes [Vacik (1975), Shatayeva (1979), Kost (1985), Horbett (1983)].

Weiss (thesis and Weiss et al.(1986)) found that changes in bath pH and ionic strength resulted in large, reversible, size-specific permeability changes in crosslinked polymethacrylic acid (PMAA) membranes. Permeability changes as great as 50 were obtained by altering the bath pH and, hence, the membrane hydration. He postulated that hydration can affect permeability in three ways:

1. The effective path length changes with changing hydration. This effective path is longer than the membrane thickness since the solute must weave its

way through the membrane. Weiss used the tortuosity factor, Θ , from the Mackie and Meares(1955) porous membrane model, to account for the increase in path length.

2. Hydration affects the surface area and thickness of the membrane.
3. Steric (sieving) effects and hydrodynamic (viscous) drag against the pore walls can be altered by changes in hydration.

The tortuosity factor, surface area, and thickness do not change with solute size; only the third factor depends on solute size.

Based on the statistical porous membrane model by Mackie and Meares (1955), Weiss derived an expression relating the permeability, P , of a membrane to its hydration, H :

$$P = \frac{D^*}{\delta_o} \left[\frac{H}{2+H} \right]^2 \left[\frac{1}{1+H} \right]^{\frac{1}{3}} \quad (1.1)$$

H is defined as the ratio of the fluid volume to the solid volume of the swollen membrane ($H = v_w/v_s$). D^* is the intramembrane diffusion coefficient in the absence of tortuosity effects and δ_o is the membrane thickness at zero hydration. This expression is independent of solute size, is valid only for solutes much smaller than the pore size, and assumes an isotropically swelling membrane. It does not include steric or hydrodynamic hindrance effects. Although the expression was found to agree reasonably well with the data obtained using the smaller solute (N-(3-sulfopropyl acridinium inner salt(NSPA), M.W.=301), it could not explain the 50-fold changes in permeability for the larger solute (Lissamine-dextran(Lis-dex), M.W.=10,000). It was concluded that the diffusion of Lis-dex was restricted by sieving effects or hydrodynamic drag, or both.

Nussbaum (1986) developed a theoretical equilibrium swelling model, based on a micro model of flat charged slabs connected by springs. He derived an equation relating hydration to membrane fixed charge, \bar{c}_m^f , and the local ionic

environment:

$$H = H_o + H_1(\bar{c}_m^s)^2 \exp \left[-H \frac{l_r}{l_d} \right] \quad (1.2)$$

The Debye length l_d depends on the local ionic environment. The membrane fixed charge depends on the internal pH which, in turn, depends on the pH and ionic strength of the surrounding bath. The three adjustable parameters, l_r , H_o , and H_1 , must be determined empirically. This model is discussed further in Section 6.3.

1.2.2 Effects of Crosslinks on Membrane Permeability

The mesh structure formed by polymer chains and crosslinks acts as a sieve, allowing smaller molecules to diffuse through but stopping larger molecules. In this thesis, the free volume theory of diffusion is used to model the diffusion of a solute through a highly swollen membrane mesh. According to this theory (Sections 1.3.3 and 5.3), the diffusion coefficient depends on three factors—hydration, crosslink density, and solute size. By holding two of these factors constant, the dependence of the diffusion coefficient on the third can be determined. For this reason, the hydrations of variously crosslinked membranes should be identical if comparisons are to be made between diffusivity and crosslink density.

Though there have been many studies on diffusion through swollen gel membranes, only a handful have focused on the role played by the crosslinks [Kirstein (1985), Wisniewski (1976), Wood (1983), Lee (1978), Chen (1979), Korsmeyer (1981), Pusch (1982), Kopeček et al.(1971), Reinhart and Peppas (1983), Moynihan et al.(1986), Peppas and Moynihan (1985)]. These studies have failed to find a precise relationship between diffusivity and crosslink density. In most of the crosslink studies, changes in diffusivity were attributed to changes in crosslink density. It is uncertain, however, just how much of the diffusivity change was truly due to changes in crosslink density; the variations in hydration from membrane to membrane, albeit small, were enough to cause some of the observed

change.

Weiss [(1986) and Weiss et al.(1986)] found the membrane composition to have a significant effect on the transport properties of crosslinked PMAA membranes. Not surprisingly, the higher the base crosslink density in the membrane, the lower the permeability at a given pH. Of particular interest is Weiss' finding that the maximum permeabilities of variously crosslinked membranes were similar, but the more heavily crosslinked membranes had much lower minimum permeabilities than the lightly crosslinked membranes. Weiss speculated that this was due to changes in restricted diffusion; at high hydrations, steric and hydrodynamic hindrance are less important, whereas, at low hydrations, small differences in hydration result in large restriction changes. The question of whether sieving depends on hydration will be discussed in Section 1.3.3.

Several studies have demonstrated that solute diffusivity depends on the base crosslink density and mesh size of polymer membranes [Kirstein (1985), Wisniewski (1976), Wood (1983), Lee (1978), Chen (1979), Korsmeyer (1981), Pusch (1982)]. Gaseous diffusion is also affected by the crosslink density [Trostyanskaya (1970), Barrer (1948)]. Kopeček et al. (1971) studied the diffusion of NaCl and MgSO₄ through charged and neutral HEMA based gel membranes. They found the permeability, P, decreased with increasing crosslink (ethylene dimethacrylate (EDMA)) density. For the neutral membranes (HEMA), P_{NaCl} varied between $4.44 \times 10^{-8} cm^2/sec$, for the heaviest crosslinked membrane, and $14.5 \times 10^{-8} cm^2/sec$, for the lightest crosslinked membrane. It was assumed that the hydration did not vary much from membrane to membrane. For the neutral membranes, the volume fraction of polymer in the swollen membranes varied between 0.5516 and 0.6646. Although this is only a 20% variation (60% variation in hydration), compared to a 226% variation in permeability, as will be seen in this thesis, a small change in hydration can result in a large change in permeability. Nevertheless, it is doubtful that the hydration changes alone can

account for the 226% change in permeability.

Reinhart and Peppas (1984 Part II) performed experiments on the diffusion of bovine serum albumin (BSA, $\text{dia} \approx 62 \text{ \AA}$) through water-swollen poly(vinyl alcohol) (PVA) membranes of various crosslink densities. They found that the normalized diffusion coefficient (the ratio of the diffusion coefficient in the membrane to that in pure solvent) increased dramatically as the molecular weight between crosslinks, \overline{M}_c , was increased. The molecular weight between crosslinks was found to depend on the base crosslink density; the more heavily crosslinked the membrane, the smaller \overline{M}_c . Although they claimed the hydration did not vary significantly from membrane to membrane, in fact, they reported that the equilibrium degree of swelling, Q_m ($Q_m = 1 / (\text{swollen volume fraction of polymer}) = H + 1$), varied from $Q_m = 11.00$ to $Q_m = 19.65$ (an 86.5% change in hydration). This may be insignificant compared to the 4383.3% increase in the normalized diffusion coefficient and the 161.3% increase in \overline{M}_c , but the results would be more convincing had the hydrations truly been constant. Their plot of the normalized diffusion coefficient vs. \overline{M}_c looks, functionally, very similar to the theoretical free volume theory [Yasuda (1969 Part III:Equation 7)] plot of D/D_0 vs. H (Figure 1.1), which is independent of crosslink density.

Reinhart and Peppas (1984 Part II) calculated the average mesh size of the membrane, based on P.G.deGennes' (1979) membrane mesh model. The average mesh size ranged from 63 \AA for the most heavily crosslinked membrane to 124 \AA for the most lightly crosslinked membrane. These approximate mesh sizes are on the order of the hydrodynamic diameter of the BSA molecule ($\text{dia} \approx 62 \text{ \AA}$).

Moynihan et al. (1986) studied the diffusion of phenylalanine through water-swollen PHEMA membranes. The crosslink density of the membranes was varied while attempting to maintain constant hydration from membrane to membrane by adjusting the base polymer content. Again, the hydrations were not constant; they varied by 13.24%, from $H = 0.68$ to $H = 0.77$. The molecular weight

between crosslinks, \overline{M}_c , varied by 101.5% (from 1700 to 3425 g/mole). The normalized diffusion coefficient increased significantly with increasing \overline{M}_c . The diffusivity in the most lightly crosslinked membrane ($\overline{M}_c = 3425$ g/mole) increased 482.8% over the diffusivity in the most heavily crosslinked membrane ($\overline{M}_c = 1700$ g/mole).

1.3 Diffusion Models

1.3.1 Porous Membrane Models

Weiss (thesis and Weiss et al.(1986)) used the Mackie and Meares porous membrane model (1955) to derive an expression relating permeability to hydration. The expression does not include solute size or steric hindrance, and was found to be inadequate when applied to the Lis-dex permeability data. This is not surprising; the Lis-dex molecules are large enough, compared to the mesh size, to be restricted in their motion by the membrane mesh.

Unlike the Mackie and Meares theory, the theories of Bean (1972) and Anderson and Quinn (1974) take into account both steric and hydrodynamic hindrance of solutes diffusing through porous networks. However, a pore model which assumes stationary pores of constant shape, location, and length may not be appropriate for hydrated polymer gel networks in which the "holes" in a mesh of fluctuating chains are continually changing in shape, size, and location. The hydrated polymer gels are considered homogeneous, with a random mixture of polymer and solvent; there is no component separation. Conversely, porous membranes are viewed as being composed of distinct regions filled either with polymer or solvent. The pores are either polymer chains or water filled channels, with no mixing of the two components.

D/D₀ vs. H from free volume theory

beta=5 sieve factor=1

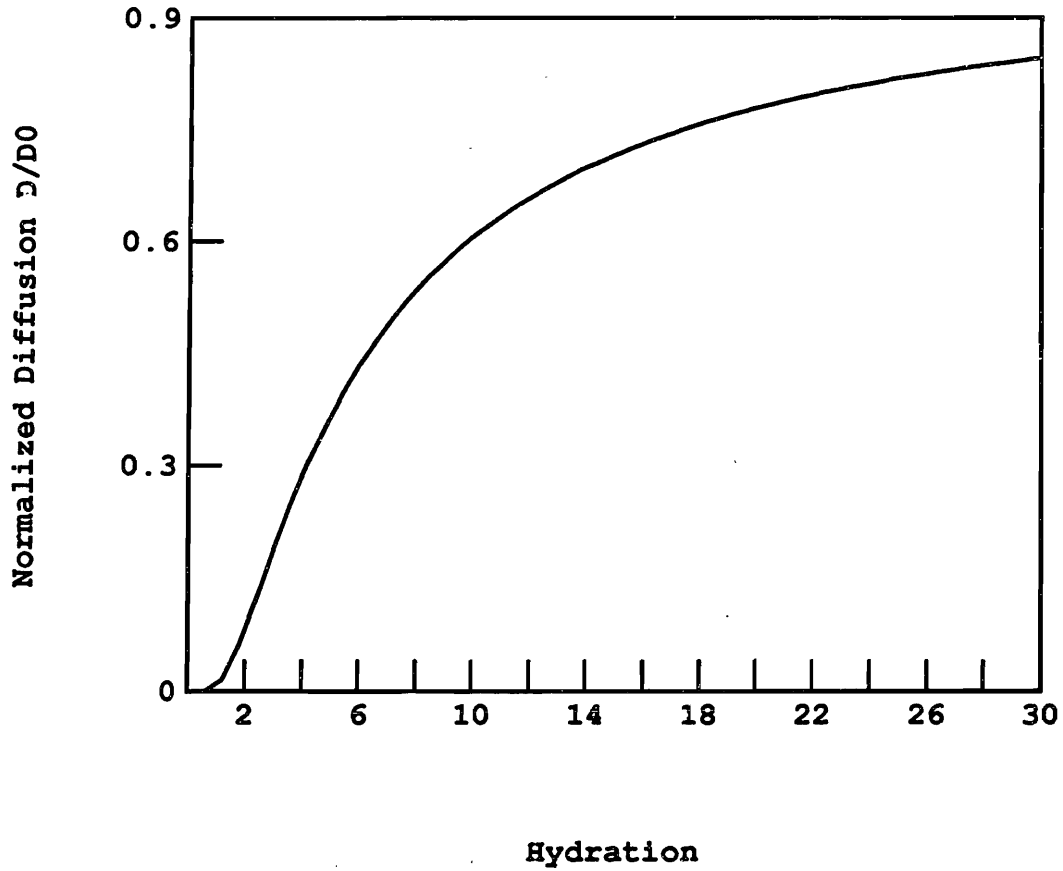


Figure 1.1: Theoretical free volume theory plot of D/D_0 vs. H [Yasuda (1969 Part III:Equation7)].

1.3.2 Nonporous Membrane Models

The pore models [Weiss, Mackie and Meares, Bean] are probably not appropriate for membranes with a mesh-like structure, such as the PMAA membranes studied in this project. Thus, the most promising models appear to be those of Yasuda (1969 PartIII) and Ogston (1973).

Ogston's approach is based on a stochastic model of diffusion applied to sedimentation and diffusion of compact macromolecules in hydrated solutions of uncrosslinked polymer chains. The expression obtained for the ratio of solute diffusivity in the polymer material to that in pure water is:

$$\frac{D}{D_0} = \exp\left(-\pi^{1/2} r l^{1/2}\right) \quad (1.3)$$

where r is the sum of the solute radius and the fibrous obstacle radius, and l is the length of the chain per unit volume. This equation is similar in form to the free volume term in Yasuda's theory. The experimental data examined by Ogston were consistent with this expression but, alas, the polymer chains were uncrosslinked, hence the model may not account sufficiently for the effect of restricted diffusion.

1.3.3 Free Volume Diffusion Models

In some respects, the free volume theory is a crude model. It is not based on rigorous molecular or hydrodynamic theory. Nevertheless, the resulting expression for the diffusion coefficient is simple and has been proven to be quite accurate when compared to diffusion data from several studies [Yasuda et al.(1968 PartI, 1969 PartII), Chen and Osterhoudt (1985), Wisniewski et al.(1980), Peppas and Reinhart (1983 PartI, 1984 PartII), Moynihan et al.(1986), Zenter (1978), Ratner (1973), Refojo (1979), Wilkens and Long (1957), Meares (1958), Fujita et al.(1960), Rosenbaum et al.(1967), Dennison (1986)].

The free volume theory originated as a model for self-diffusion in a

one-component system. Cohen and Turnbull (1959) developed a model for liquid self-diffusion (gradient in labelled molecules but no true concentration gradient) based on the free volume, v_f , within the liquid. The liquid molecule is depicted as a hard sphere which can diffuse to an adjacent void only if a neighboring molecule forfeits a space large enough to accommodate the diffusing molecule. This space, or free volume, becomes empty as a result of thermal fluctuations of molecules. The diffusion coefficient is then related to the probability of finding a hole of volume greater than a critical volume (presumably the volume of the liquid molecule). The probability of finding such a space depends on the average free volume per molecule.

The Cohen and Turnbull model was extended, by Fujita (1961), to a two-component mixture of small solvent molecules and uncrosslinked polymeric solids. The diffusion coefficient is again related to the probability of finding a hole with volume greater than a critical volume, but now the probability depends on the average free volume of the entire two-component system. Fujita expressed the average free volume, V_f , as a function of the volume fraction of solvent.

The free volume theory was further extended by Yasuda et al. (1969 Part III) to homogeneous three-component systems consisting of a solute diffusing through the solvent in a highly swollen polymer network. The membrane system is assumed to be randomly mixed, with randomly fluctuating polymer chains. Solute transport is restricted to pure concentration driven diffusion; i.e., no convection and no pressure gradients across the membrane. This model applies only to water soluble solutes that do not interact enthalpically with the polymer and are impermeable to the membrane if not dissolved in water. The solute is depicted as a hard sphere diffusing through the water filled spaces in the membrane mesh; it cannot diffuse through the solid polymer.

As did Fujita (1961), Yasuda expressed the average free volume of the

system, $V_{f,1s}$, as:

$$V_{f,1s} = H_y V_{f,1} + (1 - H_y) V_{f,3} \quad (1.4)$$

where $V_{f,1s}$, $V_{f,1}$, and $V_{f,3}$ are the free volume of the solvent-polymer mixture, the pure solvent, and the pure polymer, respectively. H_y is the volume fraction of solvent in the membrane. The solvent molecules are assumed to diffuse only through the water filled spaces in the membrane, hence, the effective free volume available to the solute is only the free volume of water in the system:

$$V_{f,eff} = H_y V_{f,1} \quad (1.5)$$

Proceeding from a diffusion coefficient written in terms of the translational oscillating frequency of the solute, the activation free energy, entropy, and energy of diffusion, Yasuda arrived at an equation for the ratio of the solute diffusivity in the swollen membrane to the solute diffusivity in pure water:

$$\frac{D}{D_o} = \Phi(\pi r_s^2) \exp \left[\frac{-B\pi r_s^2}{V_{f,1}H} \right] \quad (1.6)$$

The exponential free volume term is the conformational probability of forming a hole large enough to allow passage of the solute. Steric hindrance is taken into account by the sieve term, Φ . This term is interpreted as the volume fraction of the system containing holes greater or equal to the solute size, or equivalently, the probability of finding such a space.

Several studies have supported Yasuda's free volume theory. Yasuda et al. (1968 PartI, 1969 PartII) found that for the solutes investigated (up to albumin, M.W.=66,000) the experimental data confirmed the free volume theory. However, for the size solutes used in their studies, the sieve effect did not yet play a role and was set equal to unity. Chen and Osterhoudt (1985) examined the transport of three sulfonated azo dyes through swollen gelatin membranes and found the data followed the dependence predicted by the free volume term of the free volume

theory, although, again, the sieve effect was insignificant. Wisniewski et al. (1980) measured the effective diffusivity of small water-soluble solutes (M.W.=20-500: urea, thiourea, glucose, sucrose, lactose, inositol, raffinose, sodium ethotrexate, NaCl, KCl, CsCl, CaCl, MgCl, LiCl) through PHEMA membranes crosslinked with ethylene glycol dimethacrylate (EGDMA). They found the normalized diffusion coefficient, D/D_o , fell exponentially with increasing solute size, and found a linear dependence of $\ln(D/D_o)$ on $1/H$. The data used by Peppas and Reinhart (1983 PartI, 1984 PartII) and by Moynihan et al.(1986) validated the free volume term, as did several other studies on diffusion in PHEMA membranes [Zentner (1978), Ratner (1973), Refojo (1979)]. The last three studies did not consider the effects of crosslinks. The following investigators interpreted diffusion data in terms of the free volume theory : Wilkens and Long (1957), Meares (1958), Fujita et al.(1960), Rosenbaum et al.(1967).

Although the free volume term is well understood, the few expressions that have been formulated for the sieve term have not compared favorably with experimental data. The term is thought to be related to the crosslink density and effective solute size. According to Peppas and Reinhart (1983 PartI), who, in their new theory, came up with the same expression as Yasuda, the sieve term is a function of the molecular weight between crosslinks. They proposed several expressions for the sieve term. One expression later proved to be wrong (1983 PartII), another expression was accurately fit to PVA membrane data (1983 PartII), and a third expression was accurately fit to PHEMA membrane data [Moynihan (1986)]. None of the data fits were presented in the papers.

Dennison (1986) compared the Yasuda free volume theory to data obtained from her experiments with diffusion of globular solutes (Cyanocobalamin (Vitamin B12), Lysozyme, Chymotripsinogen, Ovalbumin, Albumin—M.W. 1350-66,000) through crosslinked poly(ethylene oxide) membranes. With the sieve term set equal to unity, the theory predicted the correct functional form but grossly

overpredicted solute diffusivities. In an attempt to develop a theoretical expression for the sieve term, Dennison derived three distribution functions for the mesh sizes based on distance and molecular weight between crosslinks. Two of these models still overpredicted the diffusivities; the third model (similar to the Ogston model (1973)), predicted diffusivities of the correct magnitude, but resulted in too broad a distribution.

Dennison suggested that the sieve term does not allow for chains that cannot move out of the way of the diffusing solute. It seems, however, that the fault lies not with the sieve term but with the exponential term. The sieve term represents the fraction of mesh spaces which are large enough to accommodate the solute. For a given membrane, this fraction should be constant. From membrane to membrane, it should depend only on crosslink density and solute size. The exponential term represents the conformational probability of forming a hole of sufficient size to allow diffusion of the solute. It seems reasonable that this probability depends on the ease with which the chains can fluctuate. This issue is discussed further in Section 5.3.

Chapter II

Background

The swelling of poly(methacrylic acid) (PMAA) membranes is governed by the interplay between electrostatic double layer repulsive forces between the membrane's fixed charge groups and linear restoring forces created by the crosslinks. These forces can be modulated by altering the ionic strength or pH of the surrounding bath, or by altering the effective crosslink density of the membrane.

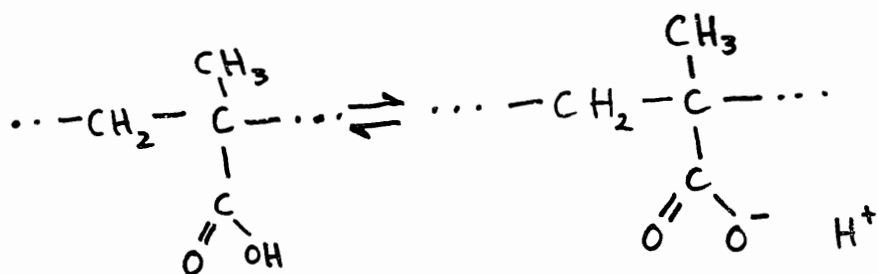
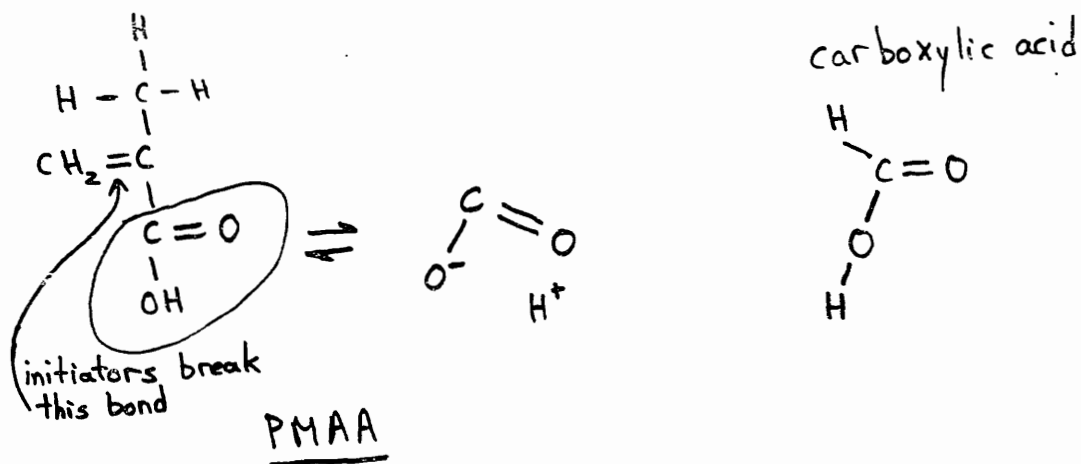
2.1 Membrane Chemical Structure

Membranes were synthesized according to the one-step process developed by Nussbaum (1986). The polymer chains are composed of methacrylic acid (MAA) monomers whose structure is shown in Figure 2.1. The monomer's carboxylic acid group can become ionized ($pK \approx 4.5$), producing a net negative charge. The double bond between the $C = CH_2$ is broken by the initiators (ammonium persulfate (AP) and sodium metabisulfite (SMBS)), allowing the monomers to bond to one another and form a polymer chain (PMAA). The structure of the crosslinker, triethylene glycol dimethacrylate (TEGDMA), is shown in Figure 2.1. The two methacrylate groups can each bond to two PMAA carboxylic acid groups. In this way, PMAA chains are crosslinked to one another, creating a sieve (mesh) structure whose mesh size depends on the amount of crosslinker added.

2.2 Swelling Controls—Ionic Strength and pH

The external controls on membrane swelling are the ionic strength and the pH of the surrounding bath. Bath pH affects the membrane fixed charge density. The ionic strength of the bath affects both the Debye shielding of the charge

methacrylic acid (MAA)



triethylene glycol dimethacrylate (TEGDMA)
with 4 PMAA chains attached

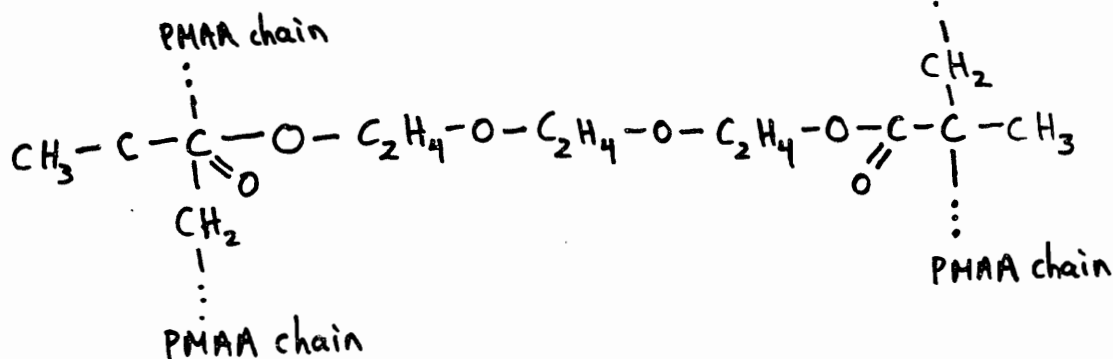


Figure 2.1: Membrane chemical structure, showing formation of PMAA chains and crosslinking of chains.

groups and the charge density.

2.2.1 pH

The fixed charge density of the membrane can be controlled by the surrounding bath pH. The membrane is uncharged at low pH. As the pH is raised, the hydrogen ions become dissociated from the carboxyl groups, leaving a net negative fixed charge (Figure 2.1). Titration experiments [Nussbaum (1986)] have determined that the effective pK of PMAA is ≈ 5.5 . Figure 2.2 is a titration curve for PMAA, showing the increase in negative fixed charge with an increase in pH. Electrostatic double layer repulsive forces between the charge groups cause the mesh spaces to enlarge and the membrane to swell. The membrane swells to the point at which the mechanical restoring force created by the crosslinks balances the electrostatic repulsive force. In summary, higher pH is concomitant with increased hydrogen dissociation; this leads to a greater fixed charge density which, in turn, leads to greater swelling. The water-filled spaces within the mesh enlarge, making it "easier" for the solute to diffuse through.

2.2.2 Ionic Strength

Debye Length

Separated by a distance of a Debye length or less, the polymer chains can exert an electrostatic repulsive force upon one another. If the distance between chains is much greater than a Debye length, the membrane will not swell. By altering the Debye length, the ionic strength of the surrounding bath can be used to control membrane swelling.

A Debye shield can be thought of as a cloud of counter ions surrounding the fixed charge on a polymer chain. Within a Debye length of the polymer chain, the electric field has decayed to $1/e$ of its value at the site of the fixed charge. In one dimension, the polymer chain can be pictured as in Figure 2.3. The potential,

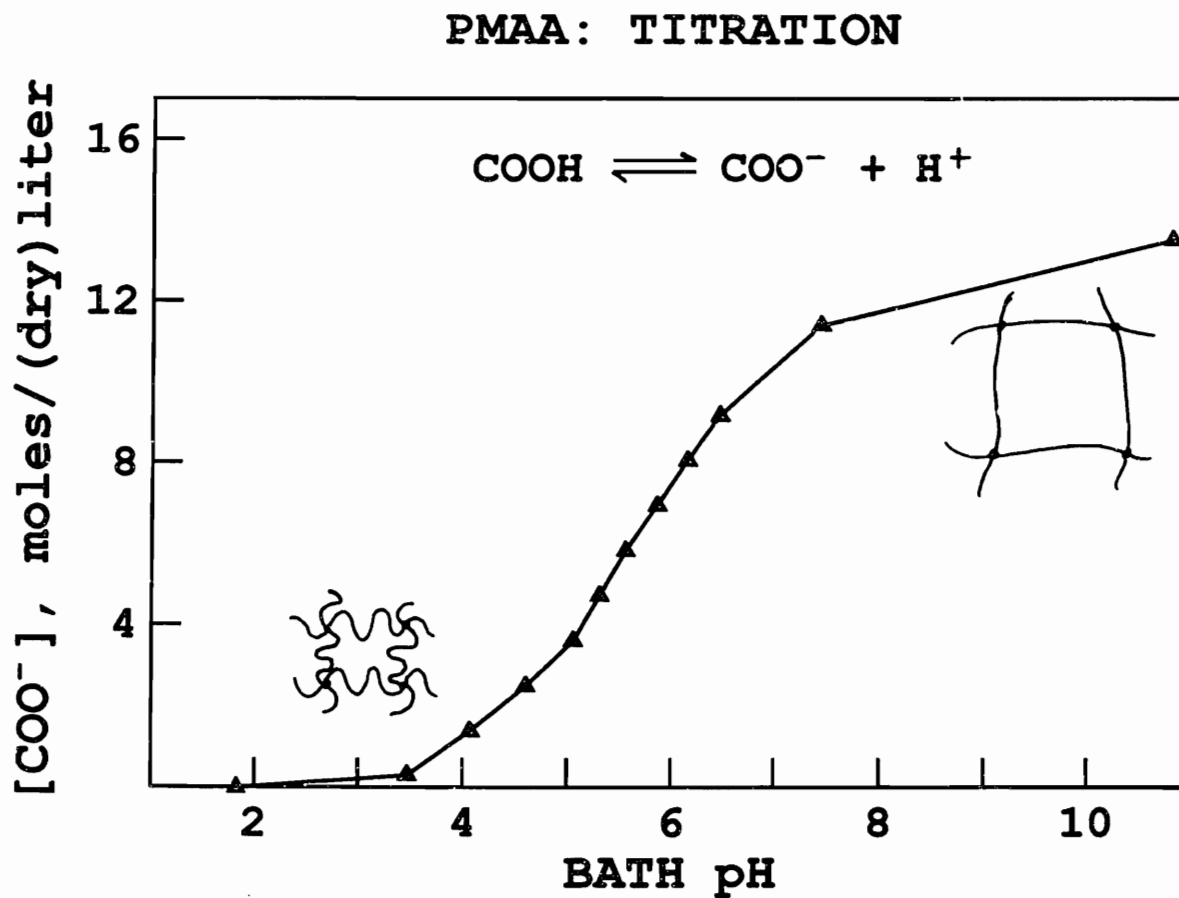


Figure 2.2: PMAA titration curve, showing increase in negative fixed charge groups with increase in pH [Nussbaum(1986)].

$$\nabla^2 \Psi(x) = \frac{-\rho_{\mu}(x)}{\epsilon}$$

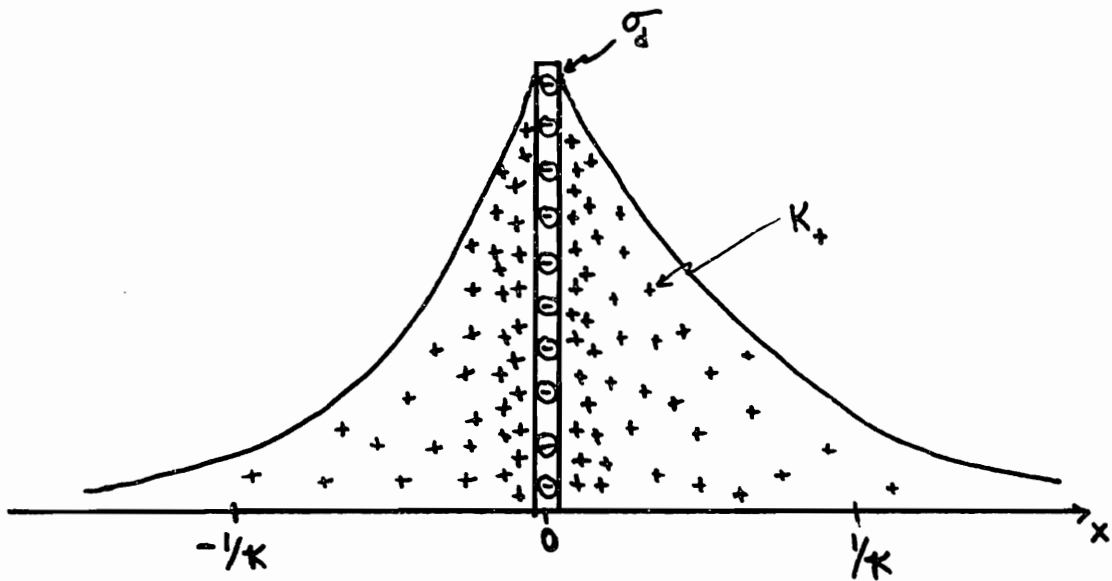


Figure 2.3: Charged polymer chain with surrounding ion cloud. The potential decays to $1/e$ of its value at $x=0$ in one Debye length.

Ψ , in the surrounding bath satisfies Poisson's equation:

$$\nabla^2 \Psi(x) = -\frac{\rho_u(x)}{\epsilon} \quad (2.1)$$

where ρ_u is the charge density in the fluid phase and ϵ is the dielectric constant. If the bath consists of an electrolyte such as KCl, the free charge density is:

$$\rho_u(x) = F(c_K(x) - c_{Cl}(x)) \quad (2.2)$$

where $c_K(x)$ and $c_{Cl}(x)$ are the local concentrations at the point x , and F is the Faraday constant.

The concentrations at x can be written in terms of those at a reference point of zero potential by using the Poisson Boltzmann equation, which applies to an equilibrium condition in which the net flux, Γ , (diffusion plus migration) of each ion species is zero:

$$\Gamma(x) = -D\nabla c(x) - \frac{z_i}{|z_i|} u \nabla \Psi c(x) = 0 \quad (2.3)$$

where u is the ionic mobility. The Boltzmann equation, written for the i th ion species is:

$$c_i(x) = c_i^o \exp \left[-\frac{z_i F \Psi(x)}{RT} \right] \quad (2.4)$$

where c_i^o is the ion concentration at a point in the bath where the potential has decayed to zero. Rewriting Poisson's equation (and recognizing that $c_{K^+}^o = c_{Cl^-}^o \equiv c^o$) gives the Poisson-Boltzmann equation:

$$\frac{d^2 \Psi(x)}{dx^2} = -\frac{F}{\epsilon} c^o \left[\exp \left(-\frac{F \Psi(x)}{RT} \right) - \exp \left(+\frac{F \Psi(x)}{RT} \right) \right] \quad (2.5)$$

For $|\frac{F\Psi(x)}{RT}| \ll 1$, the above equation can be approximated by:

$$\frac{d^2\Psi(x)}{dx^2} = \frac{2c_oF^2}{\epsilon RT}\Psi(x) = \kappa^2\Psi(x) \quad (2.6)$$

where

$$\frac{1}{\kappa} = \sqrt{\frac{\epsilon RT}{2c_oF^2}} \quad (2.7)$$

is the Debye length. With the boundary conditions $\Psi(x \rightarrow \infty) \rightarrow 0$ and $E_x(x = 0^+) = \sigma_d/\epsilon$, where σ_d is the surface fixed charge on the chain, the potential is:

$$\Psi(x) = \frac{\sigma_d}{\epsilon\kappa} \exp(-\kappa x) \quad (2.8)$$

The latter boundary condition assumes that $E=0$ inside the rod. This expression clearly shows that the potential decays to $1/e$ of its value at $x = 0^+$ in one Debye length (Figure 2.3).

The Debye length depends on the ionic strength, c_o , of the surrounding bath. As the ionic strength increases, more counterions are available to shield the fixed charge, thereby shrinking the Debye length and the distance within which the electrostatic repulsive force can act upon another chain. Macroscopically, the membrane deswells; microscopically, the chains comprising the mesh come closer together.

Charge Density

In Sections 2.2.1 and 2.2.2(Subsection Debye Length), a microscopic model for the charge of each chain and for the potential between network chains was used to motivate the effect of pH and ionic strength on swelling. The macroscopic volume charge density of the membrane is related to the surface charge pictured in Figure 2.3 via Donnan Equilibrium theory and normalization to membrane water content.

In addition to determining the Debye length within the membrane, the

external bath ionic strength affects the intramembrane hydrogen concentration by altering the Donnan equilibrium between the membrane and the surrounding bath.

A charged membrane can be viewed as having a double layer of charge on each face. The potential decays according to Equation 2.8, both just inside and just outside the membrane (Figure 2.4). Within the membrane bulk ($\frac{1}{\kappa} \leq x \leq (\delta - \frac{1}{\kappa})$) and within the external bath ($x \geq (\delta + \frac{1}{\kappa})$ and $x \leq -\frac{1}{\kappa}$), charge neutrality is the rule.

The Boltzmann equation provides a relation between the external and internal concentrations of each ionic species:

$$\frac{\bar{c}_{H_+}}{c_{H_+}} = \frac{\bar{c}_{K_+}}{c_{K_+}} = \frac{c_{Cl_-}}{\bar{c}_{Cl_-}} = \exp \left[-\frac{F \Delta \Psi_D}{RT} \right] \quad (2.9)$$

where overbars denote concentrations inside the membrane. $\Delta \Psi_D$ is the Donnan potential drop across the membrane double layer; i.e., $\Delta \Psi_D = \Psi(x = 0^+) - \Psi(x = 0^-)$ where 0^+ and 0^- are at least a Debye length from the membrane interface. The net free charge must be zero in the bulk bath and bulk membrane:

$$F \left(-\bar{c}_{COO_-} + \bar{c}_{H_+} + \bar{c}_{K_+} - \bar{c}_{Cl_-} \right) = 0 \quad (2.10)$$

$$F \left(c_{H_+} + c_{K_+} - c_{Cl_-} \right) = 0 \quad (2.11)$$

where \bar{c}_{COO_-} is the concentration (moles/liter of membrane water) of dissociated carboxyl groups within the membrane, that is, the volume charge density within the membrane.

Using Equations 2.9 and 2.11 to eliminate the internal membrane concentrations from Equation 2.10 results in a quadratic equation in \bar{c}_{H_+} and c_{Cl_-} . Solving for \bar{c}_{H_+} :

$$\bar{c}_{H_+} = \frac{c_{H_+} \bar{c}_{COO_-}}{2c_{Cl_-}} + \frac{c_{H_+}}{2} \sqrt{\left(\frac{\bar{c}_{COO_-}}{c_{Cl_-}} \right)^2 + 4} \quad (2.12)$$

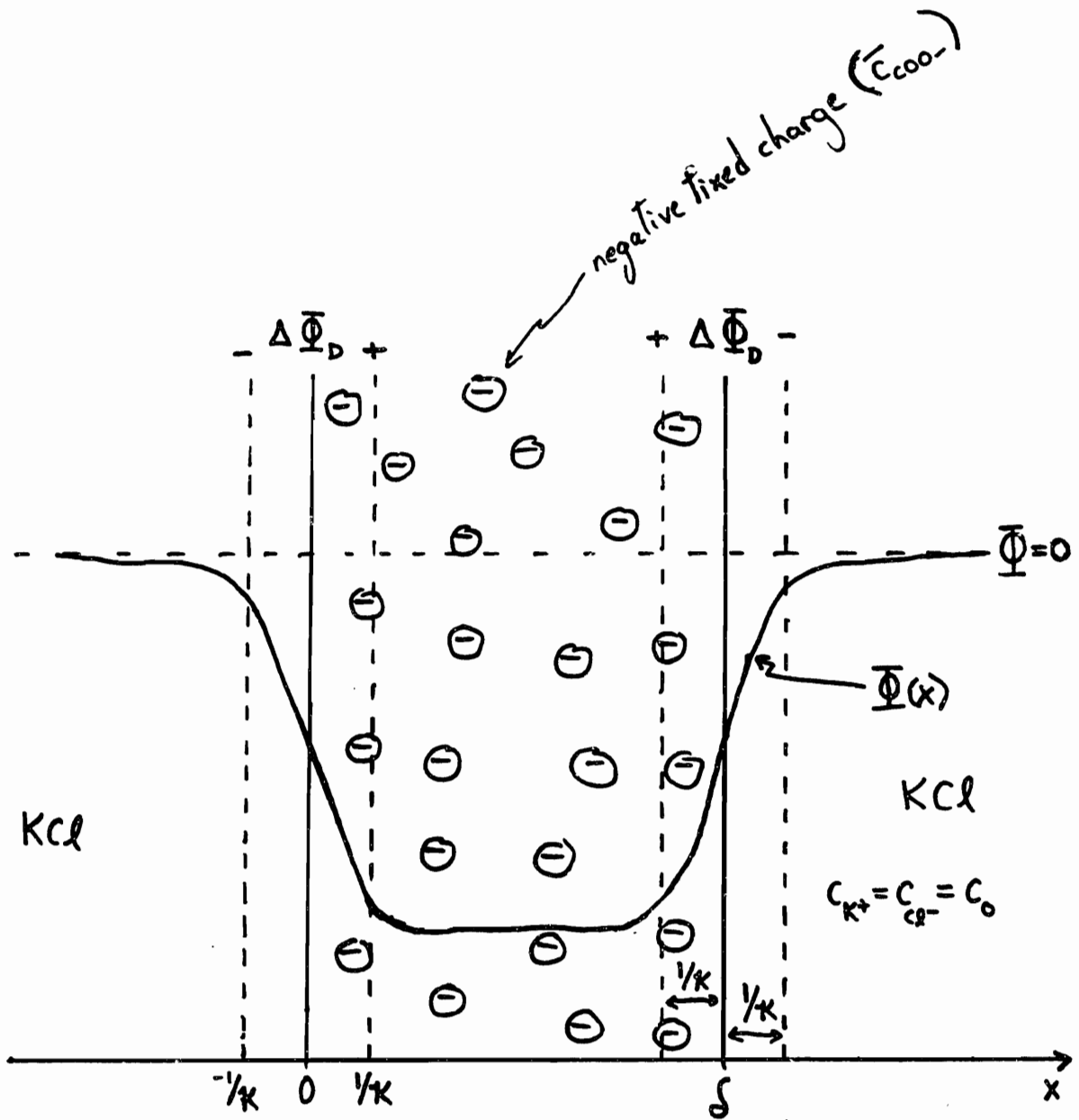


Figure 2.4: Membrane with double layer of charge on each face. A debye length away from the membrane surfaces, charge neutrality holds.

c_H is assumed to be constant. For the time being, \bar{c}_{COO-} will also be considered constant (The error associated with this approximation will be examined by finding the change in \bar{c}_{COO-} , due to the change in \bar{c}_{H+}). With \bar{c}_{COO-} constant, it is clear from Equation 2.12 that raising the external ionic strength (raising c_{Cl-}) lowers the concentration of $H+$ ions within the membrane (The $K+$ ions move in to preserve charge neutrality.).

Once \bar{c}_{H+} is altered, the membrane charge instantaneously adjusts in accordance with the chemical reaction law for the dissociation of membrane charge groups:

$$\bar{c}_{H+}\bar{c}_{COO-} = K_m\bar{c}_{COOH} = K_m(\bar{c}_{mo} - \bar{c}_{COO-}) \quad (2.13)$$

\bar{c}_{COOH} is the concentration (moles/wet liter) of undissociated carboxyl groups, \bar{c}_{mo} is the total concentration (moles/wet liter) of carboxyl groups (dissociated plus undissociated), and K_m is the dissociation constant for the membrane carboxyl group. Solving for \bar{c}_{COO-} :

$$\bar{c}_{COO-} = \frac{K_m\bar{c}_{mo}}{\bar{c}_{H+} + K_m} \quad (2.14)$$

shows that the increase in external ionic strength leads to an increase in \bar{c}_{COO-} and, ultimately, to a greater membrane hydration. In terms of moles/dry liter of carboxyl groups, \bar{c}_{mos} :

$$\bar{c}_{mo} = \frac{\bar{c}_{mos}}{H} \quad (2.15)$$

Returning to Equation 2.12, it can be seen that the increase in \bar{c}_{COO-} raises the original first order estimate of \bar{c}_{H+} . Although \bar{c}_{H+} does, indeed, decrease as the ionic strength increases, it decreases less than the original estimate.

At low ionic strengths, the predominant effect of a change in ionic strength is a change in membrane fixed charge. An increase in ionic strength causes the membrane to swell. At higher ionic strengths, when the majority of the charge groups are already dissociated, ionic charge shielding dominates. Now, an increase in ionic strength causes the membrane to deswell.

2.2.3 Slab Swelling Model

To better understand the swelling process and how it is affected by ionic strength and fixed charge, one can use a simple model [Nussbaum (1986)] which depicts the membrane strands as a series of flat solid slabs, each with a surface charge (Figure 2.5). By using the two slab model, the fields in regions (a) and (b) can be found by solving Poisson's equation in each region (where the free charge density is the sum of the ionic strengths). The repulsive force, given in Equation 2.16, is found by integrating the stress tensor over a surface surrounding one of the slabs:

$$\pi_{rep} = \frac{2}{\epsilon} \sigma_m^2 \exp \left[-\frac{W}{1/\kappa} \right] \quad (2.16)$$

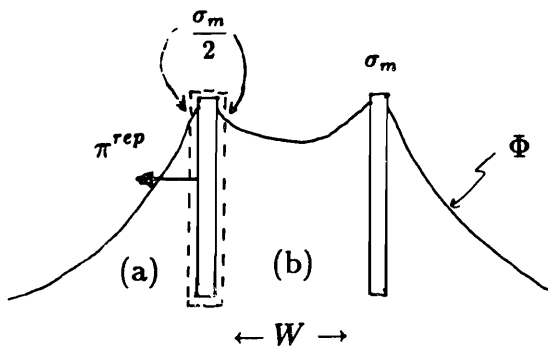
It depends on the surface fixed charge density, σ_m , which is controlled by the pH of the surrounding bath, and is inversely proportional to the Debye length, $1/\kappa$, which is inversely proportional to the ionic strength of the surrounding bath (Equation 2.7).

2.3 Crosslink Density

There are two distinct ways in which the crosslink density affects solute transport— by limiting how much the membrane can swell and by restricting solute motion through the mesh. As seen in Figure 2.6, with both membranes at identical pH, the more lightly crosslinked membrane is more hydrated than the heavily crosslinked membrane.

Two membranes with identical hydrations can have different permeabilities. The two membranes in Figure 2.6 have the same hydration but different crosslink densities. The left membrane is more heavily crosslinked. A large solute is restricted by the mesh as it diffuses through the left membrane, but it can push its way through the mesh on the right. The more heavily crosslinked membrane acts as a sieve to the large solute. A small solute would be unhindered by the

Swelling—Ionic Strength and Fixed Charge



$$\nabla^2 \Phi = -\frac{\rho_f}{\epsilon} = -\frac{1}{\epsilon} \sum_i z_i F c_i$$

$$\pi_{rep} = \frac{2}{\epsilon} \sigma_m^2 \exp \left[-\frac{W}{(1/\kappa)} \right]$$

$$\frac{1}{\kappa} = \text{Debye length} \propto \frac{1}{\sqrt{c_0}}$$

Figure 2.5: Slab swelling model

Limits Hydration



$$\begin{aligned} p H_1 &= p H_2 \\ xlink_1 &> xlink_2 \\ H_1 &< H_2 \end{aligned}$$

Acts as Sieve to Larger Solutes



$$\begin{aligned} H_1 &= H_2 \\ xlink_1 &> xlink_2 \end{aligned}$$

Figure 2.6: Effects of crosslink density on swelling and diffusion.

mesh in either case.

2.4 Solutes

Donnan partitioning (Equation 2.9) affects the concentration of charged solutes in the membrane in the same manner as it affects the internal concentration of ions. For a membrane with negative fixed charge, the internal concentration of a negative solute is suppressed and the internal concentration of a positive solute is enhanced. To eliminate this effect in the transport experiments performed in this study, neutral solutes were used.

Chapter III

Methods and Materials

3.1 Membrane Preparation

Nine different PMAA membranes were made for the hydration and transport experiments, each with a different crosslink density. The crosslinked PMAA membranes were prepared according to the formulation in Appendix A. They were cast between two optical glass plates (from Edmund Scientific, Barrington, N.J.) separated by a 3 or 5 mil thick teflon spacer and heated in a water bath (60°C) for four hours to ensure complete polymerization. The ingredients in the recipe were mixed and then degassed for 10 minutes before casting. A 3 or 5 mil thick PTFE (Teflon) o-ring spacer, cut to the size of the glass plate, was positioned on the plate. Using a pipet, a puddle of the solution (more than enough to cover the plate) was placed in the center of the plate. Starting at one edge, the second glass plate was slowly lowered onto the bottom plate, thereby spreading the solution over the area inside the spacer. Care was taken to prevent air bubbles from forming during this step. Three or four hose clamps were used to tightly clamp the glass plates together. Excess solution was rinsed off.

The unpolymerized membrane was lowered into a pyrex bowl containing 60°C deionized water where it was heated in a vertical position. Four hours later, the sandwiched plates were pryed apart under running water with a razor blade. The membrane was carefully peeled from the plate and soaked in deionized water for 48 hours to remove impurities. Membranes were stored in a preservative solution consisting of 0.1% sorbic acid in 10% ethanol.

Since the transport time constant is proportional to the square of the membrane thickness, 3 mil membranes were used for the transport experiments. The more durable 5 mil membranes were used for the hydration experiments in which the membranes were handled a great deal. The membranes are denoted by

Table 3.1: Membranes used in experiments, differing in crosslinker and water content. SX/Y: X=volume crosslinker; Y=half volume water

	S.05/Y	S.1/Y	S.2/Y	S.4/Y	S.6/Y
S.X/.5				S.4/.5	
S.X/1	S.05/1	S.1/1	S.2/1	S.4/1	S.6/1
S.X/2		S.1/2	S.2/2	S.4/2	

SX/Y, where X is the volume of crosslinker (triethylene glycol dimethacrylate (TEGDMA)) per 10ml of monomer (methacrylic acid (MAA)), and Y is half the volume of water (in ml) added at the time of casting. In order to study the correlation between membrane composition, specifically percentage of crosslinker and volume fraction of polymer, and membrane transport, the membranes in Table 3.1 were cast and used for subsequent hydration and transport experiments.

3.2 Hydration Experiments

The swelling of charged membranes can be controlled chemically by varying the pH or by varying the ionic strength of the surrounding bath. The membrane's weakly acidic fixed carboxyl groups become ionized with increasing pH ($pK \approx 5.5$). Microscopically, the spaces within the mesh of polymer chains and crosslinks enlarge as a result of an increase in the electrostatic repulsive force between the charge groups. Macroscopically, the membrane swells. The bath ionic strength determines the Debye length (amount of charge shielding) and, through Donnan partitioning, affects the membrane fixed charge as well. All experiments were performed in bath solutions of 0.05M KCl. Consequently, the Debye length was constant for all experiments and the fixed charge was altered solely through pH changes.

Membrane water content, thickness, and diameter were measured as a function of pH, at constant ionic strength (0.05M), for each membrane

formulation. Membrane water content is given in terms of hydration, defined as the ratio of the fluid volume v_w to the solid volume v_s of the membrane:

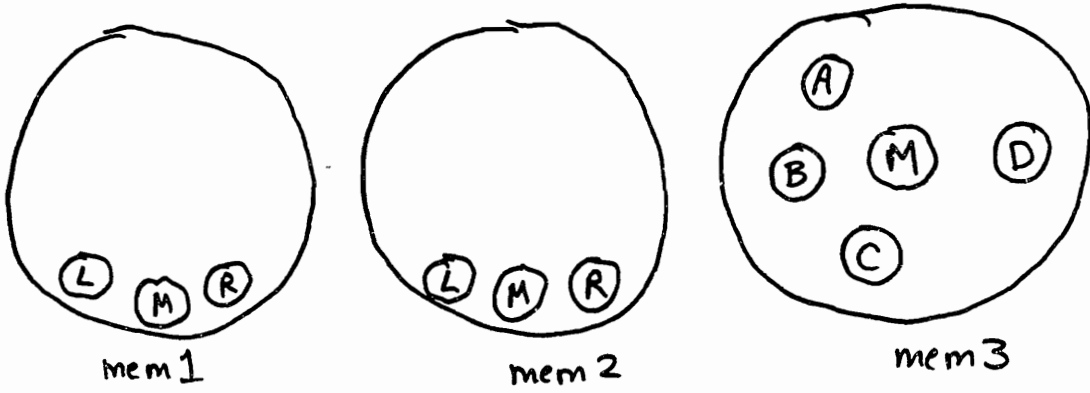
$$H = v_w/v_s .$$

Circular discs (11/16" dia) were cut, with sharpened brass cork bores, from at least one membrane from each formulation. To determine the degree of homogeneity within a membrane, 3-5 discs were cut from different regions of the same membrane for three membrane formulations (S.2/1, S.4/1, S.6/1). To determine the degree of homogeneity between different membranes from the same batch, discs were cut from three different S.2/1 membranes made from the same batch at the same time. Figure 3.1 is a drawing of the S.2/1, S.4/1, and S.6/1 membranes, showing the locations from which the discs were cut.

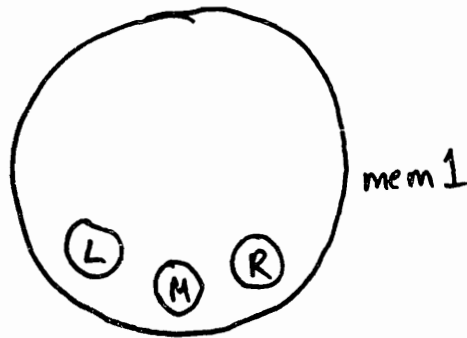
Since discs were cut from membranes which had previously been stored in a preservative solution of unknown pH, the discs may not all have been at the same pH at the time they were cut. Consequently, weight and diameter measurements are not used for comparisons between membranes; only the hydration measurements are appropriate for such comparisons. However, discs cut from the same membrane were assumed to be at equal pH's at the time of cutting, therefore weight and diameter comparisons between discs within the same membrane are valid.

The discs were equilibrated in a succession of buffered pH solutions ranging from pH3 to pH5.6 (approximately pH3, 4, 5, 5.6). pH was measured with an Orion Ross pH electrode and Orion model 231 pH meter. To examine to what extent the swelling process is reversible, discs were deswelled in reverse order from pH5.6 back down to pH3. Each disc was equilibrated in the appropriate pH buffer for at least 24 hours. Before taking any measurements, surface water droplets were removed by patting each side of the disc several times with plastic wrap. Plastic wrap was used, rather than paper towel or filter paper, since it does not draw water from the disc. The disc was then placed in a small plastic dish,

S.2/1



S.4/1



S.6/1

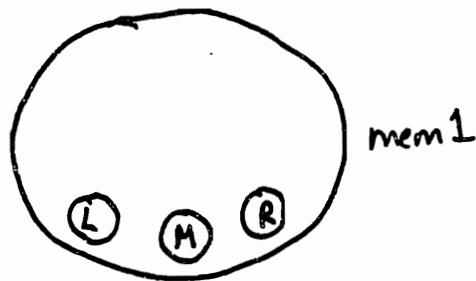


Figure 3.1: S.2/1, S.4/1, and S.6/1 membranes, showing locations of discs.

covered with a lid to prevent evaporation, and weighed.

Immediately after weighing the disc, the thickness of the disc was quickly measured using a short circuit sensing micrometer. After gently positioning the disc on the anvil, the micrometer was adjusted until the resistance scale registered a sharp decrease in electrical resistance, indicating that the micrometer had made contact with the membrane surface.

Despite the effort made to take quick thickness measurements, the surface of some discs began to dry whereas the surface of other discs became damp. Heavily hydrated discs often 'sweated' beads of water onto the surface, causing the micrometer to make electrical contact before touching the actual surface of the disc. Conversely, the surfaces of the more heavily crosslinked discs dried; thus electrical contact was not made until the micrometer slightly compressed the disc. The membranes were thin enough such that these seemingly minor problems had a significant effect on the measurement. Due to the resulting large error bars, the thickness measurements were later abandoned.

After taking one weight measurement and one thickness measurement, the disc was reimmersed in the same pH buffer where it remained until each of the other discs had been measured in a similar fashion. The entire process was then repeated twice for the set of discs, amounting to 3 weight and 3 thickness measurements for each disc. All measurements were averaged. The mean weights and thicknesses, with their standard deviations and percent errors, are given in Tables 3.2 and 3.3. In calculating the mean and s.d. weights and thicknesses for the S.2/1, S.4/1, and S.6/1 discs, the sum of the means of each disc was divided by the total number of discs (total number of discs: S.2/1:11, S.4/1:3, S.6/1:3). The dry weights were calculated in the same way.

Table 3.2: Mean weights for every disc at each pH. For the S.2/1, S.4/1, and S.6/1 weights, all intra and intermembrane discs were used in calculating the mean and s.d. for that membrane.

mem	pH	mean(g)	s.d.	% error
S.05/1	3.2	0.0403	0.0001	0.24
	4.0	0.0451	0.0002	0.55
	5.0	0.0822	0.0008	1.02
	5.6	0.1517	0.0013	0.85
	5.2	0.0971	0.0019	2.00
	4.0	0.0485	0.0005	1.02
	3.2	0.0398	0.0005	1.35
dw	0.0125			
S.1/2	3.2	0.0395	0.0001	0.15
	3.9	0.0441	0.0001	0.25
	5.0	0.0771	0.0012	1.54
	5.7	0.1343	0.0010	0.73
	5.2	0.0894	0.0006	0.72
	4.0	0.0467	0.0002	0.45
	3.2	0.0391	0.0005	1.17
dw	0.0140			
S.1/1	3.2	0.0395	0.0002	0.57
	4.0	0.0436	0.0005	1.17
	5.0	0.0726	0.0009	1.27
	5.5	0.1156	0.0011	0.91
	5.2	0.0849	0.0006	0.70
	4.0	0.0456	0.0001	0.28
	3.2	0.0387	0.0013	3.32
dw	0.0143			
S.2/2	3.3	0.0499	0.0014	2.87
	4.0	0.0558	0.0009	1.65
	5.0	0.0874	0.0012	1.37
	5.5	0.1384	0.0021	1.49
	5.1	0.1041	0.0009	0.90
	4.0	0.0595	0.0006	0.99
	3.2	0.0516	0.0008	1.52
dw	0.0208			
S.2/1	3.1	0.0378	0.0014	3.70
	4.0	0.0414	0.0016	3.86
	4.8	0.0580	0.0022	3.79
	5.4	0.0851	0.0028	3.29
	4.9	0.0651	0.0026	3.99
	4.0	0.0422	0.0017	4.03
	3.1	0.0380	0.0015	3.95
	dw	0.0168	0.0006	3.57

mem	pH	mean(g)	s.d.	% error
S.4/2	3.3	0.0355	0.0012	3.44
	4.0	0.0383	0.0008	2.00
	5.0	0.0550	0.0010	1.82
	5.6	0.0855	0.0011	1.23
	5.2	0.0617		
	4.0	0.0392		
	3.2	0.0344		
dw	0.0169			
S.4/1	3.1	0.0386	0.0004	1.04
	4.0	0.0413	0.0006	1.45
	4.8	0.0536	0.0009	1.68
	5.3	0.0687	0.0043	6.26
	4.9	0.0593	0.0004	0.67
	4.0	0.0424	0.0006	1.42
3.2	0.0389	0.0006	1.54	
dw	0.0198	0.0001	0.51	
S.4/5	3.3	0.0394	0.0002	0.61
	4.0	0.0417	0.0004	0.85
	5.0	0.0537	0.0002	0.29
	5.6	0.0761	0.0005	0.59
	5.1	0.0599	0.0004	0.71
	4.0	0.0429	0.0005	1.19
3.2	0.0392	0.0006	1.44	
dw	0.0199			
S.6/1	3.1	0.0371	0.0006	1.62
	4.0	0.0395	0.0010	2.53
	4.8	0.0485	0.0014	2.89
	5.3	0.0681	0.0034	4.99
	5.0	0.0542	0.0016	2.95
	4.0	0.0403	0.0011	2.73
3.2	0.0373	0.0009	2.41	
dw	0.0203	0.0015	7.53	

Table 3.3: Mean thicknesses for every disc at each pH. For the S.2/1, S.4/1, and S.6/1 thicknesses, all intra and intermembrane discs were used in calculating the mean for that membrane.

mem	pH	mean(um)	s.d.	% error
S.05/1	3.2	16.9333	0.9504	5.61
	4.0	17.2000	0.3606	2.09
	5.0	21.3333	0.6110	2.86
	5.6	26.9000	0.9644	3.57
	5.2	23.3667	1.9655	8.43
	4.0	17.0333	1.1547	6.75
	3.2	17.1000	0.9539	5.56
S.1/2	3.2	16.3667	0.7234	4.40
	3.9	16.3667	0.4041	2.44
	5.0	21.3667	0.6110	2.85
	5.7	24.1333	0.3215	1.33
	5.2	20.1333	0.7572	3.78
	4.0	15.7667	0.5033	3.17
	3.2	15.3000	0.4359	2.88
S.1/1	3.2	15.0667	0.5132	3.38
	4.0	16.3333	0.2082	1.29
	5.0	19.3000	0.8185	4.25
	5.5	23.0333	0.6807	2.95
	5.2	20.0667	1.1930	5.93
	4.0	16.2333	1.1846	7.30
	3.2	14.9333	0.8021	5.36
S.2/2	3.3	13.5000	0.6083	4.52
	4.0	14.6667	0.1528	1.02
	5.0	16.9333	0.8387	4.96
	5.5	21.0000	1.9079	9.10
	5.1	17.1667	0.2082	1.22
	4.0	14.4000	0.6083	4.24
	3.2	13.4667	0.3788	2.82
S.2/1	3.1	15.353		
	4.0	15.875		
	4.8	16.403		
	5.4	18.868		
	4.9	17.267		
	4.0	15.081		
	3.1	15.005		

mem	pH	mean(um)	s.d.	% error
S.4/2	3.3	13.3333	0.7572	5.70
	4.0	13.8667	0.2517	1.80
	5.0	15.8667	0.2309	1.45
	5.6	19.5667	1.3614	6.95
	5.2	16.4000		
	4.0	13.6000		
	3.2	13.2000		
S.4/1	3.1	14.122		
	4.0	14.26		
	4.8	15.39		
	5.3	17.86		
	4.9	15.48		
	4.0	14.02		
	3.2	14.45		
S.4/5	3.3	13.5667	0.0577	0.44
	4.0	15.0000	1.0149	6.73
	5.0	15.6667	0.1155	0.77
	5.6	18.2333	0.5859	3.24
	5.1	16.0333	0.1155	0.75
	4.0	15.2333	0.9713	6.37
	3.2	13.9667	0.7638	5.44
S.6/1	3.1	13.433		
	4.0	13.02		
	4.8	14.93		
	5.3	16.39		
	5.0	14.57		
	4.0	13.19		
	3.2	13.57		

Finally, the diameter of each disc was measured using a ruler. Only one diameter measurement was necessary due to the consistency of this measurement. The diameters are listed in Table 3.4. In calculating the diameters for the S.2/1, S.4/1, and S.6/1 discs, the diameters of all the discs were averaged. The standard deviations in these averages were all less than 3%.

The discs were then placed in the next pH buffer solution and allowed to equilibrate. Hydration values were calculated after lyophilizing the disc and measuring the dry weight. The volume hydration was calculated using the following equation:

$$H = \frac{W_t - W_s}{W_s} \left(\frac{\rho_p}{\rho_f} \right) \quad (3.1)$$

where W_t is the total weight of the swollen membrane, W_s is the dry weight, ρ_p is the polymer density, and ρ_f is the fluid density. For a swollen membrane $\rho_f \approx 1$ and $\rho_p \approx 1.33$ [Weiss xlink paper].

3.3 Transport Experiments

3.3.1 Equipment

The transport properties of PMAA membranes were studied by measuring the flux of two neutral fluorescent solutes across each membrane. The experimental apparatus is based on that used by Weiss [Weiss (1986)], but has been modified and improved by Paul Grimshaw [Grimshaw et al.(1988) submitted]. The transport cell (Figure 3.2) was made from 1/4 inch black poly(methyl methacrylate) and consists of two 100ml half cells with 3.8cm^2 windows. After gently placing the membrane between two #2219 sponge rubber gaskets and clamping it between the two half cells, the cells were each filled with 100ml of 0.05M KCl. The baths were circulated by a dual channel peristaltic pump and were mixed by magnetic stirring bars. To minimize the buildup of stagnant fluid layers, the inlet tubing was inserted just above and on either side of

Table 3.4: Diameters for every disc at each pH. For the S.2/1, S.4/1, and S.6/1 diameters, all intra and intermembrane discs were used in calculating the diameter for that membrane.

membrane	pH	diameter(cm)
S.05/1	3.2	16.6
	4.0	17.5
	5.0	21.3
	5.6	27.2
	5.2	24.3
	4.0	18.3
	3.2	17.0
S.1/2	3.2	17.1
	3.9	17.9
	5.0	21.7
	5.7	26.6
	5.2	23.2
	4.0	18.1
	3.2	16.7
S.1/1	3.2	17.0
	4.0	17.6
	5.0	21.9
	5.5	25.4
	5.2	22.7
	4.0	17.9
	3.2	17.1
S.2/2	3.3	20.9
	4.0	22.0
	5.0	25.9
	5.5	30.9
	5.1	27.7
	4.0	22.8
	3.2	21.3
S.2/1	3.1	1.68
	4.0	1.77
	4.8	2.00
	5.4	2.26
	4.9	2.08
	4.0	1.80
	3.1	1.72

membrane	pH	diameter(cm)
S.4/2	3.3	16.7
	4.0	17.8
	5.0	20.2
	5.6	23.2
	5.2	19.8
	4.0	17.4
	3.2	16.8
S.4/1	3.1	1.70
	4.0	1.78
	4.8	1.93
	5.3	2.21
	4.9	2.00
	4.0	1.81
	3.2	1.75
S.4/.5	3.3	17.4
	4.0	17.9
	5.0	19.6
	5.6	22.2
	5.1	20.2
	4.0	18.3
	3.2	16.8
S.6/1	3.1	1.70
	4.0	1.79
	4.8	1.92
	5.3	2.17
	5.0	2.00
	4.0	1.81
	3.2	1.74

the membrane, thus forcing the returning fluid to flow adjacent to the membrane surface.

The pH and temperature of the baths were monitored with temperature probes, Orion Ross pH electrodes, and Orion Research model 231 pH meters. pH was controlled via computer by four Metrohm model 665 Dosimat automatic burettes, thus permitting pH control in both directions (acid (HCl) and base (KOH)) in each half cell. Temperature was maintained at 20°C by continuously circulating the bath through tubing immersed in coolant, while simultaneously heating the bath via computer controlled PTFE insulated chromel heating coils placed in the half cells.

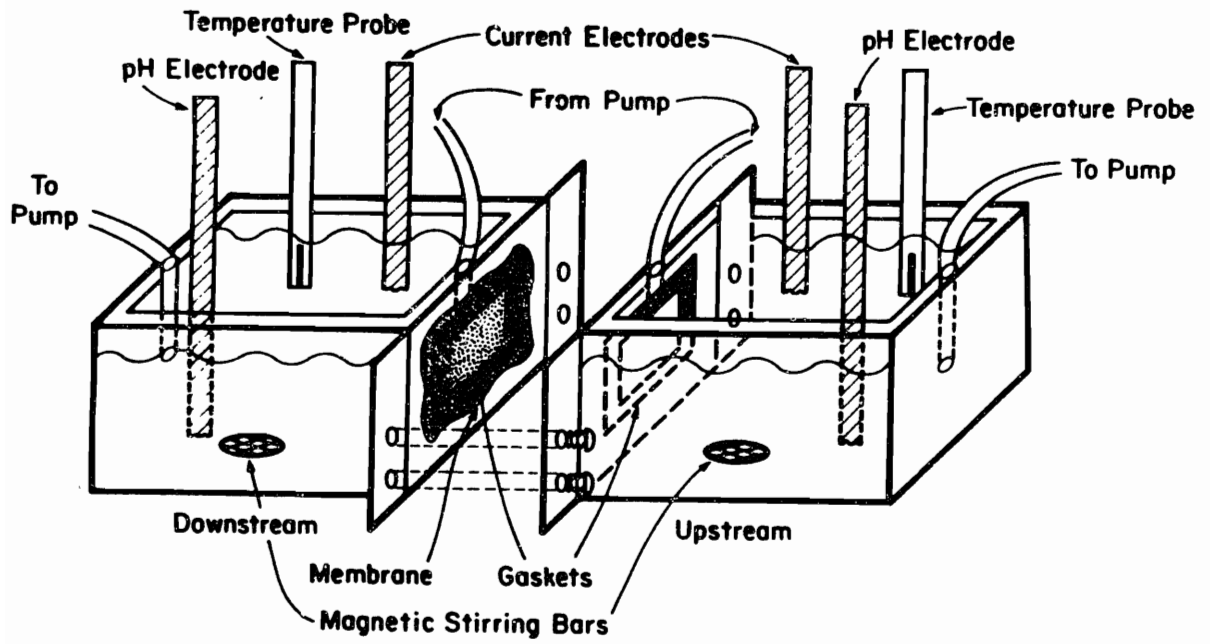


Figure 3.2: Transport Cell

The apparatus for measurement of fluorescent solute concentration on the downstream side is shown schematically in Figure 3.3. The fluid on the downstream side was circulated by the peristaltic pump to a flow-through cuvette (Hellma #171 special optical glass or Starna 47F quartz glass) in an SPF-500 Spectrofluorometer (SLM/Aminco Instruments, Inc.). The spectrofluorometer excited one of the fluorescent solutes at the appropriate excitation wavelength and detected its fluorescence at the corresponding emission wavelength. To measure the concentration of the second fluorescent solute in these dual-tracer experiments, the downstream fluid was next circulated to a flow-through cuvette in a Shimadzu RF-530 Fluorescence HPLC Monitor. The Shimadzu automatically normalized the fluorescence output to the reference excitation signal. A multichannel chart recorder (Linseis model LS-44) recorded the fluorescence and reference excitation output from the Spectrofluorometer and the normalized fluorescence output from the Shimadzu. These signals, as well as the up and downstream pH's and temperatures, and the amounts of acid and base added by the Dosimats, were then fed to an IBM computer equipped with a Metrabyte Dash-16 A/D card.

3.3.2 Protocol for Transport Experiments

Each membrane was preconditioned before a transport experiment by preswelling, deswelling, and again swelling the membrane in a 0.05M KCl solution with either KOH or HCl added. The membrane was clamped between the two half cells which were then filled with 100ml of 0.05M KCl solution. Solutions in all hydration and transport experiments were of .05M ionic strength. Temperature and pH were under computer control, with the up and downstream solutions initially set to pH4.5. There were no transmembrane pH gradients in these experiments; the downstream pH was always the same as the upstream pH. Temperature was maintained at 20°C throughout each experiment.

After establishing a baseline with no dye present for 10-15 minutes, the two

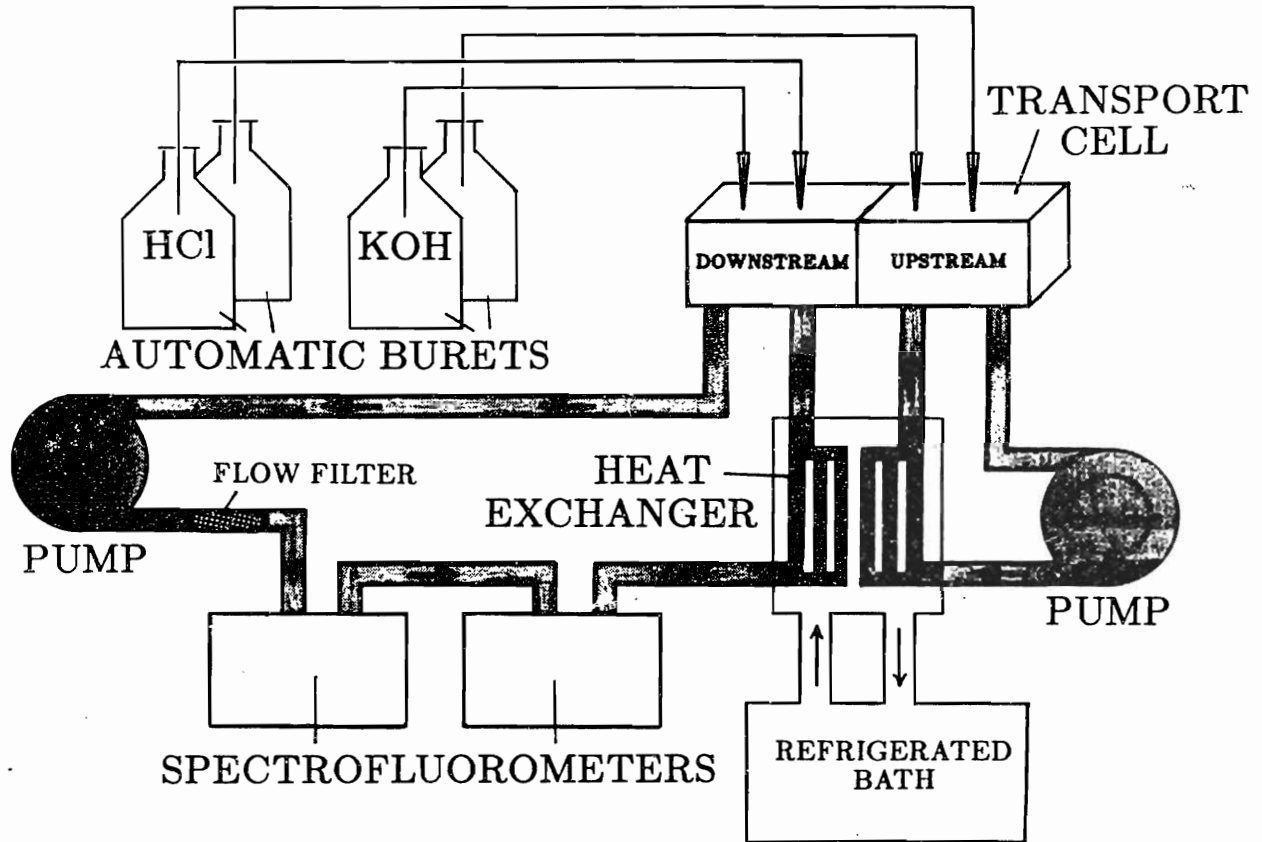


Figure 3.3: Transport Experiment Setup [Grimshaw et al.(1988)]

Table 3.5: Dyes: Their molecular weight, excitation λ , emission λ

dye	M.W.	ex peak	em peak
Lis-dex	10,000	570 nm	590 nm
NSPA	301	358 nm	488 nm

water soluble neutral solutes (Lissamine-dextran (Lis-dex) conjugate synthesized by Molecular Probes, Eugene, OR and N-(3-sulfopropyl) acridinium inner salt (NSPA) from Molecular Probes) were added to the upstream side at a concentration of approximately 10^{-5} M. Neutral, as opposed to charged, solutes were used in order to eliminate the effects of Donnan partitioning on the diffusion of the solute.

Table 3.5 lists the two solutes, their MW, and their excitation and emission wavelengths. The emission and excitation spectra of these two solutes are sufficiently separated to allow distinct detection of each solute. The solutes also complement one another in size; Lis-dex is on the order of, and NSPA is much smaller than, the mesh size. The fluorescence properties of the two dyes were found to be insensitive to pH in the ranges used for these experiments. Unfortunately, in some experiments it appeared that the solutes, especially the NSPA, were binding to the apparatus tubing and pump filter at higher pH's and detaching at lower pH's.

The experiment was monitored for at least two hours, until it was determined that both solutes had reached a steady flux. A constant slope on the solute concentration curve signified steady state.* At this time, the pH on both sides was changed, by addition of HCl or KOH, via computer and the experiment again monitored for a few hours until a new steady state flux was established. For the majority of experiments, the pH sequence was:

* Whether or not steady state had truly been reached was somewhat ambiguous since the determination was based on whether the fluorescence trace on the chart recorder 'looked straight'.

pH4.5 → pH3 → pH5.5 → pH4.5 → pH3.

The real time downstream fluorescence intensity was recorded on both the chart recorder and computer for later use in calculating membrane permeabilities. The permeability P was computed from the rate of change of downstream dye concentration c_d [moles/liter] by [Weiss (1986)]:

$$P = \frac{\Delta c_d V_d}{\Delta t A c_u} \quad (3.2)$$

where c_u is the upstream dye concentration in moles/liter, V_d [liters] is the downstream bath volume, and A [cm^2] is taken to be the area defined by the membrane gasket[†] (Figure 3.2). The permeability for each solute at each pH was calculated from the slope of the steady state portion of the corresponding section of the downstream fluorescence intensity curve.

In order to compute the permeability, the downstream fluorescence intensity must be related to $\Delta c_d/c_u$. The absolute values of c_d and c_u need not be known; only their ratio need be known. Therefore, during periods of steady state, the downstream dye concentration was calibrated relative to the upstream concentration by adding a small amount of upstream bath to the downstream side. For instance, in transferring 10ul of upstream solution to the downstream side, $10 \times 10^{-6} \times c_u$ moles of dye is transferred. Δc_d is now $10^{-5} c_u/V_d$ moles/volume. The corresponding jump in measured fluorescence intensity can then be related to $\Delta c_d/c_u$. Suppose the jump in fluorescence intensity is h units. Then the change in fluorescence intensity, Δf_d , at any point on the fluorescence

[†] Although the membrane area changes with pH, the calculation of P assumed that A was constant. This assumption is plausible to the extent that an increase in the stagnant fluid layer accompanies an increase in membrane area (due to a "bulge" in the membrane), and that these two effects on transport oppose and cancel one another.

intensity curve is related to the change in downstream dye concentration by:

$$\frac{(\Delta c_d/c_u)}{(10^{-5}/V_d)} = \frac{\Delta f_d}{h} \quad (3.3)$$

The permeability is then:

$$P = \frac{\Delta f_d}{\Delta t} \frac{1}{hA} 10^{-2} cm/sec \quad (3.4)$$

which can be determined from the steady state slope of the fluorescence intensity curve. Calibrations were made before each pH change, at a time when a discontinuity in the downstream concentration curve would be least distracting to the eye. Lis-dex calibrations consisted of 25ul or 50ul of upstream solution while NSPA calibrations were typically 500ul.

Chapter IV

Results

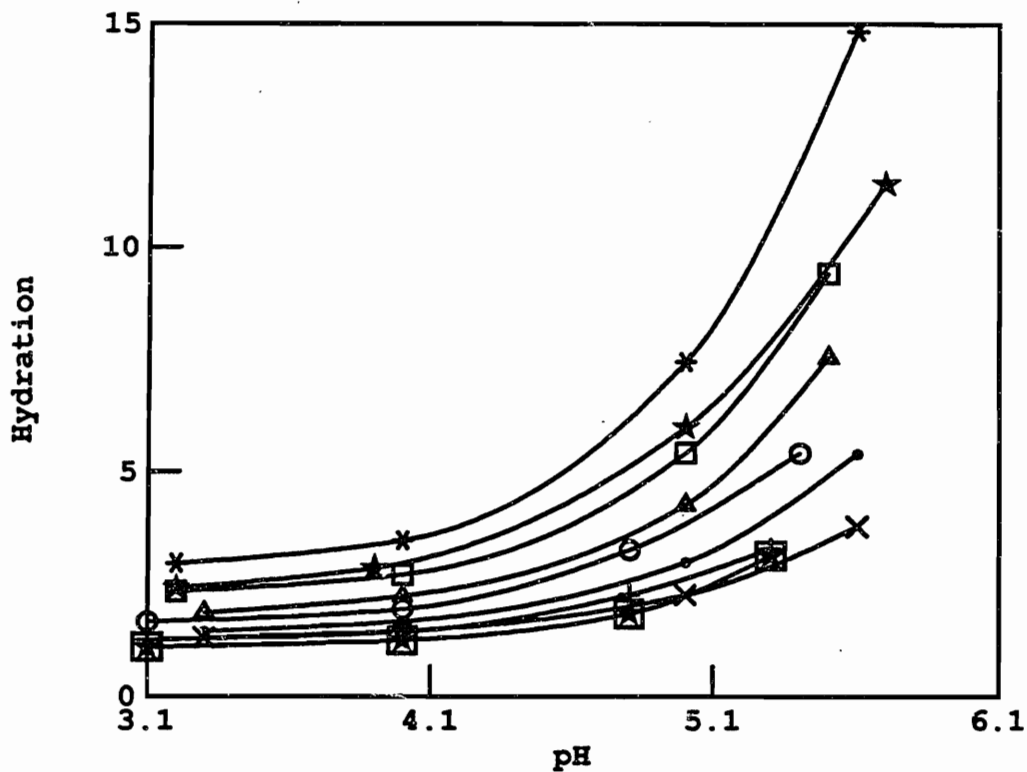
4.1 Hydration vs. pH

Figure 4.1 compares the results of the hydration experiments for each membrane formulation. As pH increases, hydration steadily increases for each membrane. At a given pH, the more heavily crosslinked the membrane, the lower the hydration, confirming that the crosslinks do indeed restrict membrane swelling. Similarly, the greater the volume fraction of polymer at the time of casting, the lower the hydration at a given pH. For the two membranes having the least (S.05/1) and greatest (S.6/1) amount of crosslinker, the hydration differs by a factor of 4 at pH5.4.

4.2 Errors and Membrane Homogeneity

The hydrations given in Figure 4.1 are actually the mean hydrations for each disc. Furthermore, to avoid cluttering the figure, error bars are omitted. The error bars are shown in Figure 4.2; they refer to inconsistencies in the multiple weight measurements ($\% \text{ error} = (\text{s.d.}/\text{mean}) * 100$). The errors in the weight measurements are no greater than 8.2%, with all but 3 weight errors no greater than 3.5% (Table 3.2 shows the mean weights and s.d.'s for each disc except the S.2/1, S.4/1, and S.6/1 discs.). The error bars in all subsequent figures refer to this measurement error. Table 4.1 lists the mean hydration, standard deviation, and percent error for each disc. In calculating the means and standard deviations for the S.2/1, S.4/1, and S.6/1 discs, the mean weights (including dry weights) for every disc were used (total number of discs: S.2/1:11, S.4/1:3, S.6/1:3). The mean hydration and standard deviation for each individual S.2/1, S.4/1, and S.6/1 disc is not shown in Table 4.1. No hydration measurement error is greater than

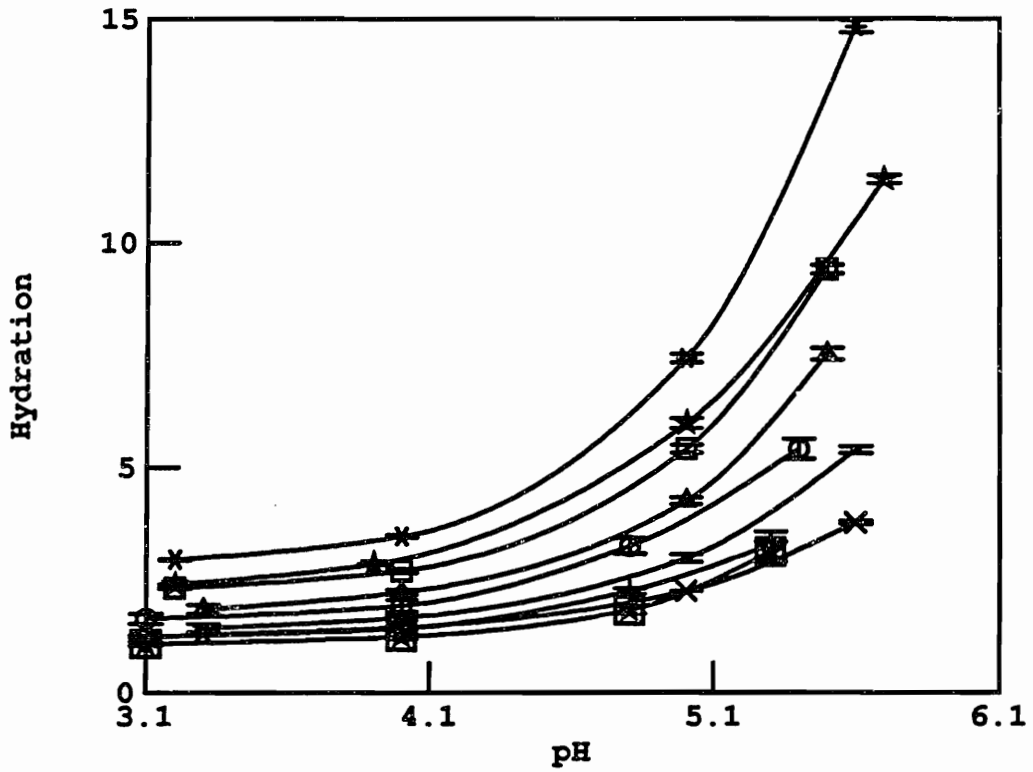
Membrane Hydration vs. pH



S.05/1:aster S.1/2:stars S.1/1:squares
S.2/2:triangles S.2/1:circles S.4/2:dots
S.4/1:plus S.4/.5:cross S.6/1:boxed stars

Figure 4.1: Hydration vs. pH for each membrane, without error bars. At a given pH, hydration increases with decreasing crosslink density.

Membrane Hydration vs. pH



S.05/1:aster S.1/2:stars S.1/1:squares
S.2/2:triangles S.2/1:circles S.4/2:dots
S.4/1:plus S.4/.5:cross S.6/1:boxed stars

Figure 4.2: Hydration vs. pH for each membrane, with error bars.

Table 4.1: Mean hydrations for each disc. For the S.2/1, S.4/1, S.6/1 hydrations, all intra and intermembrane discs were used in calculating mean hydration and standard deviation.

mem	pH	mean	s.d.	%error	mem	pH	mean	s.d.	%error
S.05/1	3.2	2.9651	0.0102	0.34	S.4/2	3.3	1.4533	0.0957	6.59
	4.0	3.4745	0.0264	0.76		4.0	1.6781	0.0602	3.60
	5.0	7.4336	0.0894	1.20		5.0	2.9882	0.0785	2.63
	5.6	14.8332	0.1371	0.85		5.6	5.3828	0.0828	1.23
	5.2	9.0166	0.2066	2.29		5.2	3.5111		
	4.0	3.8390	0.0526	1.37		4.0	1.7477		
	3.2	2.9101	0.0572	1.97		3.2	1.3724		
S.1/2	3.2	2.4203	0.0055	0.23	S.4/1	3.1	1.2628	0.0269	2.13
	3.9	2.8621	0.0105	0.37		4.0	1.4442	0.0403	2.79
	5.0	5.9809	0.1124	1.88		4.8	2.2704	0.0605	2.66
	5.7	11.4134	0.0936	0.73		5.35	3.2847	0.2888	8.79
	5.2	7.1461	0.0612	0.86		4.9	2.6533	0.0269	1.01
	4.0	3.0967	0.0211	0.68		4.0	1.5181	0.0403	2.65
	3.2	2.3776	0.0433	1.82		3.2	1.2830	0.0403	3.14
S.1/1	3.2	2.3389	0.0208	0.89	S.4/.5	3.3	1.3104	0.0160	1.22
	4.0	2.7176	0.0473	1.74		4.0	1.4665	0.0237	1.62
	5.0	5.4159	0.0858	1.58		5.0	2.2658	0.0103	0.45
	5.5	9.4066	0.0979	1.04		5.6	3.7711	0.0302	0.80
	5.2	6.5568	0.0553	0.84		5.1	2.6855	0.0283	1.05
	4.0	2.9071	0.0119	0.41		4.0	1.5446	0.0342	2.22
	3.2	2.2662	0.1219	5.39		3.2	1.2940	0.0377	2.91
S.2/2	3.3	1.8662	0.0917	4.92	S.6/1	3.1	1.1007	0.0393	3.57
	4.0	2.2401	0.0588	2.62		4.0	1.2579	0.0655	5.21
	5.0	4.2618	0.0769	1.81		4.8	1.8476	0.0917	4.96
	5.5	7.5260	0.1315	1.75		5.35	3.1317	0.2228	7.11
	5.1	5.3311	0.0600	1.13		5.0	2.2210	0.1048	4.72
	4.0	2.4770	0.0376	1.52		4.0	1.3103	0.0721	5.50
	3.2	1.9728	0.0501	2.54		3.2	1.1138	0.0590	5.30
S.2/1	3.1	1.6625	0.1108	6.66					
	4.0	1.9475	0.1267	6.51					
	4.8	3.2617	0.1742	5.34					
	5.4	5.4071	0.2217	4.10					
	4.9	3.8238	0.2058	5.38					
	4	2.0108	0.1346	6.69					
	3.1	1.6783	0.1188	7.08					

10.33%, with all but 3 errors $\leq 6.59\%$.

For most of the hydration experiments, only a small portion of one membrane was used to determine the hydration for that membrane formulation as a whole. The question is: If the disc was cut from a different region of the same membrane or from an entirely different membrane of the same formulation, would its hydration be different, and if so, how much? To answer this question, hydration experiments were performed to determine the homogeneity between different membranes from the same formulation batch (intermembrane) as well as between regions within one membrane (intramembrane). 5 discs were cut from mem.3 from an S.2/1 batch and 3 discs each were cut from mem.1 and mem.2 from the same S.2/1 batch. 3 discs were also cut from different regions of one S.4/1 and one S.6/1 membrane.

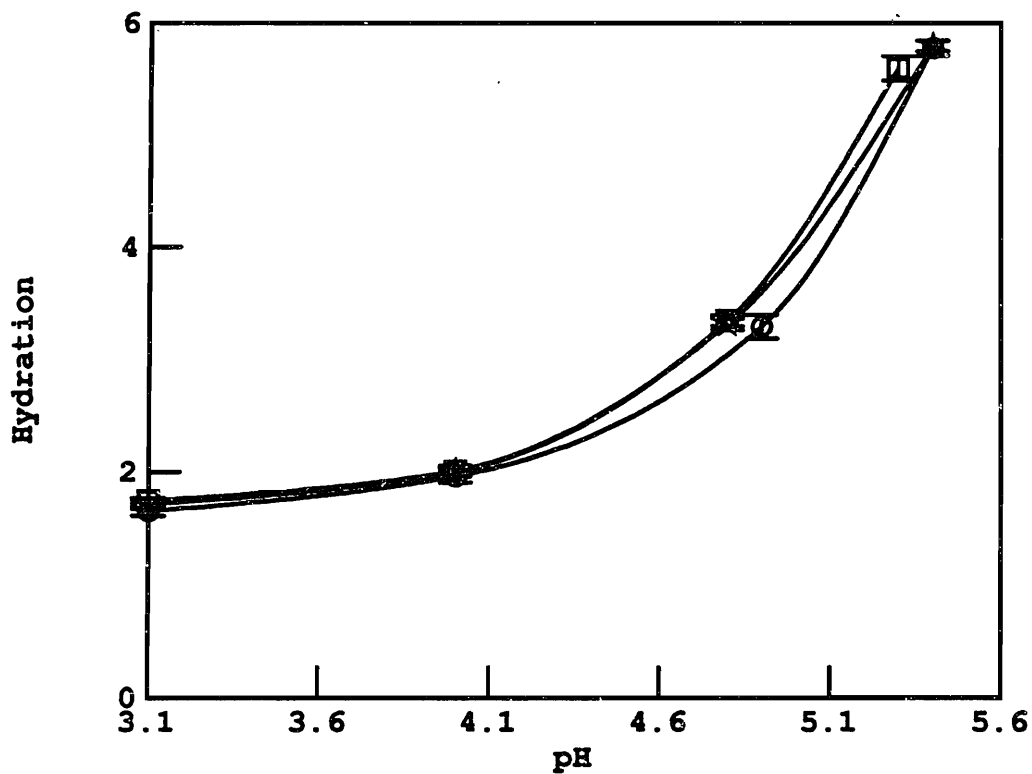
The hydration experiments showed little variation between different regions of the same membrane and between different membranes from the same formulation batch. This is an important result since the membrane used in the corresponding transport experiment was not the same as that used in the hydration experiment. * To later make legitimate comparisons between the hydration and transport data, it is important that the membranes be homogeneous both within a single membrane and from membrane to membrane within the same batch. The percent errors $((s.d./mean)*100$, using mean of discs from each S.2/1 membrane, i.e., the mean of the 3 discs (using mean of each disc) from mem1 (Figure 3.1), the mean of the 3 discs from mem2, and the mean of the 5 discs from mem3 were compared.) in intermembrane hydration are all $\leq 2.55\%$, no greater than the measurement errors (Figure 4.3).

Although only the hydration measurements are appropriate for

*Due to the fragility of the membranes it was necessary to use 5 mil membranes for the hydration experiments. Ideally, the membrane used in the corresponding transport experiment would be the same membrane from which the hydration disc was cut. Instead, since the diffusion time constant is proportional to the square of the membrane thickness, 3 mil membranes were used in the transport experiments.

Membrane Hydration vs. pH (Inter S.2/1)

Middle plug from each mem. in S.2/1



S.2/1, Mem1, M: circles S.2/1, Mem2, M: squares

S.2/1, Mem3, M: stars

Figure 4.3: Hydration vs. pH for intermembrane discs (S.2/1), with error bars

intermembrane comparisons (Section 3.2), all three measurements (weight, diameter, and hydration) reveal the homogeneity within a single membrane. The percent errors in intramembrane weights are all $\leq 6.26\%$, again well within the experimental weight measurement errors. The percent errors in intramembrane diameters are all $\leq 3.01\%$ (Figure 4.4). Intramembrane hydration, with error bars, is shown in Figure 4.5. Intramembrane % error was calculated by finding the mean and s.d. for the discs within one membrane (using the mean measurement for each disc). The largest intramembrane hydration error is 8.8%.

The hydration data taken twice at each pH, once during the ascending pH sequence and again during the descending sequence, indicate that the swelling process is essentially reversible. Figure 4.6 shows weight vs. ascending pH and descending pH for an S.2/1 membrane. At a given pH, the ascending weight is slightly greater than the descending weight. This figure is representative of the results obtained for the other membrane formulations as well. The percent differences between ascending and descending weights, measured at the same pH, are no greater than 14.60%, with all but 5 differences $\leq 3.60\%$. The diameter data support the conclusion that membrane swelling is largely reversible (Figure 4.7). The percent differences between ascending and descending diameters are $\leq 6.25\%$, with all but 5 differences $\leq 3.64\%$.

As a bonus, the data provide a test for isotropic swelling by comparing weights to diameters. If the membrane swells isotropically, the ratio of swollen weight to base weight should be equal to the the ratio of swollen to base diameter. The differences between W/W_o and $(d/d_o)^3$ are $\leq 34.26\%$, with all but 3 errors $\leq 17\%$. Figure 4.8 shows W/W_o vs. $(d/d_o)^3$ for four membranes.

4.3 Transport Results

Transport experiments were carried out on nine membrane formulations using two neutral fluorescent solutes: Lis-dex (MW 10,000) and NSPA (MW 301)

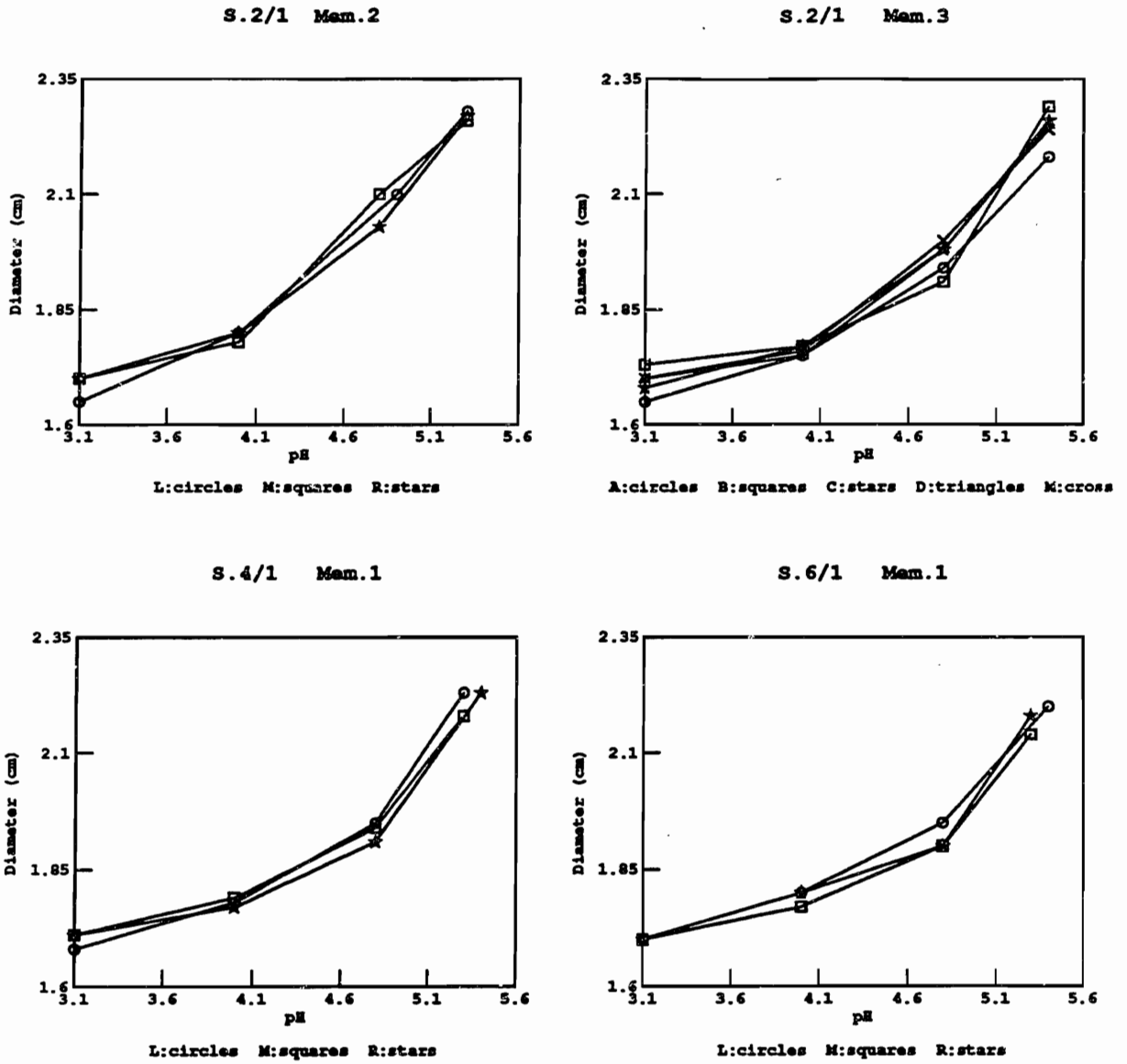


Figure 4.4: Diameter vs. pH for intramembrane discs. See Chapter III for definition of A, B, C, D, L, M, R.

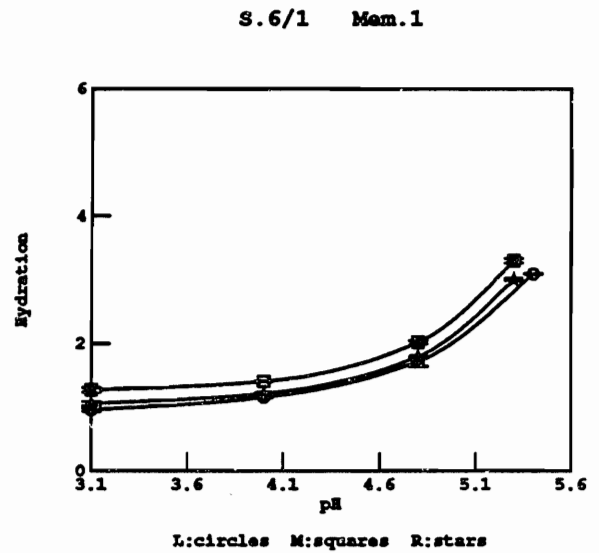
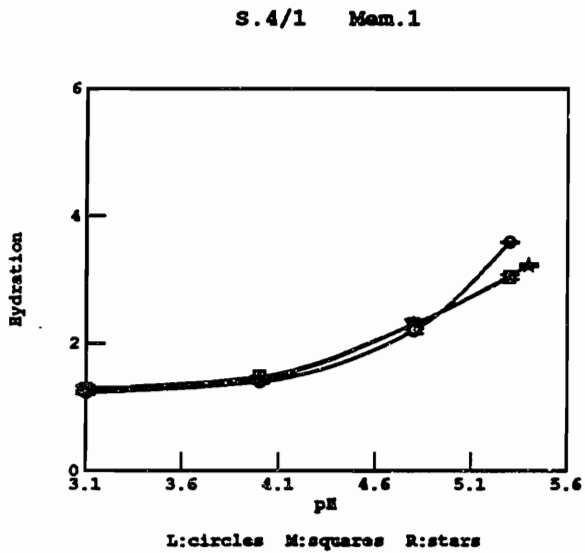
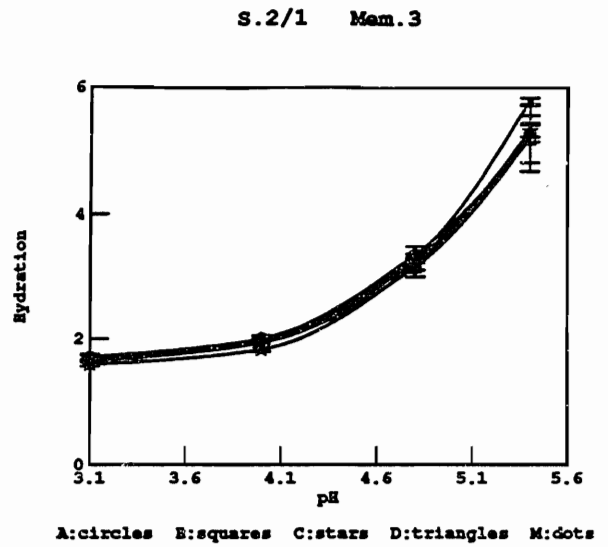
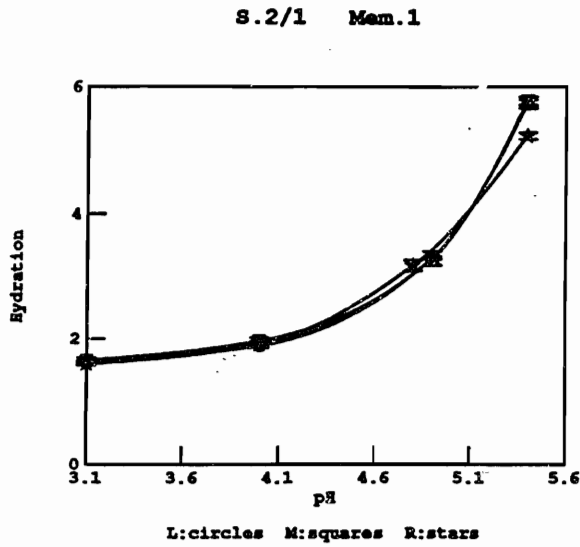


Figure 4.5: Hydration vs. pH for intramembrane discs, with error bars. See Chapter III for definition of A, B, C, D, L, M, R.

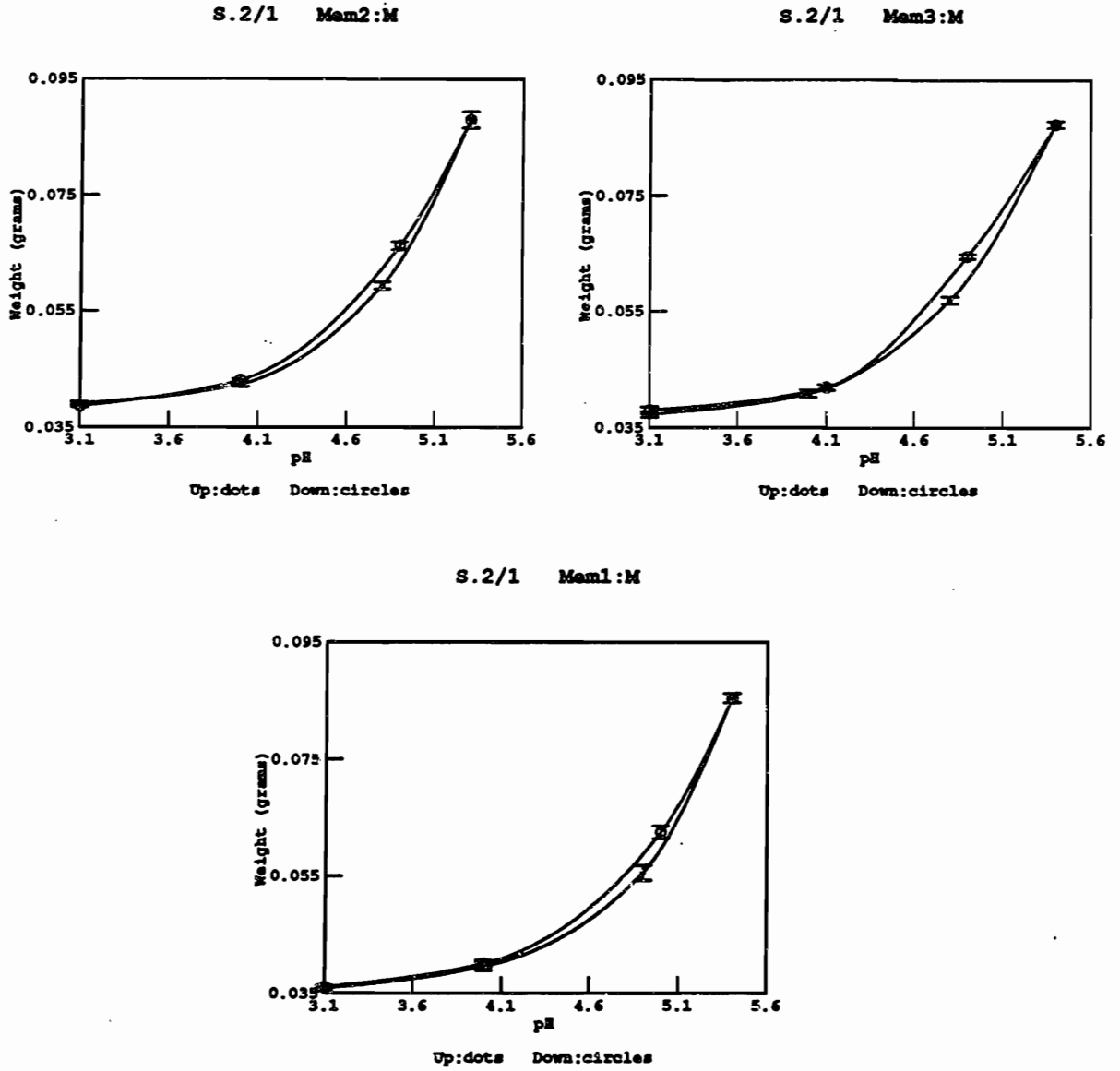


Figure 4.6: Weight at ascending pH vs. weight at descending pH for 3 discs, with error bars.

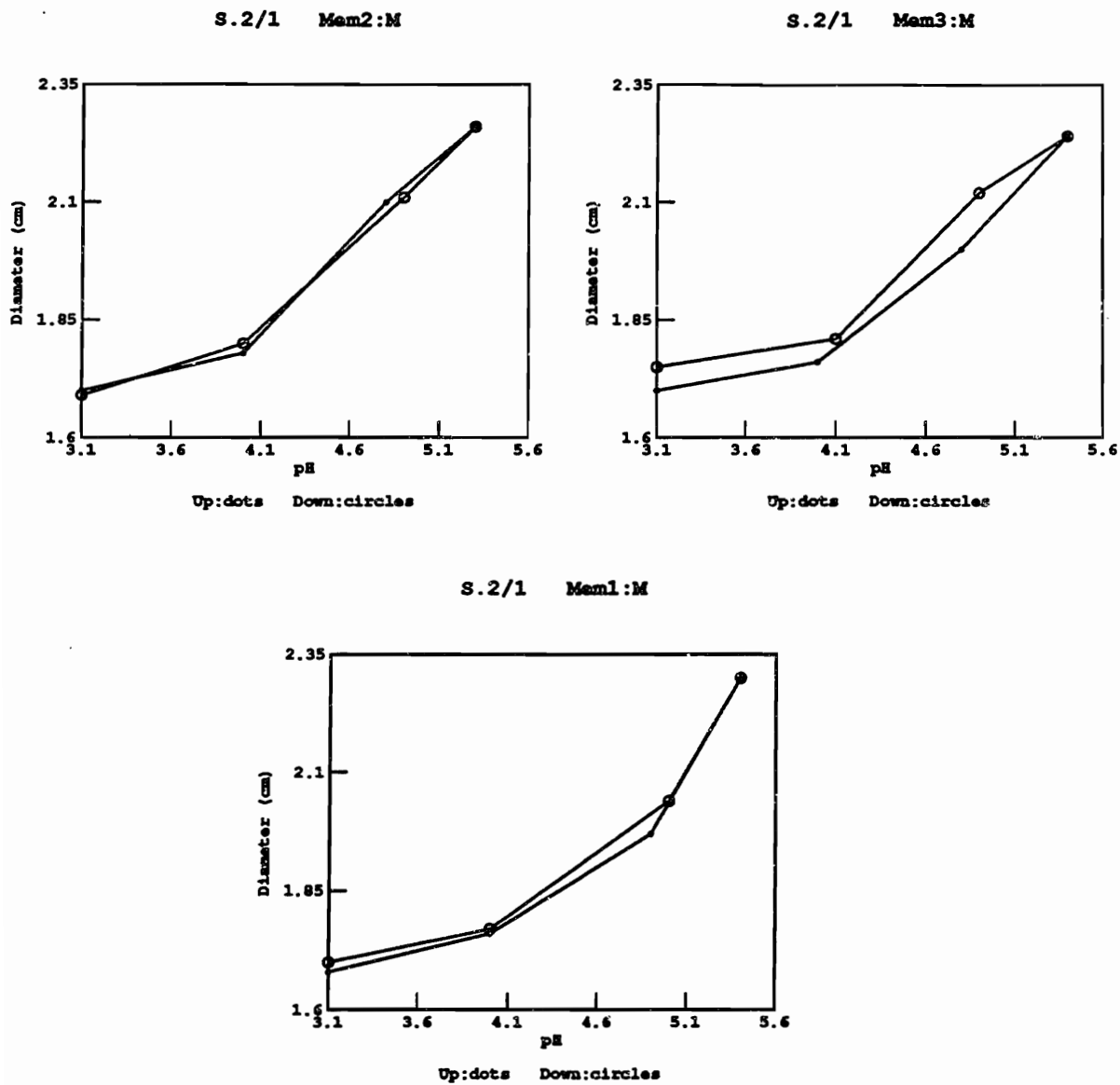


Figure 4.7: Diameter at ascending pH vs. diameter at descending pH for 3 discs.

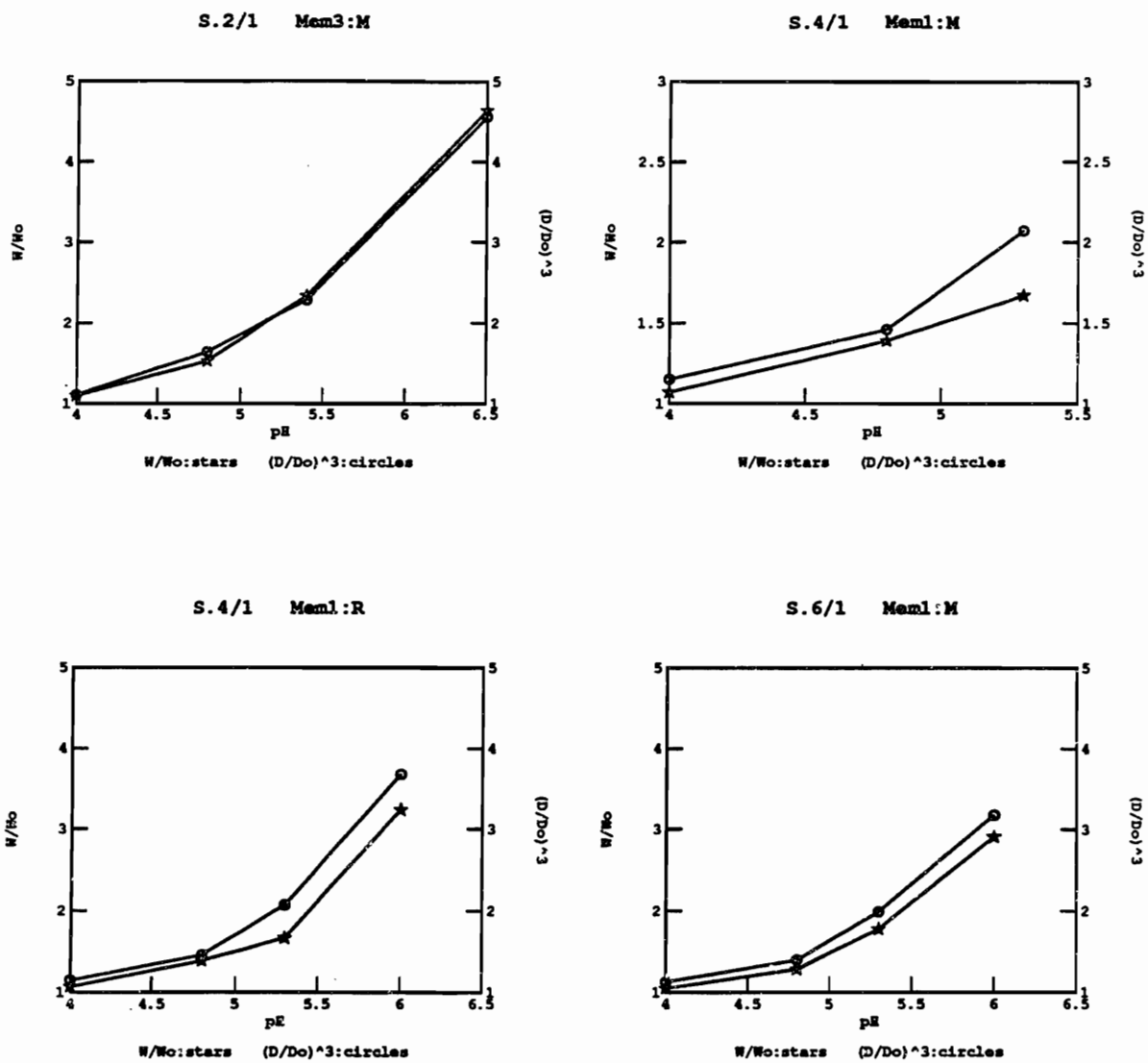


Figure 4.8: W/W_o vs. $(d/d_o)^3$, showing isotropic swelling.

(Table 3.5). The membrane compositions vary in the percentage of crosslinker and the volume fraction of polymer added at the time of casting. These two parameters control the average mesh size in the membrane, the mobility of the polymer chains, and the membrane's swelling properties. Dual-tracers were used in order to shed some light on the "sieving effect" which presumably would only hamper the transport of the larger solute.

Figure 4.9 shows the raw data from a typical transport experiment (S.1/1 membrane). At the starting pH of 4.5, transport of Lis-dex to the downstream side was observed about 30 minutes after its addition to the upstream side. Upon lowering the pH to 3 by addition of HCl to both sides of the membrane, Lis-dex flux decreased considerably. Raising the pH to 5.5 resulted in an increase in flux greater than that at pH4.5. The effects of pH on the transport of NSPA were not nearly so dramatic. At pH4.5, NSPA dye appeared on the downstream side a few minutes after adding it to the upstream side. The subsequent pH changes altered the NSPA flux only slightly in comparison to the Lis-dex flux. The calibrations (Section 3.3.2), performed once at the beginning of the experiment and again before each pH change (except pH3), are also shown in Figure 4.9.

Using equation 3.4, the permeability was calculated for each pH using the slope from the steady-state portion of the corresponding pH section of the fluorescent intensity curve in Figure 4.9. Table 4.2 lists the permeabilities for Lis-dex and NSPA.

Figure 4.10 is data from one transport experiment performed on an S.4/.5 membrane, one of the more heavily crosslinked membranes. At pH3, the membrane was closed[†] to Lis-dex ($P=2.25e-9 \pm 6.4e-9$ cm/sec), whereas the permeability to NSPA ($P=.87e-4$ cm/sec) was relatively large. At pH5.5, the permeability to Lis-dex increased quite dramatically (by a factor of 58 if the upper

[†]The downstream Lis-dex concentration curve looked horizontal to the eye. Due to the noise, however, there was a large uncertainty (relatively large error bars: $\pm 6.4e-9$) in the calculated slope of $2.25e-9$ cm/sec.

Normalized downstream concentration of Lis-dex & NSPA

Raw data from chart recorder

S.1/1

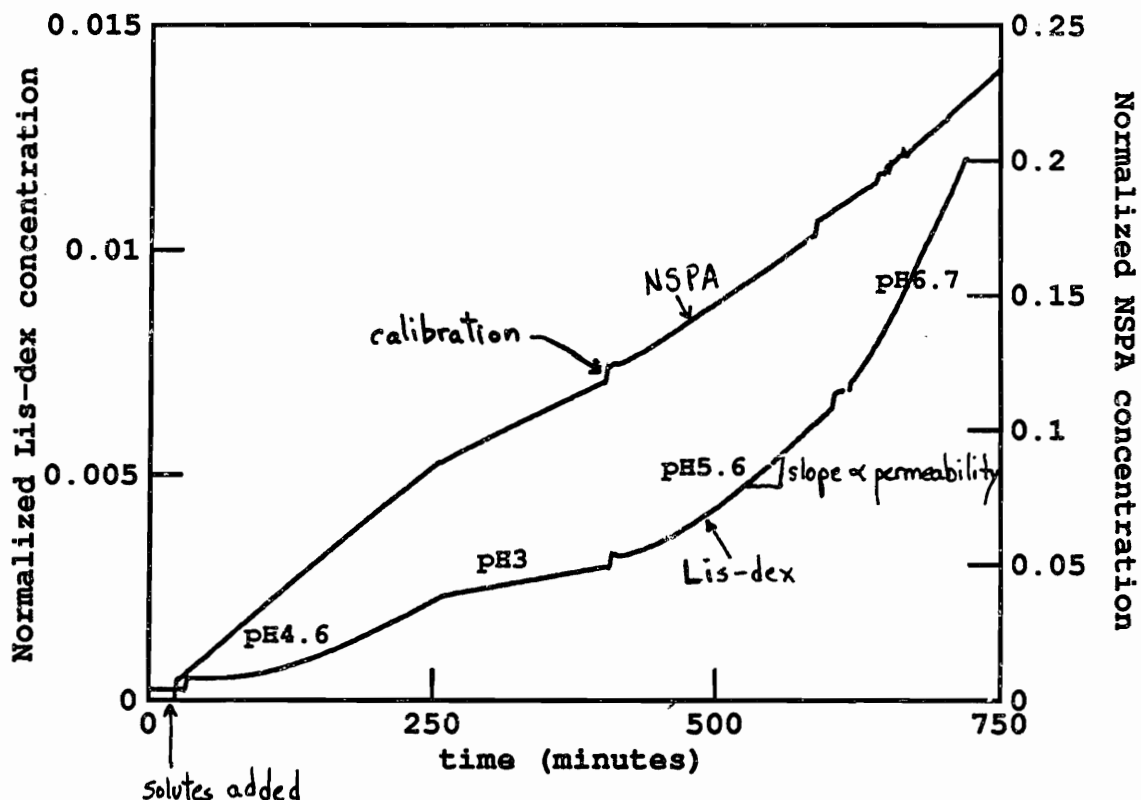


Figure 4.9: Raw transport data for Lis-dex and NSPA from chart recorder, showing downstream normalized concentration of both solutes. Prior to $t=0$, the membrane had been preconditioned by cycling from low pH to high pH and back to low pH, following which the solutes were added.

Table 4.2: Lis-dex and NSPA permeabilities for each membrane formulation at each pH. pH's are given in the same order in which they occurred in the corresponding transport experiment. *No transport: concentration curve looked horizontal to the eye.

mem	pH	Lis-dex permeability	NSPA permeability
S.05/1	4.6	8.55e-6 +/- 1.4e-8	7.5e-5
	3	8.0e-6 +/- 2.3e-7	9.25e-5
	5.75	1.61e-5 +/- 1.35e-7	9.55e-5
S.1/2	4.6	6.2e-6 +/- 5.3e-8	1.42e-4
	3	5.2e-6 +/- 4.8e-8	1.263e-4
	5.45	1.03e-5 +/- 6.0e-8	1.185e-4
	4.6	6.5e-6	7.25e-5 +/- 1.9e-5
	3	5.4e-6	9.85e-5
S.1/1	4.6	4.68e-6 +/- 11e-9	8.8e-5
	3.15	1.5e-6 +/- 9.6e-8	6.8e-5
	5.55	7.14e-6 +/- 5e-8	1.05e-4
	6.7	1.85e-5 +/- 7.8e-8	1.34e-4
S.2/2	4.7	5.04e-6 +/- 4.6e-8	9.28e-5 +/- 1.8e-6
	3	2.6e-6 +/- 3.2e-8	9.45e-5 +/- 1.6e-5
	5.45	8.54e-6 +/- 6.4e-8	9.85e-5 +/- 8.0e-6
	4.6	5.56e-6 +/- 11.8e-8	8.3e-5
S.2/1	4.6	1.34e-6 +/- 4.7e-8	6.7e-5
	3	3.88e-7 +/- 4.4e-8	6.8e-5
	5.6	2.48e-6 +/- 4.4e-8	9.13e-5
	4.55	1.2e-6 +/- 1.8e-8	7.74e-5
S.4/2	4.6	1.13e-6 +/- 1.5e-8	1.025e-4 +/- .04e-4
	3	5.58e-7 +/- 1.25e-8	8.9e-5 +/- 2e-6
	5.45	2.36e-6 +/- 2.3e-8	9.85e-5
	4.6	1.65e-6 +/- 3.0e-8	8.7e-5 +/- 2e-5
S.4/1	4.65	1.97e-7 +/- 6.1e-9	5.3e-5
	3.1	5.6e-8 +/- 5.7e-9	6.55e-5
	5.6	6.57e-7 +/- 1.4e-8	7.2e-5 +/- 1.3e-5
S.4/.5	4.6	2.69e-8* +/- 3.1e-9	6.2e-5
	3	2.25e-9* +/- 6.4e-9	4.35e-5 +/- 2.4e-5
	5.5	5.15e-7 +/- 2.4e-8	7.9e-5
	4.6	8.34e-8* +/- 4.7e-8	6.3e-5 +/- 4e-6
	3	1.975e-8* +/- 2.04e-8	4.62e-5
S.6/1	4.6	5.4e-9* +/- 3.9e-9	3.405e-5 +/- 6e-7
	3	6.6e-9* +/- 3.3e-9	2.635e-5
	5.5	6.4e-9* +/- 2.1e-9	4.75e-5
	3	no transport	2.61e-5
	7	1.0e-6 +/- 8.7e-8	8.25e-5

error bar is used for the pH3 permeability ($P=8.65e-9$ cm/sec), by a factor of 200 if the mean pH3 permeability ($P=2.25e-9$ cm/sec) is used) whereas the permeability to NSPA remained fairly constant ($P=1.6e-4$ cm/sec). This demonstrates the selectivity of this membrane, which can be made either open or closed to Lis-dex, while remaining open at all times to NSPA.

In contrast, Figure 4.11 is data from one transport experiment performed on an S.05/1 membrane, the most lightly crosslinked membrane. The membrane is essentially open to both Lis-dex and NSPA regardless of pH. While the permeability to Lis-dex does increase at the higher pH (by 101.3%, from $P=8.0e-6$ to $P=1.6e-5$ cm/sec), the effect is not nearly as pronounced as it is with the more heavily crosslinked membrane, S.4/.5.

Figures 4.12 and 4.13 show the permeability to Lis-dex for each membrane at each pH, with and without error bars. Each error bar is the standard deviation in the straight line fit to the corresponding steady state slope of the concentration curve (Figure 4.9). These data show the effect of crosslink density on permeability. At a given pH, as the crosslink density increases, the permeability to Lis-dex decreases.

As seen in Figure 4.14, by no means had the permeability to Lis-dex reached its upper limit at pH5.5 (The S.1/1 permeability increased by 140% from pH5.5 to pH6.7. For the S.6/1 membrane, no transport was even seen at pH5.5). Although two membranes do not constitute an extensive data set, it is reasonable to conclude that the permeabilities of the other membranes would also increase at pH 6 or 7 †. In other transport experiments performed in this lab [Grimshaw et al.(1988)], the pH was raised from pH3 to pH7. The resulting Lis-dex permeability changes were greater than the changes induced in the experiments in this thesis.

†Some of the membranes may become brittle at such high pH's. The S.6/1 membrane tore \approx 1 hour and 20 minutes after the pH had been raised to pH7, before the flux had reached a steady state. Had the membrane remained intact, the permeability would have increased beyond $1.025e-6$ cm/sec.

Membrane Permeability vs. pH

S.4/.5 Membrane (2.67% crosslinker (by volume))

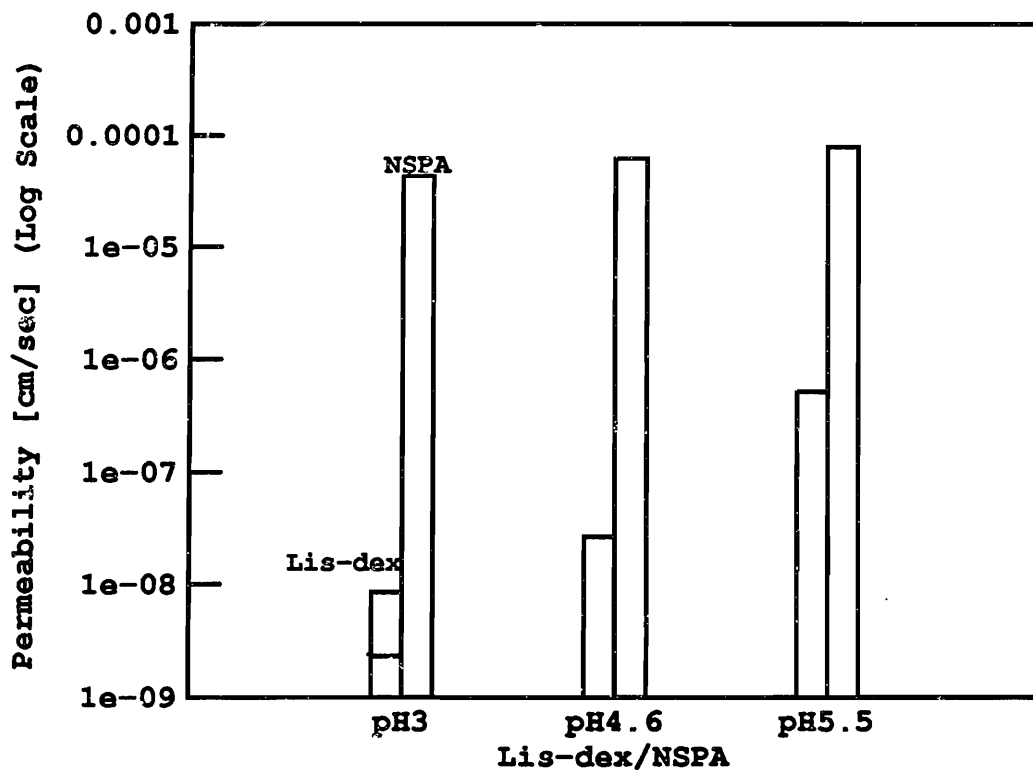


Figure 4.10: Results from transport experiment on S.4/.5 membrane, comparing Lis-dex and NSPA permeabilities. The change in Lis-dex permeability with pH is significant. The higher Lis-dex pH3 bar is the permeability using the upper error bar ($P=8.65e-9$ cm/sec); the shorter bar is the mean permeability ($P=2.25e-9$ cm/sec).

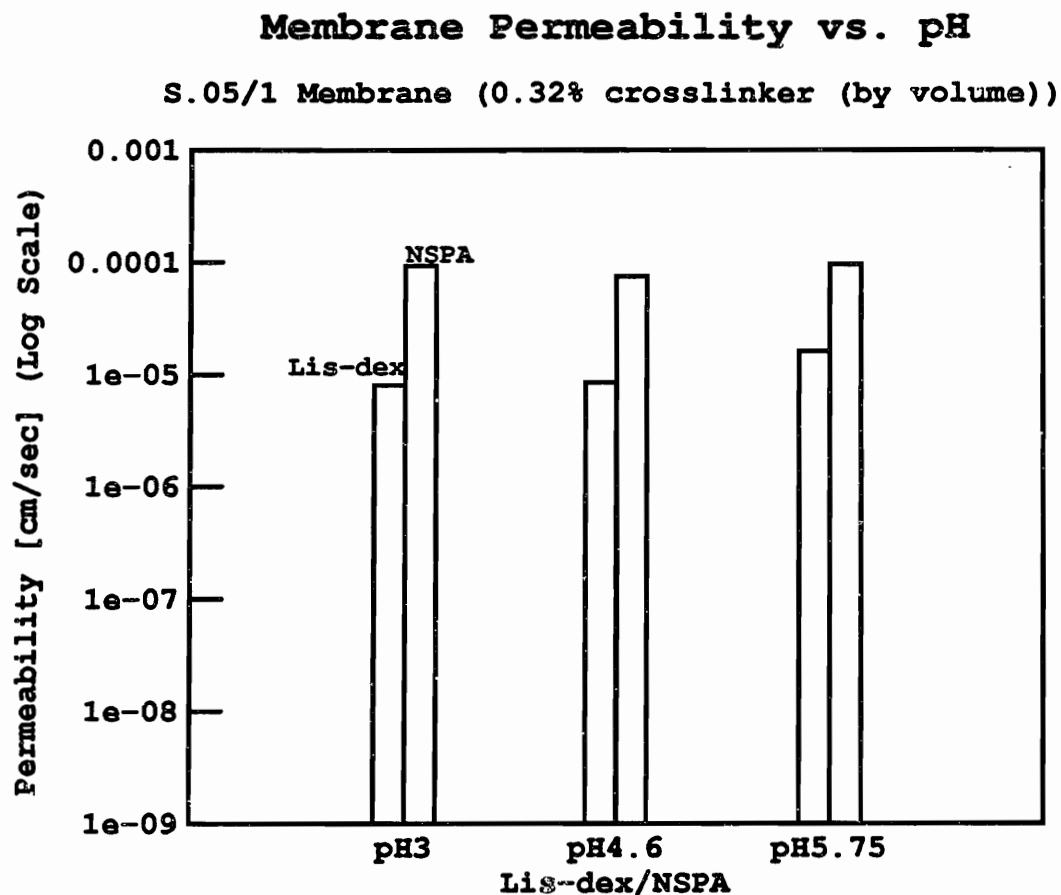
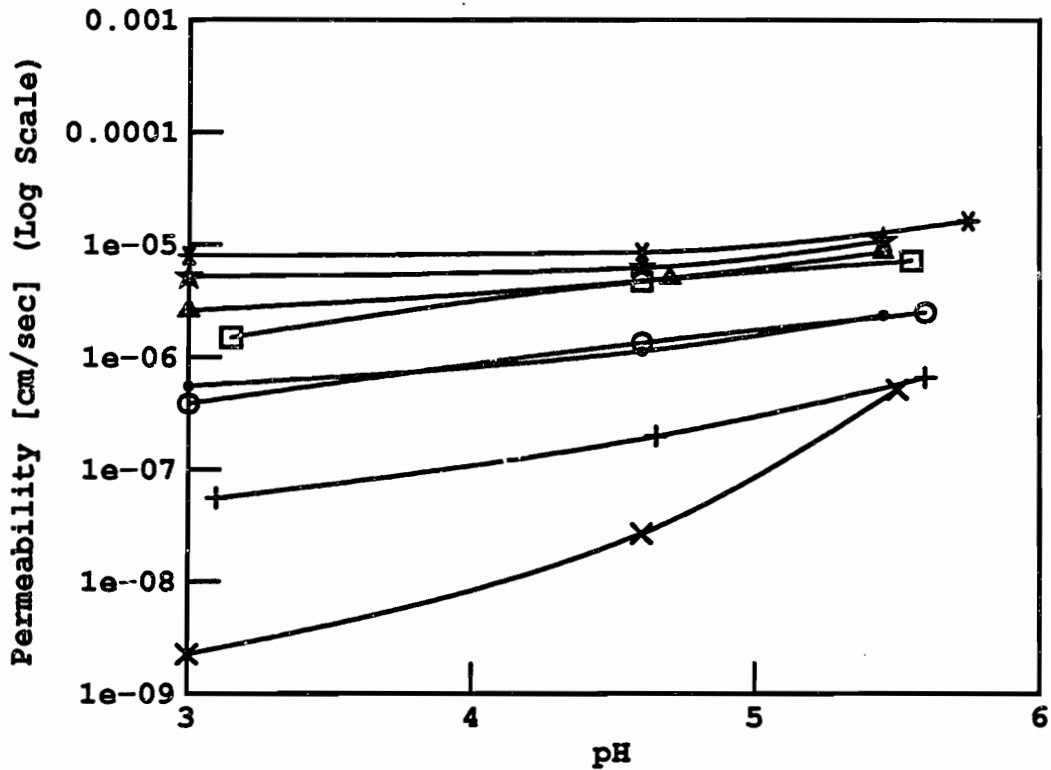


Figure 4.11: Results from transport experiment on S.05/1 membrane, comparing Lis-dex and NSPA permeabilities. The membrane is essentially open to both solutes.

Membrane Permeability to Lis-dex vs. pH



S.05/1:aster S.1/2:stars S.1/1:squares

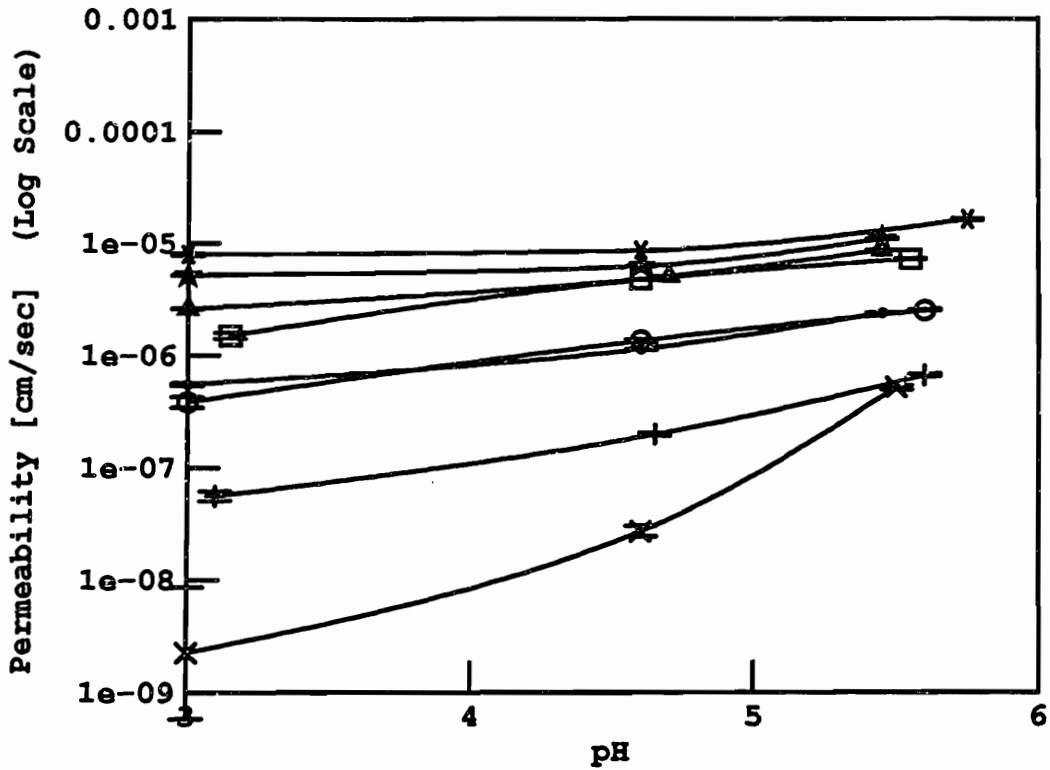
S.2/2:triangles S.2/1:circles S.4/2:dots

S.4/1:plus S.4/.5:cross

Figure 4.12: Permeability vs. pH for Lis-dex (log scale). At a given pH, permeability increases with decreasing crosslink density.

Membrane Permeability to Lis-dex vs. pH

With error bars



S.05/1:aster S.1/2:stars S.1/1:squares

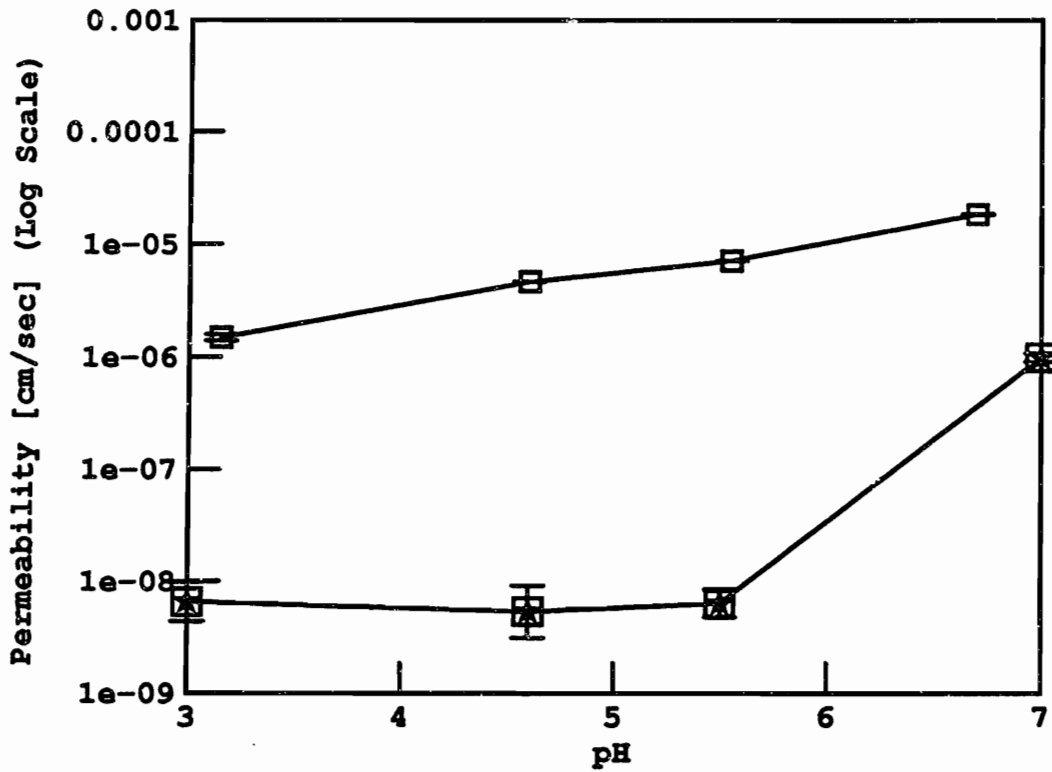
S.2/2:triangles S.2/1:circles S.4/2:dots

S.4/1:plus S.4/.5:cross

Figure 4.13: Permeability vs. pH for Lis-dex, with standard deviation error bars.

Membrane Permeability to Lis-dex vs. pH

Up to pH7



S.1/1:squares S.6/1:boxed stars

Figure 4.14: Permeability vs. pH for Lis-dex, up to pH6.7 and pH7. These were the only experiments in which the pH was raised beyond pH5.5.

Table 4.3: Percent changes in hydration and permeability compared to percentage crosslinker. % crosslinker = (vol TEGDMA /total vol)*100. % change in permeability = (perm@pH5.5-perm@ pH3)/(perm@pH3). % change in hydration = (hyd@pH5.5-hyd@pH3)/ (hyd@pH3). *Using upper error bar (P=8.65e-9 cm/sec). If the mean permeability (2.25e-9) is used, then % change in perm=22,789.

mem	% xlinker(by vol)	% change in perm	% change in hyd
S.05/1	0.32	101	400
S.1/2	0.56	108	372
S.1/1	0.64	376	302
S.2/2	1.12	228	303
S.2/1	1.27	539	225
S.4/2	2.22	323	270
S.4/1	2.50	1073	160
S.4/.5	2.67	5854*	188
S.6/1	3.70	no transport	184

Membrane permeability to Lis-dex differs by more than three and a half orders of magnitude, at the lower pH's, for the two membranes having the least (S.05/1) and greatest (S.4/.5) percentage of crosslinker (by volume).⁵ The S.4/.5 membrane has only eight times as much crosslinker (2.67% crosslinker, by volume, as opposed to 0.32%) as the S.05/1 membrane. More significantly, at a given pH, the ordering of the various membrane compositions with respect to increasing permeability is essentially the same as the ordering with respect to increasing hydration (Figure 4.1). The ordering is from the membrane with the greatest to that with the least percentage of crosslinker. The membranes with the lowest pH3 permeability (highest percentage of crosslinker) underwent the largest percent change in permeability at pH5.5. (Table 4.3). The converse is found for the hydration data in which the most loosely crosslinked membrane underwent the largest percent change in hydration.

Buried in this data is the dependence of permeability on hydration. At a

⁵The S.6/1 membrane actually has the greatest percentage of crosslinker. However, no Lis-dex transport was seen with this membrane.

given pH, each membrane is *not at the same hydration*. To separate crosslink effects from hydration effects, the permeability should be plotted as a function of hydration. This is done in Section 6.5.2.

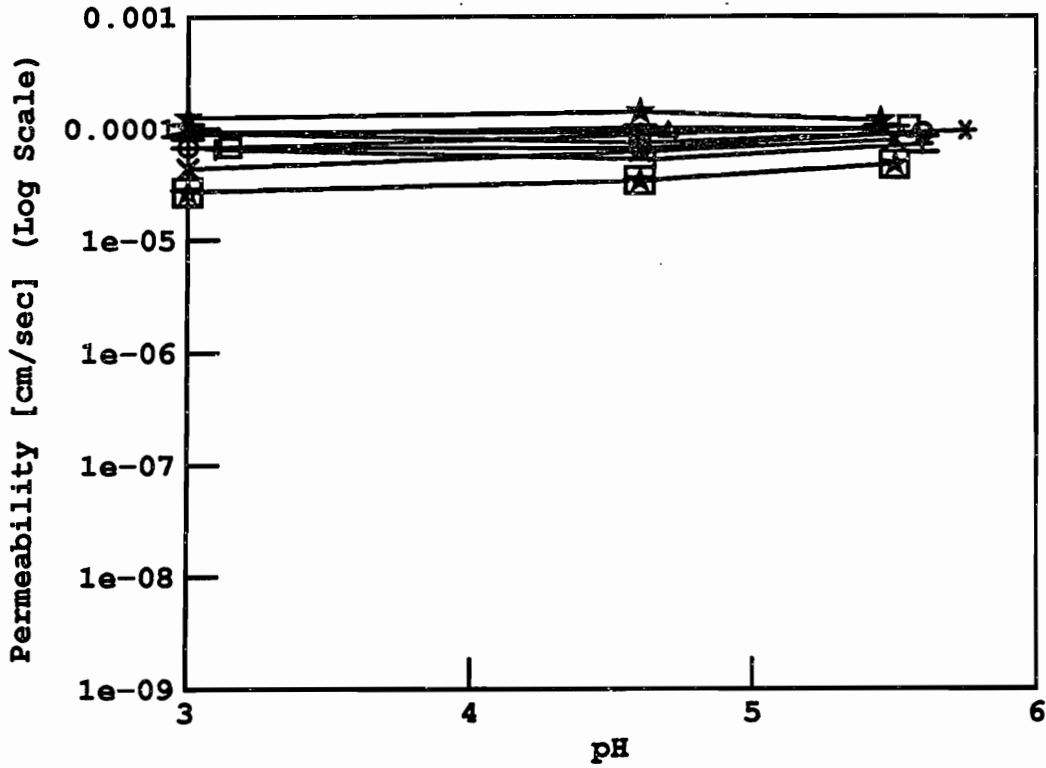
In sharp contrast to the Lis-dex permeability data, the NSPA permeability data of Figure 4.15 reveals rather modest differences in permeability from membrane to membrane, with no apparent ordering of the membrane compositions. The membranes are all open to NSPA regardless of crosslink density.

Not only are there no clear trends exhibited by the NSPA data but, for some membranes, there is a disturbing decrease, albeit small, in permeability with increasing pH. As mentioned earlier (Section 3.3.2), at times during the transport experiments unknown absorption effects were observed. These effects were attributed to pH sensitive NSPA binding to either the plastic tubing or pump filter or both. An increase in pH was accompanied by a loss of solute and vice versa. This effect was also observed with Lis-dex, although to a lesser extent.

The NSPA data of Figure 4.15 suggest that changes in permeability, with respect to pH for a given membrane and with respect to membrane composition for a given pH, are insignificant compared to apparent changes in solute flux due to NSPA absorption. Further evidence that binding has a substantial effect on the NSPA concentration on the downstream side is provided by the calibrations, shown in Figure 4.9. Within a single experiment, Lis-dex calibrations at different pH's are fairly consistent (The largest change is 25.8%; most are less than 13%), whereas NSPA calibrations vary by as much as 390%, with most varying by more than 30%.

In all cases, returning the bath pH to lower previous values caused a reversal in permeability, toward the permeability obtained at the first occurrence of that pH. Although the reverse permeability was always greater than the original permeability (Table 4.2), this is attributed to insufficient equilibration time at

Membrane Permeability to NSPA vs. pH



S.05/1:aster S.1/2:stars S.1/1:squares
S.2/2:triangles S.2/1:circles S.4/2:dots
S.4/1:plus S.4/.5:cross S.6/1:boxed stars

Figure 4.15: Permeability vs. pH for NSPA (log scale). There is no ordering of the membranes with respect to crosslinker.

each pH rather than to irreversibility. Had the experiments run longer[†], the permeability would have increased during the ascending pH sequence and decreased during the descending pH sequence; eventually, the two permeabilities would have converged to the same value.

[†]As it was, some experiments ran for close to 20 hours.

Chapter V

Theory

The free volume theory originated as a model for self-diffusion in a one-component system [Cohen and Turnbull,(1959)]. The model was later extended to two-component solvent-polymer systems [Fujita, (1961)], and then to homogeneous three-component systems consisting of a solute diffusing through the solvent in a highly swollen polymer network [Yasuda,(1969)].

5.1 One-Component System

Cohen and Turnbull (1959) developed a model for liquid self-diffusion (gradients in labelled molecules but no true concentration gradients) based on the free volume, v_f , within the liquid. The liquid molecule is viewed as a hard sphere confined to a cage defined by its neighbors. Occasionally, thermal fluctuations will redistribute the free volume of the liquid in such a way as to enlarge a molecule's cage enough to allow it to be displaced within its cage. Diffusive transport occurs if a neighboring molecule jumps into the space forfeited by the first molecule.

The free volume, v , of one molecule is defined as the volume within its cage minus the volume of the molecule. The diffusion coefficient associated with this molecule is:

$$D(v) = ga(v)u \quad (5.1)$$

where $a(v)$ is the diameter of the cage, g is a geometric factor, and u is the gas kinetic velocity of the molecules. For diffusion of a neighboring molecule to occur, v must be greater than a critical volume v^* . The average diffusion coefficient is:

$$D = \int_{v^*}^{\infty} D(v)p(v)dv \quad (5.2)$$

where $p(v)$ is the probability of finding the free volume of one molecule between v

and $v + dv$:

$$p(v) = \frac{\gamma}{\langle v \rangle} \exp \left[-\frac{\gamma v}{\langle v \rangle} \right] \quad (5.3)$$

where $\langle v \rangle$ is the average free volume (total free volume/total # of molecules) and γ corrects for overlap of the free volumes.

Since $D(v)$ is slowly varying, it is set equal to $D(v^*)$ in order to obtain an expression for D . Then $D = D(v^*)P(v^*)$ where $P(v)$ is the probability of finding a hole of volume greater than v^* :

$$P(v^*) = \int_{v^*}^{\infty} p(v) dv = \exp -\frac{\gamma v^*}{\langle v \rangle} \quad (5.4)$$

The diffusion coefficient is then:

$$D = ga^*u \exp \left[-\frac{\gamma v^*}{\langle v \rangle} \right] \quad (5.5)$$

where a^* is approximately the molecular diameter. Both the average free volume, $\langle v \rangle$, and the gas kinetic velocity, u , vary with temperature.

5.2 Two-Component System

Fujita (1961) extended the Cohen and Turnbull theory to diffusion in a two-component mixture of small solvent molecules and polymeric solids. Interpreting $\langle v \rangle$ as the average fractional free volume, V_f , of the entire two-component system, rather than the average free volume per molecule, Fujita rewrote the probability of finding a hole of volume greater than or equal to B as:

$$P(B) = \exp(-B/V_f) \quad (5.6)$$

where $B = \gamma v^*$.

The mobility of a molecule is related to the probability of it finding a void in its neighbor's cage which is larger than the critical hole size, B^* , needed to

accommodate the diffusing molecule. Fujita assumed the mobility, m_d , to be proportional to this probability:

$$m_d = A_d \exp(-B^*/V_f) \quad (5.7)$$

where A_d depends only on the size and shape of the solvent molecule. A_d and B are neither functions of temperature nor volume fraction of solvent, H_v , in the mixture.

Fujita and Kishimoto (1960) showed that V_f increases in direct proportion to the volume of solvent added to the two-component system. Reasoning that V_f should be a function of temperature and volume fraction of solvent, H_v , they expressed V_f as:

$$V_f(H_v, T) = V_f(0, T) + \beta(T)H_v \quad (5.8)$$

where $\beta(T) = \gamma(T) - V_f(0, T)$ and $\gamma(T)$ is a proportionality factor. By rewriting the above equation as:

$$V_f(H_v, T) = V_f(0, T)(1 - H_v) + \gamma(T)H_v \quad (5.9)$$

it becomes clear that $V_f(0, T)$ and $\gamma(T)$ represent the average fractional free volume in the pure polymer and in the pure solvent, respectively. This expression is identical to that given by Yasuda (1969) (Equation 5.18).

Fujita defined the diffusion coefficient, D , of the solvent as:

$$D = RTm_d \quad (5.10)$$

where R is the gas constant and T is the absolute temperature. The relative diffusivity of the two-component system (the ratio of the diffusivity in the

two-component system to the diffusivity, D_o , in pure water) is then:

$$\frac{D}{D_o} = \exp \left[-B^* \left(\frac{1}{V_f(0, T)(1 - H_v) + \gamma(T)H_v} - \frac{1}{\gamma(T)} \right) \right] \quad (5.11)$$

The solvent molecules are essentially diffusing through the solvent; not through the solid polymer. Hence, the free volume of the system can be approximated by the free volume of the solvent in the system:

$$V_f(H_v, T) \approx \gamma(T)H_v \quad (5.12)$$

The ratio of diffusivities is then:

$$\frac{D}{D_o} = \exp \left[-\frac{B^*}{\gamma(T)} \left(\frac{1}{H_v} - 1 \right) \right] \quad (5.13)$$

5.3 Three-Component System

The free volume theory was further extended by Yasuda et.al.(1969) to homogeneous three-component systems consisting of a solute diffusing through the solvent in a highly swollen polymer network. Solute transport is restricted to pure concentration driven diffusion; i.e. no convection and no pressure gradients across the membrane. This model applies only to water soluble solutes which do not interact enthalpically with the polymer and are impermeable to the membrane if not dissolved in water. The membrane system is assumed to be randomly mixed, with randomly fluctuating polymer chains. The solute is depicted as a hard sphere diffusing through the water filled spaces in the membrane mesh; the solute cannot diffuse through the solid polymer. Only if a solute molecule forfeits a large enough space can another solute molecule diffuse into the void. This space becomes empty due to thermal fluctuations of molecules.

Actually, Fujita's two-component model could be directly applied to a three-component system of solute, solvent, and *uncrosslinked* polymer chains. The

critical hole size, B^* , would now be the size of the diffusing solute rather than the size of the diffusing solvent molecule. The distinguishing feature of the three-component polymer network system is that no longer is finding a sufficiently large void in the water phase enough for successful diffusion of the solute. The spaces formed by the mesh of polymer chains and crosslinks must be large enough to accommodate the diffusing solute.

Yasuda began by writing the diffusion coefficient in terms of the translational oscillating frequency, ν , of the diffusing molecule, the activation energy, F , entropy, S , and energy of diffusion, E :

$$D = \nu \exp(-F/kT) = \nu \exp(S/k) \exp(-E/kT) \quad (5.14)$$

The entropy term can be written as the sum of two terms, each representing distinct mechanisms by which the polymer chains diminish the diffusivity of the solute compared to its diffusivity in pure solvent:

$$\frac{S}{k} = \ln W = -\frac{V^*}{V_f} + \ln \Phi(V^*) \quad (5.15)$$

V_f is the total free volume in the membrane and V^* is the volume of the diffusing solute. The first term, the free volume term, is the conformational probability of forming a hole large enough to allow passage of the solute. The second term, the sieve factor, $\Phi(V^*)$, is the probability of finding such a hole in the membrane mesh. The polymer chains decrease the amount of free volume available for diffusion and, by forming the mesh, set the upper limit on how large a molecule can diffuse through.

The diffusion coefficient for the solute diffusing through the solvent in the membrane is then:

$$D_{2,1s} = \nu \Phi(\pi r_s^2) \exp \left[-\frac{B\pi r_s^2}{V_f} \right] \exp(-E/kT) \quad (5.16)$$

1=water 13=water swollen membrane
2=solute
3=polymer

where r_s is the effective solute radius and B is a proportionality constant which includes the diffusional jump length. Yasuda chose to represent the solute size by its cross section, πr_s^2 , rather than its volume V^* . That this indeed was the proper parameter was supported by the experimental data of Colton (1969). The diffusion coefficient in pure water is:

$$D_{2,1} = \nu \exp \left[-\frac{B\pi r_s^2}{V_{f,1}} \right] \exp(-E/kT) \quad (5.17)$$

Since the solute diffuses only through water in the membrane, the energy of diffusion, E , for the solute in pure water is assumed to be the same as that for the solute in the membrane. In the pure water case, there is no mesh, hence, $\Phi = 1$.

The free volume of the membrane is the sum of the free volume of the water and the free volume of the polymer:

$$V_{f,13} = H_v V_{f,1} + (1 - H_v) V_{f,3} \quad (5.18)$$

where H_v is the volume fraction of water in the membrane (volume of water/ total volume of swollen membrane), $V_{f,1}$ is the free volume in pure water, and $V_{f,3}$ is the free volume in pure polymer. Since the solute is assumed to diffuse only through the water filled spaces in the membrane mesh, the effective free volume available to the solute is only the free volume of water in the membrane:

$$V_{f,eff} = H_v V_{f,1} \quad (5.19)$$

The relative diffusivity of the solute can then be written:

$$\frac{D_{2,1s}}{D_{2,1}} = \Phi(\pi r_s^2) \exp \left[\left(-\frac{B\pi r_s^2}{V_{f,1}} \right) \left(\frac{1}{H_y} - 1 \right) \right] \quad (5.20)$$

In this thesis, the hydration, H , is defined as the ratio of the water volume to the polymer volume:

$$\frac{1}{H} = \left(\frac{1}{H_y} - 1 \right) \quad (5.21)$$

In terms of the hydration used in this thesis, the relative diffusivity is:

$$\frac{D_{2,1s}}{D_{2,1}} = \Phi(\pi r_s^2) \exp \left[-\frac{B\pi r_s^2}{V_{f,1}H} \right] \quad (5.22)$$

The exponential term can be thought of as the probability that the solute can form a hole, by “pushing” the polymer chains aside, through which it can pass. As the hydration increases or the solute size decreases, it becomes “easier” for the solute to wieve its way through since there are fewer chains in its path. When comparing diffusivities for a small solute diffusing through membranes of various crosslink densities, it becomes apparent that this term may be wanting. For instance, consider a solute that is smaller than 100% of the mesh spaces. The sieve term is then equal to unity . Imagine the solute diffusing through two membranes; both have the same hydration but different crosslink densities. The exponential term predicts that the solute diffusivity will be the same in both membranes. But it should be easier for the solute to diffuse through the more lightly crosslinked membrane since the chains are less restricted in their movement and more apt to be pushed aside by the solute (As pictured in Figure 2.6).

This possible difficiency in the free volume term was discussed by Kopeček et al.(1971) in their paper on the diffusion of NaCl and MgSO₄ ions through charged and neutral HEMA based crosslinked gel membranes. They concluded that the free volume is proportional not to the volume fraction of solvent but, instead, to the length of the chain segments between crosslinks. The length of

these segments will determine the chain's mobility. Hence, two membranes of different crosslink density may also have different free volumes, even at the same hydration.

The sieve term in equation 5.22 can be interpreted as the probability of finding a hole in the membrane which is greater or equal to the solute size. If the membrane is so heavily crosslinked that virtually no mesh spaces are large enough for the passage of the solute, then, regardless of how hydrated the membrane is, there will be no transport. It then seems plausible to assume that the sieve term depends solely on solute size and crosslink density.

Although the free volume term is well understood, the few expressions that have been formulated for the sieve term have not compared favorably with experimental data. The term is thought to be related to the crosslink density and effective solute size. Peppas and Reinhart (1983,PartI) proposed a linear dependence of the sieve term on the mesh size. Later they concluded that this dependence was incorrect (1984,PartII). Moynihan et.al.(1986) derived another expression for the sieve factor which they claimed was supported by their experimental data— data not presented in the paper.

Peppas (1983,PartI) began with the Eyring [Glasstone,(1941)] equation for a solute diffusing in one dimension:

$$D = \lambda^2 \frac{kT}{h} \exp\left(-\frac{\Delta S^*}{R}\right) \exp\left(-\frac{\Delta H^*}{RT}\right) \quad (5.23)$$

where λ is an average diffusional jump distance, k is the Boltzmann constant, h is the Plank constant, ΔS^* is the entropy per mole, and ΔH^* is the enthalpy per mole. Peppas made the same assumptions as did Yasuda. In particular, he assumed the solute diffuses solely through the water in the highly swollen membrane; thus, the enthalpy is the same for solute diffusion in the membrane as

for diffusion in pure water. The relative diffusion coefficient is then:

$$\frac{D_{2,13}}{D_{2,1}} = \frac{\exp(\Delta S_{1,13}^*/R)}{\exp(\Delta S_{2,1}^*/R)} \quad (5.24)$$

In a manner similar to Fujita, Peppas adapted the Cohen and Turnbull theory to a three-component system. Reinterpreting the average free volume per molecule as the average fractional free volume of the system, V_f , and incorporating γ in V_f , Peppas rewrote the Cohen and Turnbull probability of finding a hole of volume v^* or greater:

$$P(v^*) = B(v^*) \exp(-v/V_f) \quad (5.25)$$

$P(v^*)$ is now the probability that a solute of volume v will find a hole of volume v^* or greater in the swollen membrane ($v^* \geq v$). $B(v^*)$ depends on the size and shape of the mesh of polymer chains and crosslinks, while the exponential term depends on the size and shape of the solute. $B(v_1^*)$ is the probability of there being a mesh space, in pure water (subscript 1), large enough to allow the passage of a solute of volume v . Obviously, $B(v_1^*) = 1$.

The entropic term can be written for the solute diffusing in the swollen membrane and for the solute diffusing in pure water:

$$-\frac{\Delta S_{2,13}^*}{R} = \ln P(v_{13}^*) = \ln B(v_{13}^*) - \frac{v_2}{V_f} \quad (5.26)$$

$$-\frac{\Delta S_{2,1}^*}{R} = \ln P(v_1^*) = \ln B(v_1^*) - \frac{v_2}{V_{f,1}} = -\frac{v_2}{V_{f,1}} \quad (5.27)$$

Peppas made the familiar assumption that only the free volume of water in the membrane is available for solute diffusion. Thus, the effective free volume is as given in equation 5.19. In this manner, Peppas arrived at Yasuda's free volume equation.

Reinhart and Peppas (1984,PartII) found that the molecular weight

between crosslinks, \overline{M}_c , was greatly affected by the initial crosslink ratio, X (X=moles of crosslinker/moles of polymer repeating unit). An increase in X corresponded to an increase in \overline{M}_c . The sieve term was postulated as having the following functional form:

$$B(v_{13}^*) = f \left[\frac{\overline{M}_c - \overline{M}_c^*}{\overline{M}_n - \overline{M}_c^*} \right] \quad (5.28)$$

where \overline{M}_c^* is the critical value of \overline{M}_c below which the solute cannot fit through the mesh spaces and \overline{M}_n is the number average molecular weight of the polymer chains before crosslinking.

The dependence of the solute diffusivity on the molecular weight between crosslinks was demonstrated by plotting \overline{M}_c versus the normalized diffusion coefficient for various poly(vinyl alcohol) (PVA) membranes (1983,PartII) and poly(2-hydroxyethyl methacrylate) (PHEMA) membranes [Moynihan,(1986)]. The plots clearly show an increase in the diffusion coefficient with \overline{M}_c . However, the membranes with a larger \overline{M}_c had a larger hydration as well. Despite the effort made to maintain constant hydration while varying the crosslink density in the PHEMA membranes, the hydration varied between 0.68 and 0.77 (a 13.24% increase). The diffusivity increased from $16.9 \times 10^{-3} \text{cm}^2/\text{s}$ to $98.5 \times 10^{-3} \text{cm}^2/\text{s}$ (a 482.8% increase). The hydration of the PVA membranes varied between 10.00 and 18.65 (an 86.5% increase), while the diffusivity ranged from $1.8 \times 10^{-8} \text{cm}^2/\text{sec}$ to $80.7 \times 10^{-8} \text{cm}^2/\text{sec}$ (a 4383% increase). The increase in the diffusion coefficient must, at least partly, be attributed to the increase in hydration, an effect represented in the free volume term. In fact, the plot of \overline{M}_c versus the normalized diffusion coefficient [Reinhart and Peppas,(1984,PartII)] looks very much like a plot of the free volume theory expression [Yasuda (1969 Part III:Equation 7)] for normalized diffusivity versus hydration (Figure 5.1).

Various expressions were developed by Peppas et al. to fit the different

D/D₀ vs. H from free volume theory

beta=5 sieve factor=1

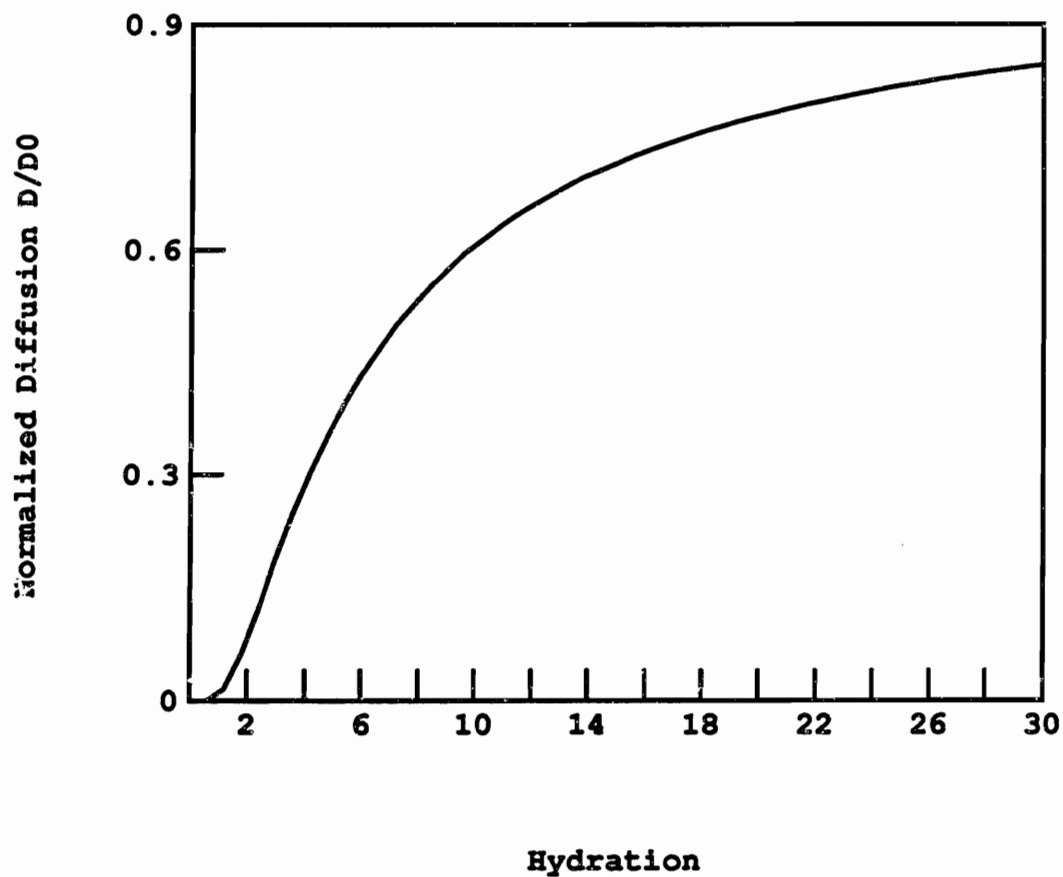


Figure 5.1: Theoretical free volume theory plot of D/D_0 vs. H [Yasuda (1969 Part III:Equation 7)].

data sets. The PVA data was accurately fit to the free volume equation by using:

$$f\left(\frac{\overline{M}_c - \overline{M}_c^*}{\overline{M}_n - \overline{M}_c^*}\right) = \left(\frac{\overline{M}_c - \overline{M}_c^*}{\overline{M}_n - \overline{M}_c^*}\right)^2 \quad (5.29)$$

Peppas and Moynihan (1985) developed an equation for diffusion in moderately swollen polymer networks:

$$\frac{D_{2,13}}{D_{2,1}} = f(\xi) \exp\left[k_3(\overline{M}_c - \overline{M}_n)\right] \exp\left[-\frac{\pi r_s^2 l_s}{HV_{f,1}}\right] \quad (5.30)$$

where ξ is the mesh size of the membrane and ξ^2 is the mesh area. Using the diffusion data from the PHEMA membranes, Moynihan et.al.(1986) used the method of least squares to determine the functional form of $f(\xi)$. They found the best fit to be $f(\xi) = \xi^2$.

Chapter VI

Discussion

6.1 Membrane Homogeneity

The hydration experiments demonstrate quite convincingly that there is minor variation in composition between membranes from the same batch. This is a significant result because it supports a major assumption made in this study—namely, that, because the 3 and 5 mil membranes are from the same batch, the 5 mil membranes used in the hydration experiments are essentially the same as the 3 mil membranes used in the transport experiments. Valid comparisons can now be made between hydration and transport data, even though the same membrane could not be used for both experiments (Section 4.2).

6.2 Membrane Formulation Trends

It was found that both hydration and Lis-dex permeability increase, for a given pH, with decreasing percent crosslinker. The membrane formulations can be ordered with respect to three properties:

1. In order of decreasing percent crosslinker.
2. In order of increasing hydration for a given pH.
3. In order of increasing Lis-dex permeability for a given pH.

These three arrangements result in almost the same ordering of the membranes (At some pH's, the Lis-dex permeability ordering was reversed between the S.1/1 and S.2/2 membranes and between the S.2/1 and S.4/2 membranes). In sharp contrast to the Lis-dex permeability ordering, the NSPA permeabilities exhibit no apparent ordering.

6.3 Swelling Model

The hydration data for each membrane was fit to Nussbaum's [1986] swelling model, given by:

$$H = H_o + H_1(\bar{c}_m^s)^2 \exp \left[-H \frac{l_r}{l_d} \right] \quad (6.1)$$

where

$$\bar{c}_m^s = \frac{K_m * \bar{c}_{mos}}{\bar{c}_{H^+} + K_m} \quad (6.2)$$

and \bar{c}_{mos} is the total concentration (moles/dry liter) of carboxyl groups, which is calculated from the amount of MAA added at the time of polymerization. In these experiments, $\bar{c}_{mos} = 15.45$. K_m is the dissociation constant for the membrane carboxyl group ($K_m = 10^{-pK} = 10^{-5.5}$). \bar{c}_{H^+} is given in Section 2.2.2.

Equations 2.12, 2.14, and 2.15 are combined to give \bar{c}_{H^+} in terms of the unknowns, H and \bar{c}_{H^+} :

$$\bar{c}_{H^+} = \frac{c_{H^+} K_m \bar{c}_{mos}}{2c_{K^+} H (\bar{c}_{H^+} + K_m)} + \frac{c_{H^+}}{2} \sqrt{\left(\frac{K_m \bar{c}_{mos}}{c_{K^+} H (\bar{c}_{H^+} + K_m)} \right)^2 + 4} \quad (6.3)$$

c_{K^+} is the ionic strength of the bath, which in these experiments was $c_{K^+} = 0.05M$. c_{H^+} is the external bath pH ($c_{H^+} = 10^{-pH}$). The debye length, l_d , is given in Equation 2.7 and again here:

$$\frac{1}{\kappa} = \sqrt{\frac{\epsilon RT}{2c_o F^2}} \quad (6.4)$$

where $c_o = 0.05M$.

The three parameters, H_o , H_1 , and l_r , were found for each membrane formulation by using a routine, written by Eliot Frank, that fits the swelling model function (Equation 6.1) to the hydration data. The fitting algorithm is a nonlinear regression analysis algorithm which minimizes the weighted square error

Table 6.1: Swelling Model Parameters

mem	H_0	H_1	l_r [cm]
S.05/1	2.95765	10.2257	2.09324e-8
S.1/2	2.3749	28.9157	4.31505e-8
S.1/1	2.33953	8.78326	2.90462e-8
S.2/2	1.99302	6.79454	3.24096e-8
S.2/1	1.65864	16.9183	6.47994e-8
S.4/2	1.51244	7.22799	5.36441e-8
S.4/1	1.24957	20.9767	11.3562e-8
S.4/.5	1.31886	6.97526	8.00249e-8
S.6/1	1.10456	8.12671	7.5846e-8

of the function. Figure 6.1 shows the swelling model fit to hydration data for an S.2/2 membrane. The fits for the other membranes are equally good. Table 6.1 lists the parameters for each membrane. With the three parameters known for each membrane formulation, it is possible to interpolate hydrations at any pH for any membrane.

6.4 Hydration vs. Crosslinker Concentration and Solvent Volume

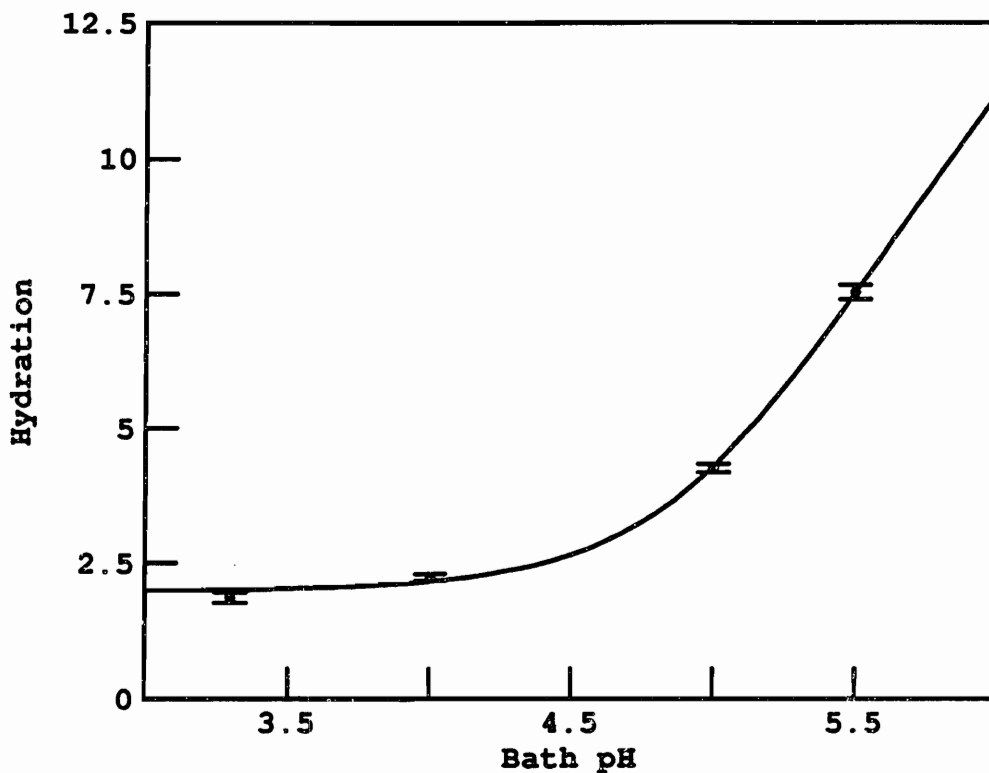
For a given pH, membrane swelling decreased with crosslinker concentration (Figure 4.1). This comes as no surprise since the crosslinks exert a mechanical restoring force which resists further chain separation.

Using Nussbaum's swelling model, the hydration was interpolated at the same pH for each membrane. The following figures compare membrane hydration to the volume of crosslinker and water added at the time of polymerization. Figure 6.2 shows hydration versus crosslinker for S.X/1 and S.X/2 membranes, at four pH's. These bar graphs show how the volume of crosslinker affects the membrane's hydration; the solvent volume is constant in each graph. Figure 6.3 shows hydration versus water content for S.1/Y, S.2/Y, and S.4/Y membranes at four pH's. These graphs show how the volume of water affects the membrane's

Swelling Model Fit To S.2/2 Data Points

$H_0=1.99302$ $H_1=6.79455$ $l_{ref}=3.24096e-08$ cm

$[KCL]=0.05$ $c_{mos}=15.45$ $pK=5.5$



dots: Data points from S.2/2 membrane

Figure 6.1: Swelling model function, $H = H_0 + H_1(\bar{c}_m^*)^2 \exp \left[-H \frac{l_r}{l_d} \right]$, fit to hydration data for S.2/2 membrane. This plot is typical of the other membrane hydration fits.

hydration; the volume of crosslinker is constant in each graph. A comparison of Figures 6.2 and 6.3 reveals that crosslinker has more of an effect on hydration than does water.

6.5 Lis-dex Permeability vs. Crosslinker Concentration and Solvent Volume

6.5.1 Constant pH

Figure 6.4 shows permeability versus volume of crosslinker at four pH's for S.X/1 and S.X/2 membranes. Figure 6.5 shows permeability versus volume of water at four pH's for S.4/Y, S.2/Y, and S.1/Y membranes.

The volume of water has a minor effect on hydration, but it has a substantial effect on permeability to Lis-dex. The implication is that chain mobility increases with increasing water content, allowing the solute to move through the mesh more "easily" (this is illustrated in Figure 2.6 (bottom)).

6.5.2 Constant Hydration

Previous studies relating diffusivity to crosslinker concentration have compared solute transport in membranes of various crosslinker concentrations [Kirstein (1985), Wisniewski (1976), Wood (1983), Lee (1978), Chen (1979), Korsmeyer (1981), Pusch (1982), Kopeček et al.(1971), Reinhart and Peppas (1983), Moynihan et al.(1986), Peppas and Moynihan (1985)]. Those experiments were performed under the same bath conditions for each membrane, the assumption being that the differences in hydration from membrane to membrane were negligible compared to the differences in diffusivity. The hydrations were often quite low and varied as much as 86% (Section 1.2.2). As demonstrated in the experiments in this thesis (See Figure 6.6, which plots Lis-dex permeability vs. hydration, rather than pH, and Figure 6.7.), and as predicted by the free volume

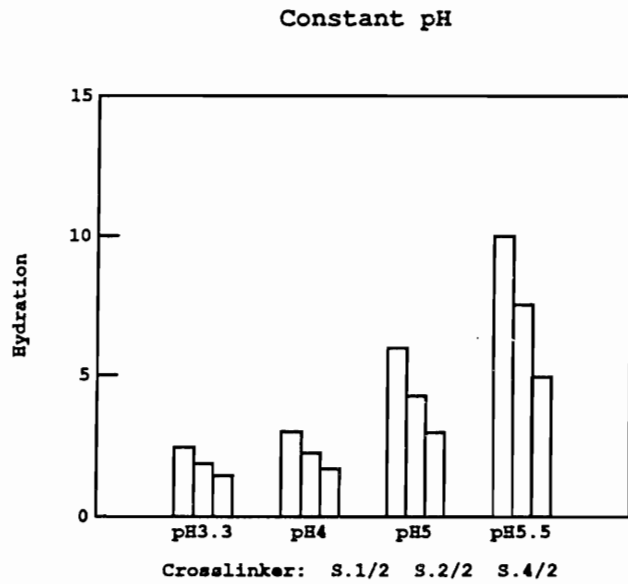
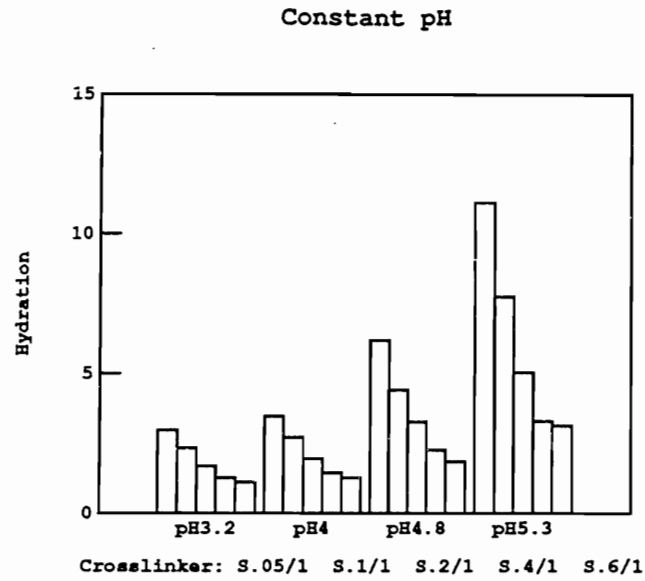


Figure 6.2: Hydration vs. volume of crosslinker for S.X/1 (top) and S.X/2 (bottom) membranes at 4 different pH values. The volume of crosslinker added at the time of polymerization has a significant effect on hydration.

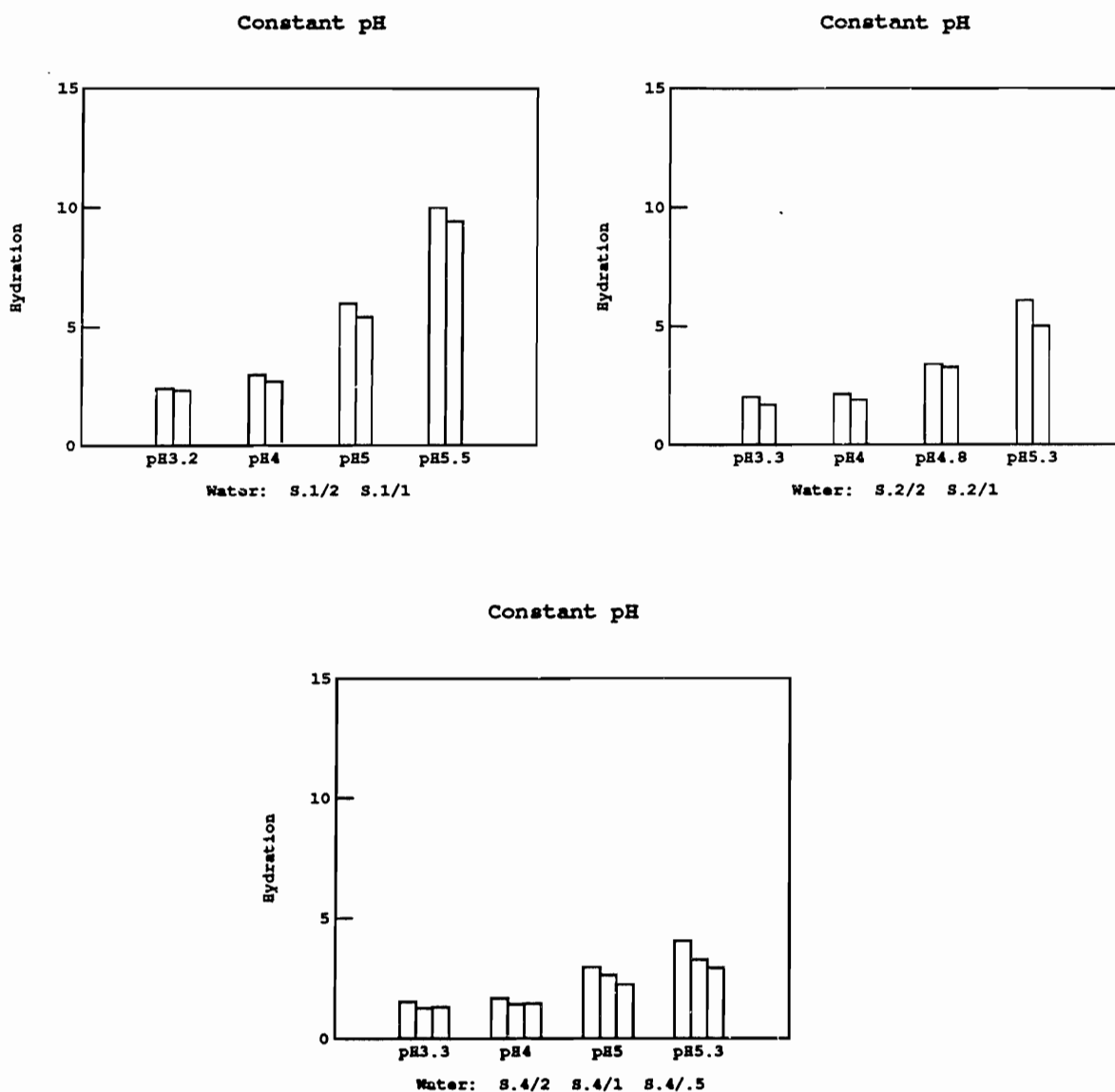


Figure 6.3: Hydration vs. volume of D.I. water for S.4/Y (bottom), S.1/Y (top left), and S.2/Y (top right) membranes at 4 different pH values. The volume of water added at the time of polymerization has less of an effect on hydration than does the volume of crosslinker.

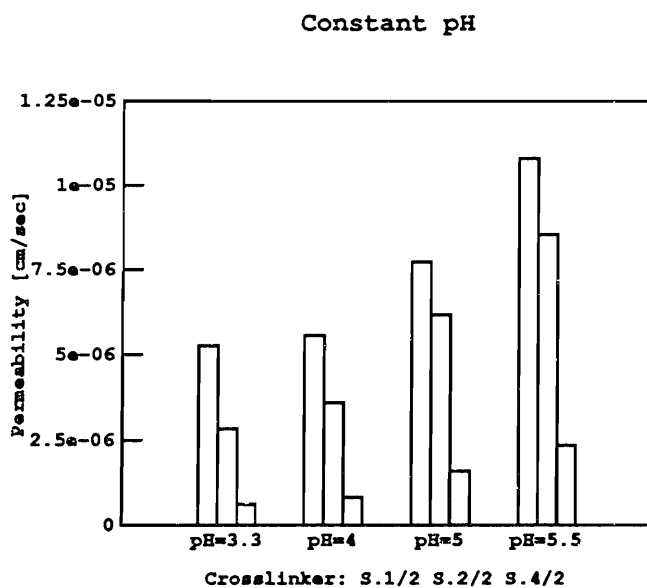
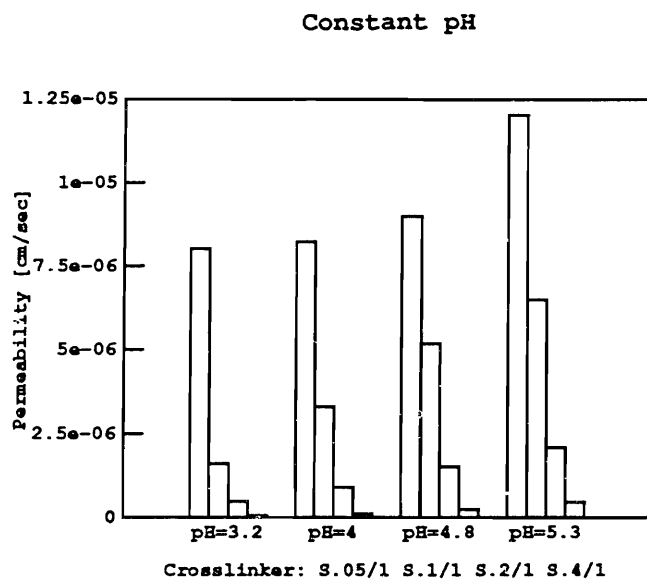


Figure 6.4: Lis-dex permeability vs. volume of crosslinker for S.X/1 (top) and S.X/2 (bottom) membranes at 4 different pH values.

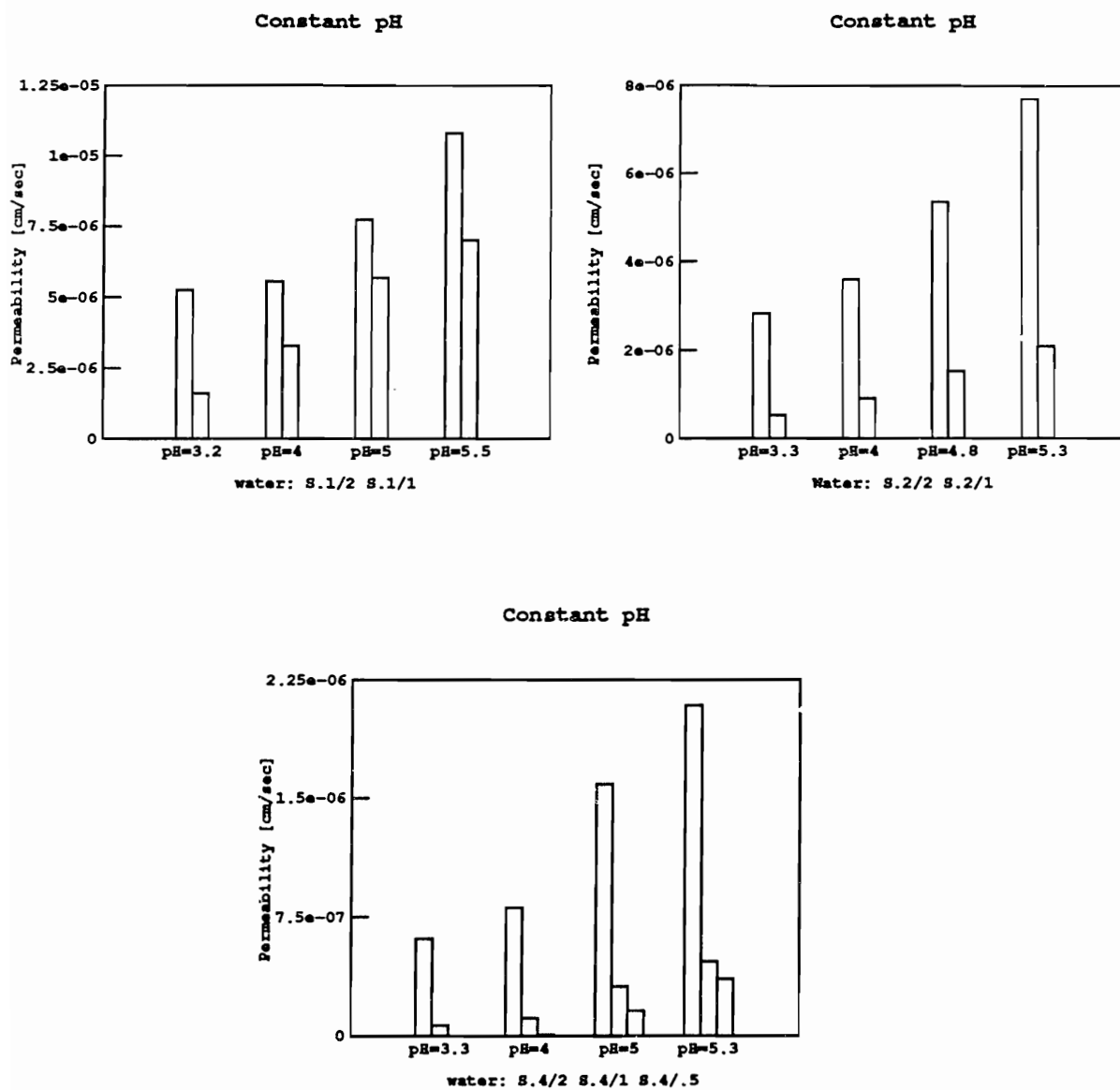


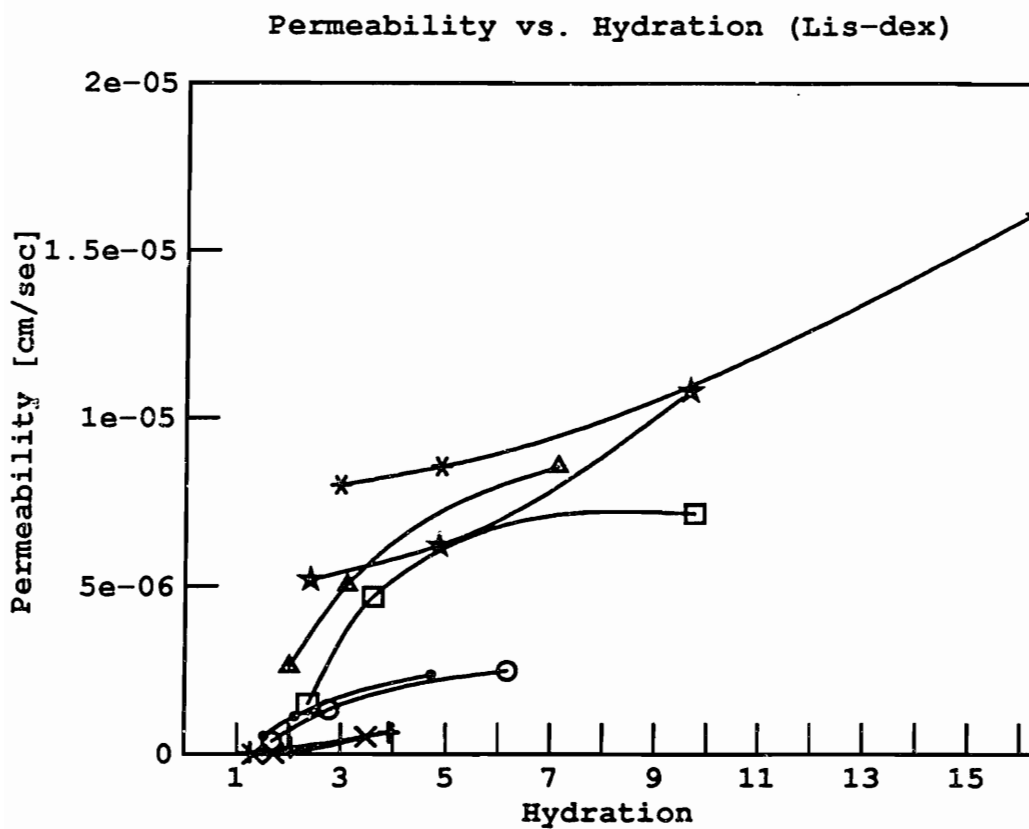
Figure 6.5: Lis-dex permeability vs. volume of water for S.4/Y (bottom), S.1/Y (top left), and S.2/Y (top right) membranes at 4 different pH values. The water added at the time of polymerization has a substantial effect on the permeability.

theory (See Figure 6.10, which is a plot of the free volume theory expression for normalized diffusivity vs. hydration), this assumption may not be valid; a small change in hydration can cause a marked change in permeability.

In these experiments, two factors affected transport: hydration and crosslink density. In order to correlate solute diffusivity with crosslinker concentration, it is necessary to hold the hydration constant. At a chosen hydration, the corresponding pH is determined by using the parameters H_0 , H_1 , and l_r , and the swelling model function (Equation 6.1). The permeability at this pH is then found by using a spline interpolation routine. In this way, it is possible to find the permeability at any hydration.

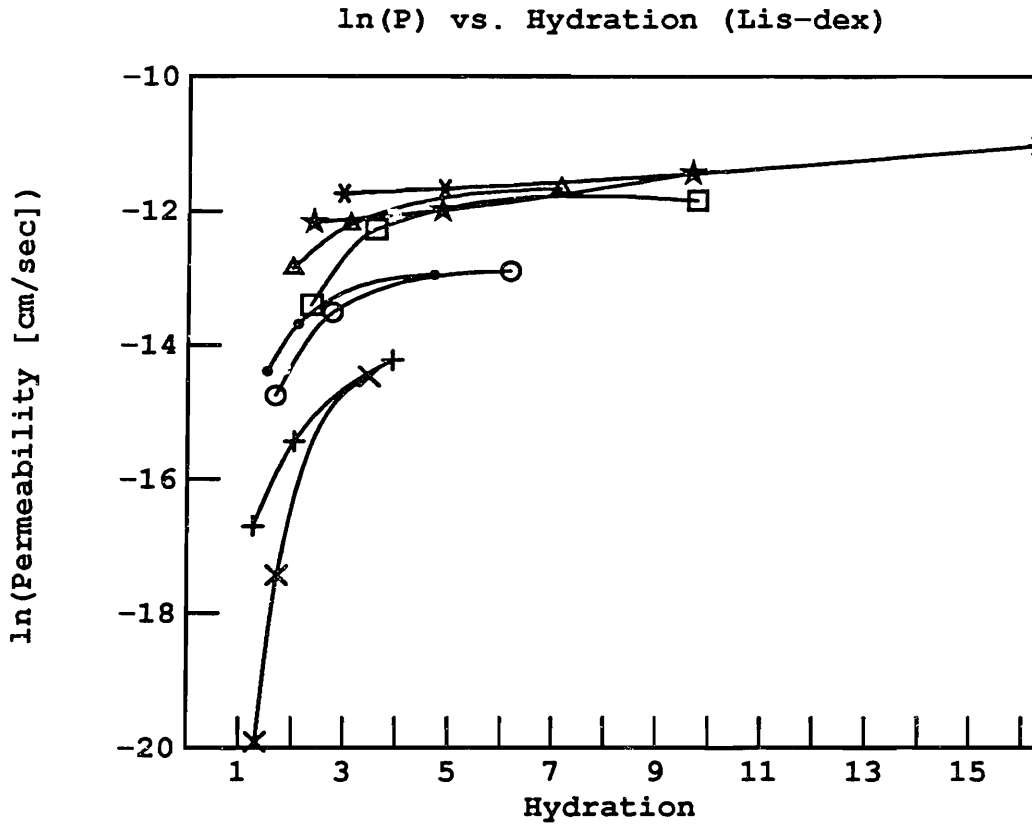
Figure 6.8 shows plots of Lis-dex permeability versus volume of crosslinker, *at constant hydration*, for S.X/1 and S.X/2 membranes. Each bar represents a different membrane, with each membrane at the hydration given below that set of bars. Figure 6.9 plots permeability versus volume of water, at constant hydration, for S.4/Y*, S.2/Y, and S.1/Y membranes. These plots show that the crosslinker concentration, alone, has an enormous effect on the diffusion of Lis-dex (Table 6.2 shows the crosslinker concentration for each membrane). At a constant hydration of 3.2, Lis-dex permeability differs by a factor of 18.7 for the two membranes having the least (S.05/1: $P=8.063e-6$ cm/sec) and greatest (S.4/.5: $P=4.101e-7$ cm/sec) percentage of crosslinker. This data also implies that the strands making up the membrane, which are in continuous random thermal motion, can actually be “pushed aside” by the diffusing solute in the more lightly crosslinked membranes (Figure 2.6 demonstrates how two membranes at the same hydration can have different permeabilities to a large solute, and how a large solute can “push” its way through the more lightly crosslinked mesh.).

* For the S.4/.5 membrane, the mean pH3 permeability ($2.25e-9$ cm/sec) was used for all calculations, fits, and figures in this Chapter.



S.05/1:aster S.1/2:stars S.1/1:squares
S.2/2:triangles S.2/1:circles S.4/2:dots
S.4/1:plus S.4/.5:cross

Figure 6.6: Lis-dex permeability vs. hydration.



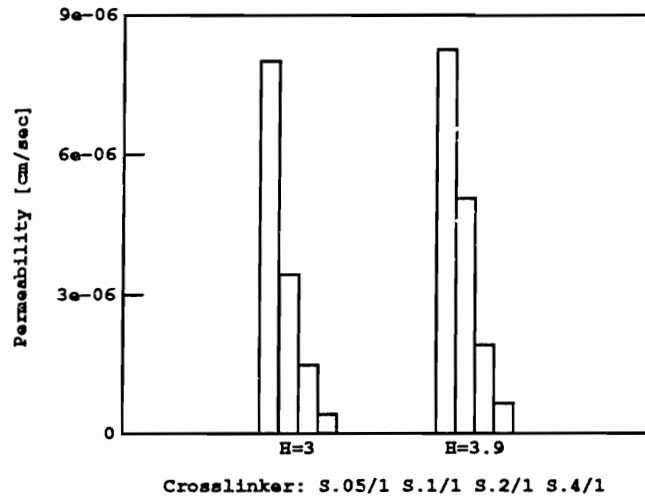
S.05/1:aster S.1/2:stars S.1/1:squares

S.2/2:triangles S.2/1:circles S.4/2:dots

S.4/1:plus S.4/.5:cross

Figure 6.7: ln(P) vs. hydration for Lis-dex, showing that, at low hydrations, a small change in hydration can cause a tremendous change in permeability.

Constant Hydration



Constant Hydration

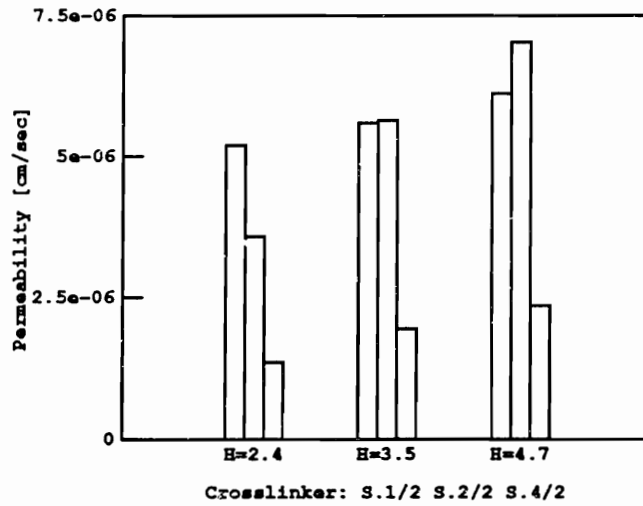


Figure 6.8: Lis-dex permeability vs. volume of crosslinker for S.X/1 (top) and S.X/2 (bottom) membranes, at *constant hydration*. Strands are more easily “pushed aside” by the diffusing solute in the more lightly crosslinked membranes.

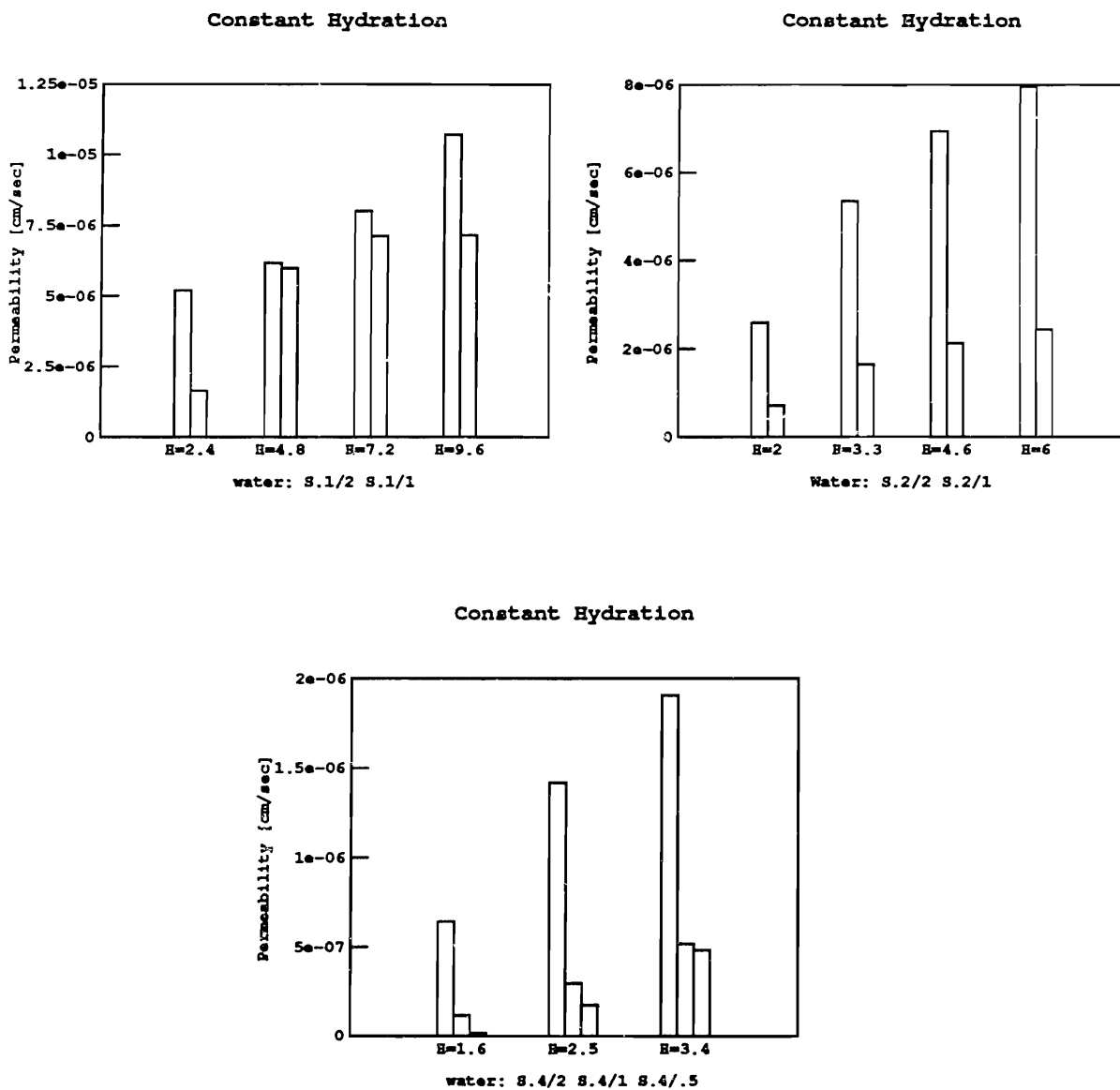


Figure 6.9: Lis-dex permeability vs. volume of water for S.4/Y (bottom), S.1/Y (top left), and S.2/Y (top right) membranes at *constant hydration*.

Table 6.2: Crosslinker concentration for each membrane. % crosslinker = (vol TEGDMA/total vol)*100.

mem	% xlinker(by vol)
S.05/1	0.32
S.1/2	0.56
S.1/1	0.64
S.2/2	1.12
S.2/1	1.27
S.4/2	2.22
S.4/1	2.50
S.4/.5	2.67
S.6/1	3.70

6.6 NSPA Permeability vs. Crosslink Density

If the membrane crosslink density has any effect on the transport of NSPA, it is so minor as to be obscured by experimental errors. This result suggests that the crosslink density may not play a significant role in the exponential free volume term. As discussed in Section 5.3, the effect of restricted chain movement is not included in the free volume term, as perhaps it should be. Since the mesh spaces are more than large enough to allow the NSPA molecules to diffuse through, any chain related hindrances to transport will be reflected in the free volume term. The chain length does not appear to have any effect on NSPA transport; but, then again, neither does the hydration.

6.7 Interpretation of Data in Terms of Free Volume Theory

6.7.1 Lis-dex Data

The free volume theory (Yasuda,[1969,PartIII]) relates the solute diffusivity to hydration, solute size, and the sieve term:

$$\frac{D}{D_0} = \Phi(\pi r_s^2) \exp \left[-\frac{B\pi r_s^2}{V_{f,1}H} \right] \quad (6.5)$$

Figure 6.10 is a plot of D/D_0 versus hydration, with $\Phi = 1$ (100% of the mesh spaces are large enough to allow the solute to diffuse through) and $\beta = \frac{B\pi r_s^2}{V_{f,1}} = 5$. As can be seen in this figure, a small change in hydration can lead to a large change in diffusivity.

Yasuda defined the permeability, P_v , as $P_v = kD$, where k is the partition coefficient:

$$k = \frac{\text{g solute/vol.hydrated polymer}}{\text{g solute/vol.solution}} \quad (6.6)$$

$$= \frac{\text{g solute/vol.solution in polymer}}{\text{g solute/vol.solution}} * \left(\frac{H}{1+H} \right) \quad (6.7)$$

If the concentration of the solute in solvent in the membrane is equal to the concentration of the solute in pure solvent, then k is simply the fractional volume of solvent in the membrane. In that case:

$$P_v = D \left(\frac{H}{1+H} \right) \quad (6.8)$$

The permeability measured in the transport experiments in this study is related to the diffusivity by:

$$P = \frac{D}{\delta} \phi \quad (6.9)$$

where δ is the thickness of the membrane. The porosity factor, ϕ , is the fraction of

D/D₀ vs. H from free volume theory

beta=5 sieve factor=1

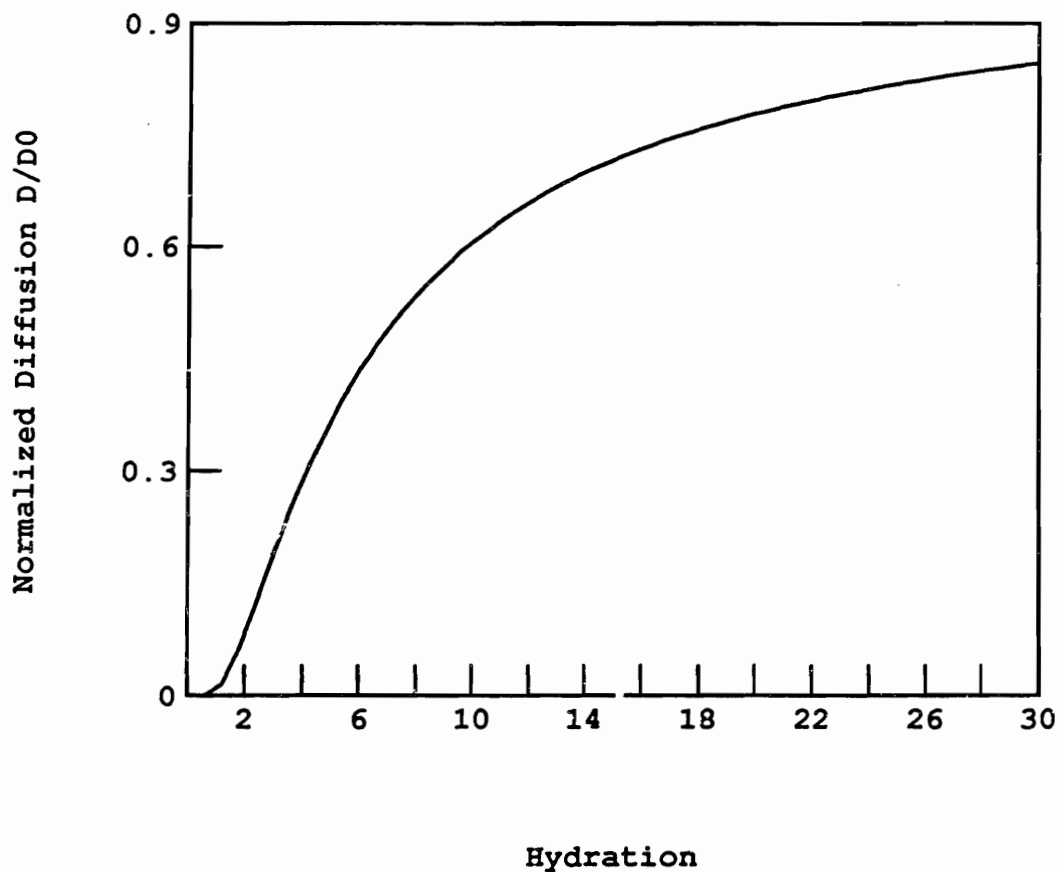


Figure 6.10: Normalized diffusion D/D_0 vs. hydration from free volume theory equation: $\frac{D}{D_0} = \Phi \exp -\frac{\beta}{H}$. Small changes in hydration can cause great changes in diffusion.

the surface area consisting of solvent. For an isotropically swelling membrane:

$$\phi = \left(\frac{H}{1+H} \right) \quad (6.10)$$

and:

$$\frac{\delta}{\delta_o} = \left(\frac{v_w}{v_s} \right)^{1/3} = (1+H)^{1/3} \quad (6.11)$$

where δ_o is the thickness of the dry membrane. The expression for P is now:

$$P = \frac{DH}{\delta_o(1+H)^{4/3}} \quad (6.12)$$

which can be written in terms of the free volume equation as:

$$P \frac{\delta_o}{D_o} = \Phi \frac{H}{(1+H)^{4/3}} \exp -\frac{\beta}{H} \quad (6.13)$$

where:

$$\beta = \frac{B\pi r_s^2}{V_{f,1}} \quad (6.14)$$

Figure 6.11 shows $P \frac{\delta_o}{D_o}$ vs. H for $\Phi = 1$ and various values of β .

Rearranging:

$$P \frac{(1+H)^{4/3}}{H} = \frac{D_o}{\delta_o} \Phi \exp -\frac{\beta}{H} \quad (6.15)$$

Figure 6.12 is a plot of $P(1+H)^{4/3}H^{-1}$ vs. $1/H$, using the data points from the transport experiments.

Taking the natural log of both sides:

$$\ln [P(1+H)^{4/3}H^{-1}] = \ln \left(\frac{D_o}{\delta_o} \Phi \right) - \frac{\beta}{H} \quad (6.16)$$

Assuming Φ to be a function only of solute size and crosslink density, a plot of $\ln[P(1+H)^{4/3}H^{-1}]$ vs. $1/H$, for each membrane, is expected to be linear, with slope $-\beta$ and with the intercept, $\ln \left(\frac{D_o}{\delta_o} \Phi \right)$, reflecting the importance of the sieve

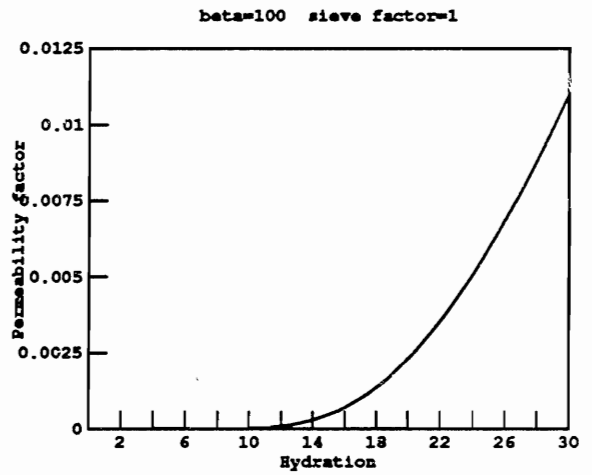
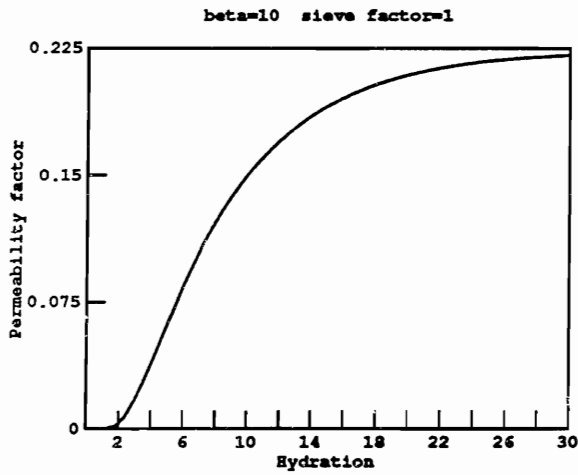
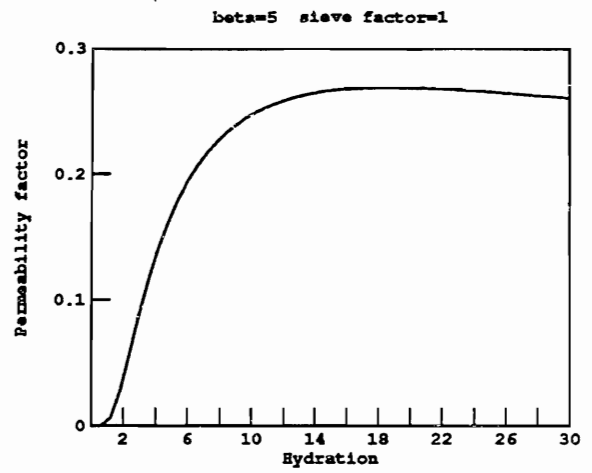
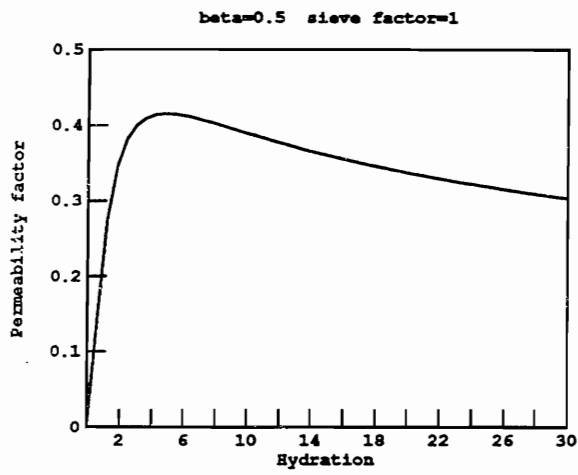
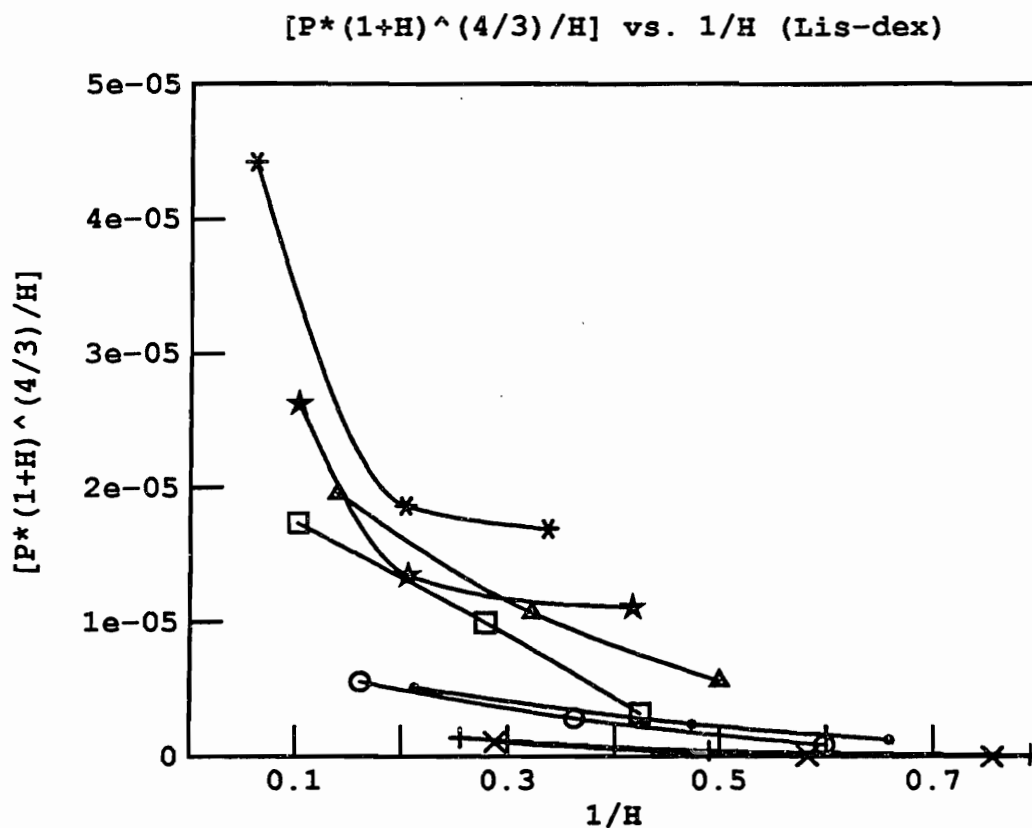


Figure 6.11: $P \frac{\delta_0}{D_0}$ vs. H from free volume theory equation: $P \frac{\delta_0}{D_0} = \Phi \frac{H}{(1+H)^{4/3}} \exp -\frac{\beta}{H}$.
 $\Phi = 1$ and $\beta=0.5, 5, 10, 100$.



S.05/1:aster S.1/2:stars S.1/1:squares
 S.2/2:triangles S.2/1:circles S.4/2:dots
 S.4/1:plus S.4/.5:cross

Figure 6.12: Plot of $\frac{P(1+H)^{4/3}}{H}$ vs. $1/H$ using Lis-dex data. Free volume theory expression is: $\frac{P(1+H)^{4/3}}{H} = \frac{D_o}{\delta_o} \Phi \exp -\frac{\beta}{H}$.

Table 6.3: Intercepts obtained from simultaneous linear least squares fit of all eight data sets. Slope= $-\beta = -5.11933$.

mem	intercept
S.05/1	-9.60777
S.1/2	-9.81901
S.1/1	-10.3368
S.2/2	-9.81777
S.2/1	-11.0301
S.4/2	-10.6031
S.4/1	-12.0407
S.4/.5	-13.703

effect. Figure 6.13 is a plot of $\ln[P(1 + H)^{4/3}H^{-1}]$ vs. $1/H$ for Lis-dex for each membrane.

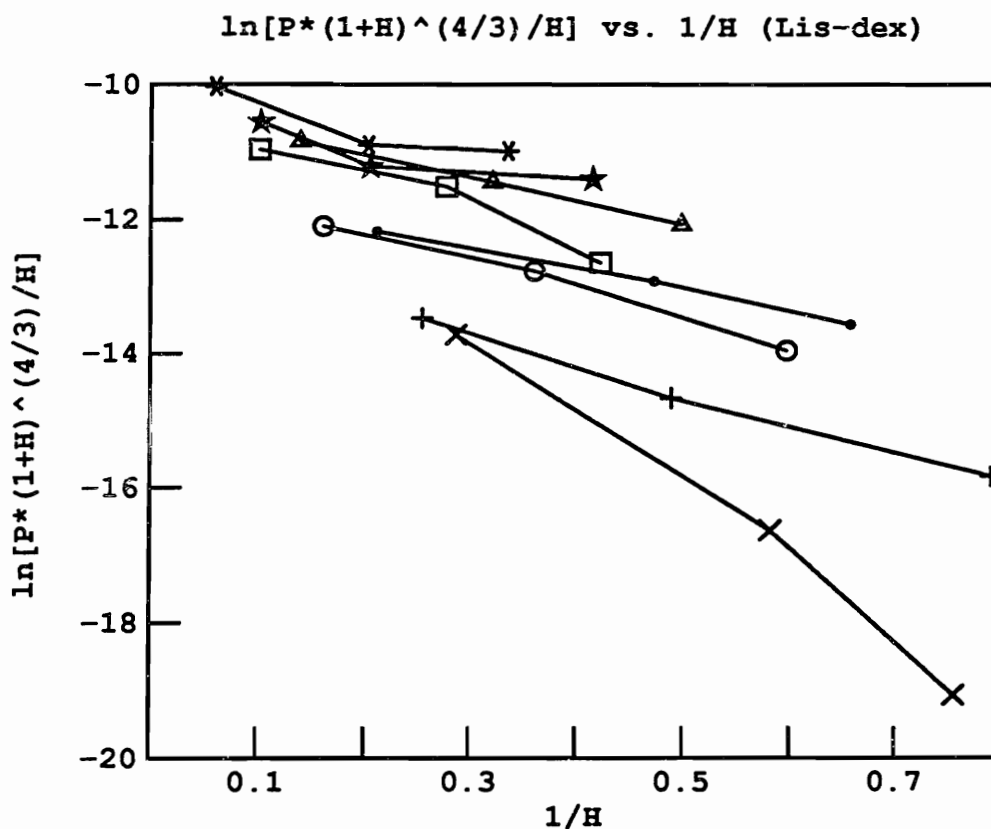
Using a linear least squares fit, each membrane data set was simultaneously fit to a line, each line having the same slope, $-\beta$, but a different intercept (Appendix B). β was found to be:

$$\beta = 5.11933 \quad (6.17)$$

Table 6.7.1 lists the intercept, $\ln\left(\frac{D_0}{\delta_0}\Phi\right)$, for each membrane. Since D_0/δ_0 is constant for each membrane, the trend in the intercepts implies that the sieve factor increases with increasing crosslink density.

Each data point was then offset by the corresponding intercept and plotted in Figure 6.14, along with a line of slope 5.11933 and zero intercept. The S.4/.5 membrane is the only one with a poor fit to the line. There was a great deal of uncertainty, however, in the pH3 point (Section 4.3).

With $\frac{D_0}{\delta_0}\Phi$ now known for each membrane, the free volume theory can be compared to the data. Figure 6.15 shows plots of P vs. H for various membranes,



S.05/1:aster S.1/2:stars S.1/1:squares

S.2/2:triangles S.2/1:circles S.4/2:dots

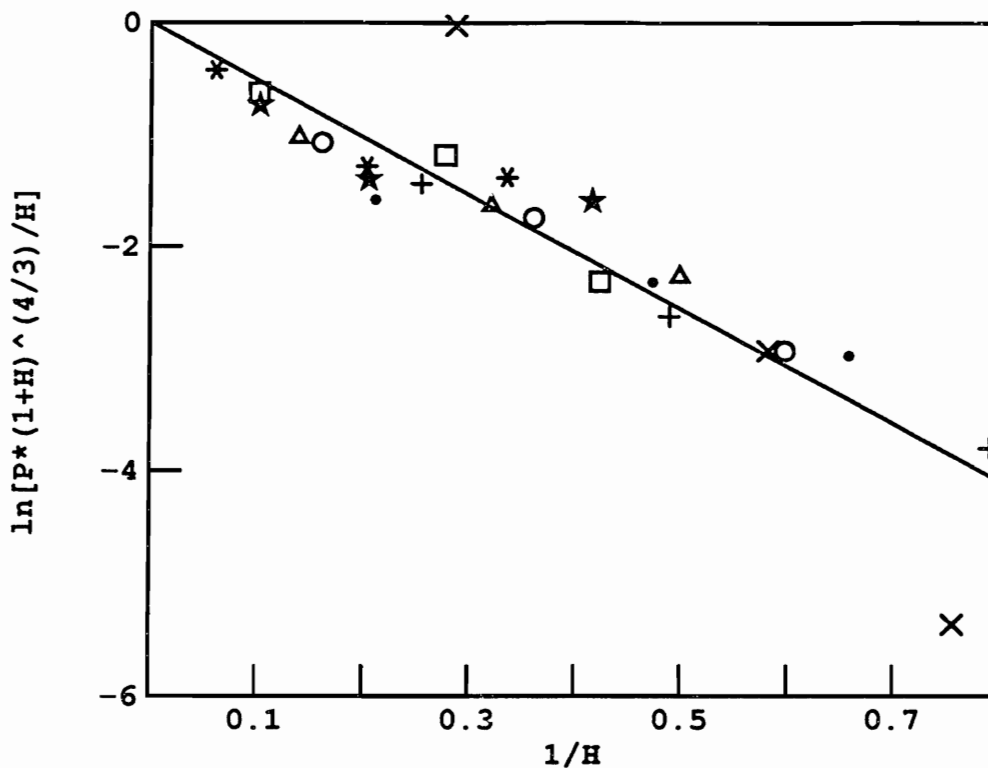
S.4/1:plus S.4/.5:cross

Figure 6.13: Plot of $\ln [P(1 + H)^{4/3}H^{-1}]$ vs. $1/H$ using Lis-dex data. Free volume theory expression is: $\ln [P(1 + H)^{4/3}H^{-1}] = \ln \left(\frac{D_a}{\delta_o} \Phi \right) - \frac{\beta}{H}$. According to the free volume theory, each membrane data set should fit a line. The slope, $-\beta$, should be the same for each data set while the intercept, $\ln \left(\frac{D_a}{\delta_o} \right)$, should be different.

$\ln[P*(1+H)^{(4/3)}/H]$ vs. $1/H$ (Lis-dex)

Intercept B_i added to each mem set

$x = \text{beta} * y$ $\text{beta} = 5.11933$



S.05/1:aster S.1/2:stars S.1/1:squares

S.2/2:triangles S.2/1:circles S.4/2:dots

S.4/1:plus S.4/.5:cross

Figure 6.14: Plot of $\ln [P(1 + H)^{4/3}H^{-1}] + \ln \left(\frac{D_0}{\delta_0} \Phi \right)$ vs. $1/H$ for Lis- dex for each membrane data set. Also shown is a line with slope $-\beta$ and zero intercept. β and the 8 intercepts were obtained using a linear least squares fit on each data set, simultaneously.

using the free volume theory equation:

$$P = \frac{D_0}{\delta_0} \Phi \frac{H}{(1+H)^{4/3}} \exp -\frac{\beta}{H} \quad (6.18)$$

$\beta = 5.11933$ and the intercepts are given in Table 6.7.1. The data points from the corresponding membrane are plotted for comparison. The data points for the other membranes were also close to their respective theoretical plots, with the exception of the S.4/.5 membrane. The poor S.4/.5 fit may be due to the large uncertainty in the pH3 permeability (Section 4.3).

The data from these experiments are accurately described by the free volume theory model, with β constant and the sieve term, Φ , different for each membrane. The sieve term plays an important role in fitting the Lis-dex data and cannot merely be set equal to unity, implying that the crosslinker concentration (or, equivalently, chain length) has a significant effect on Lis-dex diffusion, even at *constant hydration*. This, in turn, implies that chain mobility is an important factor in restricted diffusion of solutes which are on the order of the mesh size, as illustrated in Figure 2.6.

6.7.2 NSPA Data

Yasuda assumed that the sieve term was unity and plotted $\ln(D/D_0)$ vs. $1/H$ for each solute diffusing through various uncharged membranes (1968, Part I and 1969, Part II). As expected, the dependence was linear. Despite large variations in the membranes' compositions, all the data for a solute were fit to a single line. This would indeed be the case if the sieve effect was insignificant.

Figure 6.16 is a plot of $\ln[P(1+H)^{4/3}H^{-1}]$ vs. $1/H$ for NSPA, for each membrane, compared to the same plot for Lis-dex. Evidently, the sieve effect is of little importance to the transport of NSPA and the data could be convincingly fit to a single line. Even so, the data was fit to separate lines, as well as to a single line.

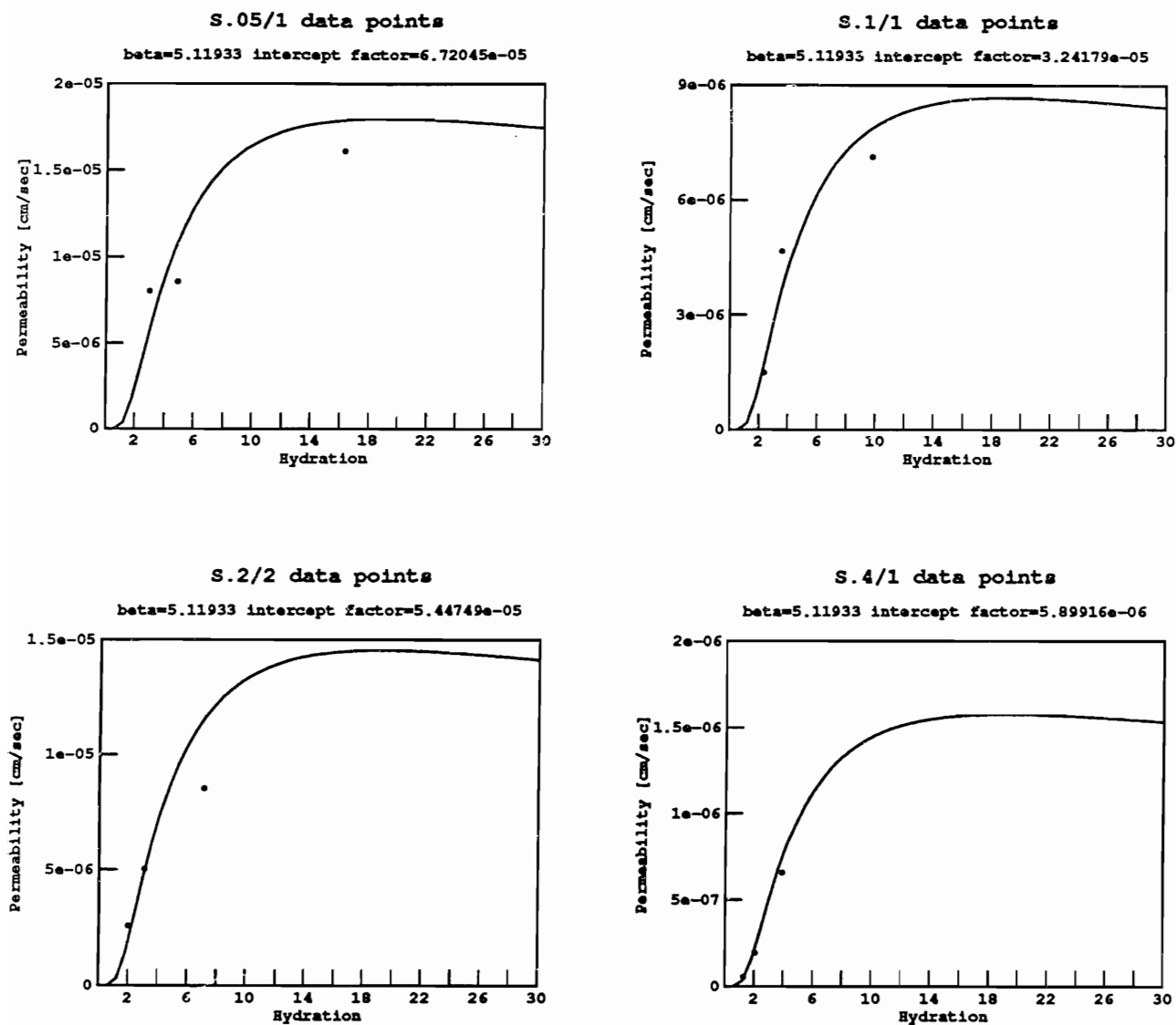
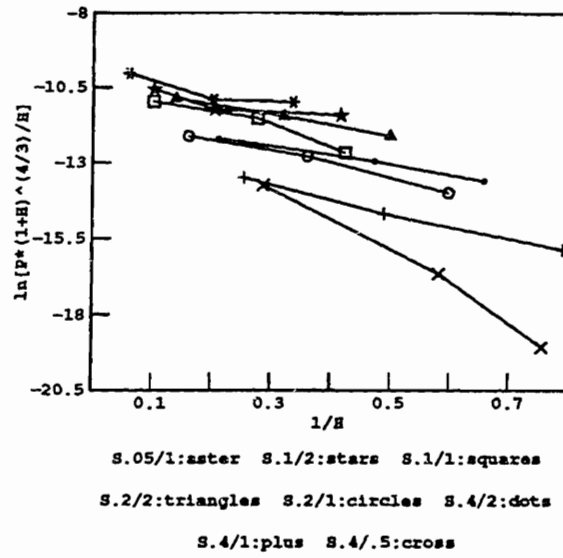


Figure 6.15: Comparison of free volume theory P vs. H (from expression $P = \frac{D_0}{\delta_0} \Phi \frac{H}{(1+H)^{4/3}} \exp -\frac{\beta}{H}$) to Lis-dex transport data. $\Phi \frac{D_0}{\delta_0}$ and β were obtained using a simultaneous linear least squares fit. Membranes: S.05/1, S.1/1, S.2/2, S.4/1

Lis-dex



NSPA

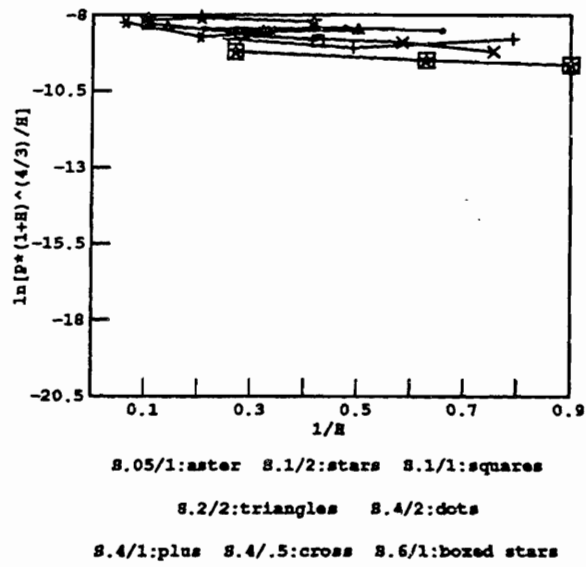
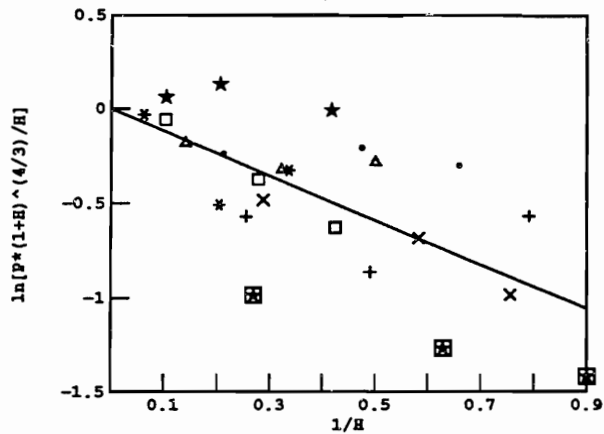


Figure 6.16: Comparison of NSPA and Lis-dex plots of $\ln[P(1+H)^{4/3}H^{-1}]$ vs. $1/H$. The NSPA data could be convincingly fit to a single line.

The lower plot in Figure 6.17 shows the results of fitting the data to multiple lines, each with the same slope, $-\beta$, but different intercepts. The data points are offset by the intercept of the corresponding line. The upper plot in Figure 6.17 is a plot of the data points fit to a single line, using the method of least squares. Data points in the upper plot were offset by the intercept -8.215. The single line fit is not much worse than the multiple intercept fit. This suggests that the sieve term does not play a role in the transport of the small solute, NSPA; the length of the chains and concentration of crosslinker are of little consequence to the diffusion of NSPA compared to the diffusion of Lis-dex.

NSPA Data Fit to a Single Line

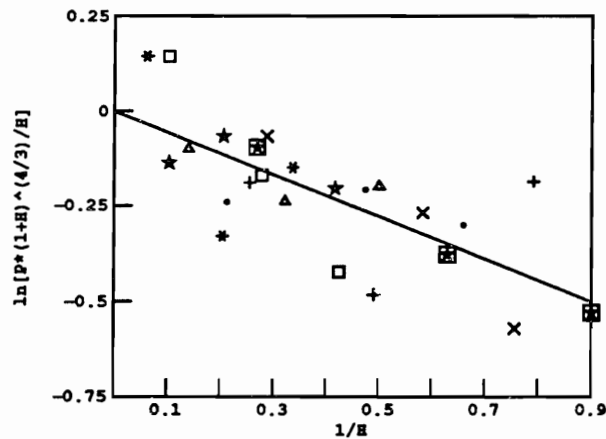
intercept=-8.215 beta = 1.17482



S.05/1:aster S.1/2:stars S.1/1:squares
S.2/2:triangles S.4/2:dots
S.4/1:plus S.4/.5:cross S.6/1:boxed stars

NSPA Data Fit to Multiple Lines

x = beta*y beta = 0.557002



S.05/1:aster S.1/2:stars S.1/1:squares
S.2/2:triangles S.4/2:dots
S.4/1:plus S.4/.5:cross S.6/1:boxed stars

Figure 6.17: NSPA data points, $y = \ln[P(1+H)^{4/3}H^{-1}]$ and $x = 1/H$, fit to multiple lines (bottom), as was done for the Lis-dex data, and a single line (top). For the lower plot, the data points were offset by the appropriate intercept. For the upper plot, the data points were offset by the intercept -8.215

Appendix A

One step recipe for PMAA membranes

10 ml methacrylic acid (MAA)

X ml triethylene glycol dimethacrylate (TEGDMA)

2Y ml deionized water

3 ml ethylene glycol

0.3 ml 40% (w/v) ammonium persulfate (AP) solution (40g AP/100ml water)

0.3 ml 15% sodium metabisulfite (SMBS) solution

The notation we have been using to denote membrane formulation is SX/Y, where X is the volume of crosslinker (TEGDMA) per 10 ml monomer, and Y is half the volume of water per 10 ml monomer. For example a S.4/1 membrane is made with 0.4 ml crosslinker and 2 ml water per 10 ml monomer.

For each membrane to be cast, prepare 2 clean, dry, optically flat glass plates and a PTFE (Teflon) spacer. Mix all ingredients together in a test tube. For each membrane, place the spacer on the bottom glass plate, and coat the glass surface inside the spacer with the fluid mixture, using a 1 ml disposable pipet to transfer the fluid. Slowly lower the top glass onto the bottom one, starting at one end and gradually lowering the other end to insure that only fluid (no air bubbles) remains between the two plates. Clamp the two plates together with hose clamps and rinse off any fluid on the outside of the plates with water. Place the plates vertically in a 60 degree water bath for 2 hours. Then separate the plates under running water using a razor blade. Let the membrane hydrate under running water before removing it from the glass plates and spacer. Then soak it in deionized water for about 24 hours to remove any unreacted ingredients.

Appendix B

Linear Least Squares Fit to Multiple Lines

Fit i data sets, simultaneously, to i lines, with each line having the same slope, A , but a different intercept, B_i [Papoulis (1965)]:

$$\begin{aligned}
 i &= \# \text{ of membranes} \\
 \sigma_x^2 &= E\{(x - \eta)^2\} = \sum_n (x_n - \eta)^2 P\{x = x_n\} \\
 &= E\{x^2\} - E^2\{x\} \\
 \eta_x &= E\{x\} = \int_{-\infty}^{\infty} xf(x)dx \\
 c &= E\{(x - \eta_x)(y - \eta_y)\} = E\{xy\} - E\{x\}E\{y\}
 \end{aligned}$$

Minimize the error, e :

$$\begin{aligned}
 e &= \sum_i E\{[y_i - (Ax_i + B_i)]^2\} \\
 &= \sum_i \int_{-\infty}^{\infty} (y_i - Ax_i - B_i)^2 f(x_i, y_i) dx_i dy_i \\
 \frac{\partial e}{\partial B_i} &= -2 \int_{-\infty}^{\infty} (y_i - Ax_i - B_i) f(x_i, y_i) dx_i dy_i = 0 \\
 B_i \int_{-\infty}^{\infty} f(x_i, y_i) dx_i dy_i &= \int_{-\infty}^{\infty} (y_i - Ax_i) f(x_i, y_i) dx_i dy_i \\
 B_i &= E\{y_i - Ax_i\} = \eta_{y_i} - A\eta_{x_i}
 \end{aligned}$$

A is found in a similar manner:

$$\begin{aligned}
 e &= \sum_i E\{(y_i - Ax_i - B)^2\} \\
 &= \sum_i E\{[(y_i - \eta_{y_i}) - A(x_i - \eta_{x_i})]^2\} \\
 &= \sum_i E\{(y_i - \eta_{y_i})^2\} - 2AE\{(y_i - \eta_{y_i})(x_i - \eta_{x_i})\} +
 \end{aligned}$$

$$\begin{aligned} & A^2 E \{ (\mathbf{x}_i - \eta_{\mathbf{x}_i})^2 \} \\ &= \sum_i (\sigma_{y_i}^2 - 2Ac_i + A^2 \sigma_{x_i}^2) \\ \frac{\partial e}{\partial A} &= \sum_i (-2c_i + 2A\sigma_{x_i}^2) = 0 \\ A &= \frac{\sum_i c_i}{\sum_i \sigma_{x_i}^2} \end{aligned}$$

References

- Anderson, J.L., Quinn, J.A. (1974), Restricted Transport in Small Pores, *Biophys. J.*, **14**:130.
- Barrer, R.M., Skirrow, G. (1948), Transport and Equilibrium Phenomena in Gas-Elastomer Systems, *J. Polym. Sci.*, **3**:549
- Bean, C.P. (1972), The Physics of Porous Membranes-Neutral Pores, in *Membranes-A Series of Advances*, Eisenman, G. (ed.), Marcel Dekker, Inc., New York, Vol.1, Ch.1, 1-54.
- Chen, S.P., Osterhoudt, H.W. (1985), Diffusion and Solubility of Some Azo Dyes in Swollen Gelatin Matrices: The Effects of Dye Size, Matrix Swell, and Dye-Matrix Interactions, *J. Appl. Polymer Sci.*, **30**:2075.
- Chen, R.Y.S. (1979), Electrolyte Transport through Crosslinked PHEMA. I. Effects of Anionic Size and Crosslinking Content, *Polym. Prepr.*, **20**(1):1005.
- Cohen, M.H., Turnbull, D. (1959), Molecular Transport in Liquids and Glasses, *J. Chem. Phys.*, **31-5**:1164.
- Colton, C.K. (1969), Ph.D. Thesis, M.I.T., Cambridge, Mass.
- deGennes, P.G. (1979), *Scaling Concepts in Polymer Physics*, Cornell University Press, Ithaca, N.Y.
- Dennison, K.A. (1986), Radiation Crosslinked Poly(Ethylene Oxide) Hydrogel Membranes, Ph.D Thesis (Chem. E.), M.I.T., Cambridge, Mass.
- Fujita, H. (1961), Diffusion in Polymer-Diluent Systems, *Fortschr. Hochpolym.-Forsch.*, **3**:1.
- Fujita, H., Kishimoto, A., Matsumoto, K. (1960), Concentration and Time-Dependence of Diffusion Coefficient for Systems Polymethyl Acrylate and N-Alkyl Acetates, *Trans. Faraday Soc.*, **56**:424.
- Glasstone, S., Laidler, K.J., Eyring, H. (1941), *The Theory of Rate Processes*, McGraw-Hill, New York, N.Y.
- Grimshaw, P.E., Grodzinsky, A.J., Yarmush, M.L., Yarmush, D.M. (1988), Dynamic Membranes for Protein Transport: Chemical and Electrical Control, *Chem. Eng. Sci.*, manuscript submitted.

- Grimshaw, P.E. (1988), Electric Control of Solute Transport Across Polyelectrolyte Membranes, PhD Thesis, (EECS), M.I.T., in progress.
- Horbett, T.A., Kost, J., Ratner, B.D. (1983), *ACS Poly. Preprints*, **24**:34.
- Kirstein, D., Braselmann, H., Vacik, J., Kopeček, J. (1985), Influence of Medium and Matrix Composition on Diffusivities in Charged Membranes, *Biotech. Bioeng.*, **27**:1382.
- Kopeček, J., Vacik, J., Lim, D. (1971), Permeability of Membranes Containing Ionogenic Groups, *J. Polymer Sci.*, **9(A1)**:2801.
- Korsmeyer, R.W., Peppas, N.A. (1981), Effects of the Morphology of Hydrophilic Polymeric Matrices on the Diffusion and Release of Water Soluble Drugs, *J. Mem. Sci.*, **9**:211.
- Kost, J., Horbett, T.A., Ratner, B.D., Singh, M. (1985), Glucose-Sensitive Membranes Containing Glucose Oxidase: Activity, Swelling and Permeability Studies, *J. Biomed. Mater. Res.*, **19(9)**:1117-1133.
- Kudela, V., Vacik, J., Kopeček, J. (1980), Strong-Acid Membranes with Enhanced Hydrophilicity, *J. Mem. Sci.*, **6**:123.
- Lee, K.H., Jee, J.G., Jhon, M.S., Ree, T. (1978), Solute Transport through Crosslinked PHEMA Membranes, *J. Bioeng.*, **2**:269.
- Mackie, J.S., Meares, P. (1955), The Diffusion of Electrolytes In a Cation-Exchange Resin Membrane. I. Theoretical, *Proc. Roy. Soc. A* **232**:498.
- Meares, P. (1958), Diffusion of AllylCl in Polyvinyl Acetate, PartI. The Steady State of Permeation, *J. Polymer Sci.*, **27**:391.
- Moynihan, H.J., Honey, M.S., Peppas, N.A. (1986), Solute Diffusion in Swollen Membranes. PartV: Solute Diffusion in Poly(2-Hydroxyethyl Methacrylate), *Polym. Eng. and Sci.*, **26**, **17**:1180.
- Nussbaum, J.H. (1986), Electric Field Control of Mechanical and Electromechanical Properties of Polyelectrolyte Gel Membranes, Ph.D. Thesis (EECS), M.I.T., Cambridge, Mass.
- Ogston, A.G., Preston, B.N., Wells, J.D. (1973), On the Transport of Compact Particles through Solutions of Chain-Polymers, *Proc. Roy. Soc. Lond., A*. **333**:297-316.

- Papoulis, A. (1965), *Probability, Random Variables, and Stochastic Processes*, McGraw-Hill, Inc., New York, 218.
- Peppas, N.A., Moynihan, H.J. (1985), *J. Appl. Polym. Sci.*, **30**:2589.
- Peppas, N.A., Lustig, S.R. (1985), The Role of Crosslinks, Entanglements, and Relaxations of the Macromolecular Carrier in the Diffusional Release of Biologically Active Materials, *Conceptual and Scaling Relationships*, Ann. NY Acad. Sci., **446**:26.
- Pusch, W., Walch, A. (1982), Membrane Structure and its Correlation with Membrane Permeability, *J. Mem. Sci.*, **10**:325.
- Ratner, B.D., Miller, I.F. (1973), *J. Biomed. Mater. Res.*, **7**:353.
- Refojo, M.F., Leong, F.L. (1979), *J. Polym. Sci., Polym. Symp.*, **66**:227.
- Reinhart, C.T., Peppas, N.A. (1983), Solute Diffusion in Swollen Membranes. Part I. A New Theory, *J. Mem. Sci.*, **15**:275-287.
- Reinhart, C.T., Peppas, N.A. (1984), Solute Diffusion in Swollen Membranes. Part II. Influence of Crosslinking on Diffusive Properties, *J. Mem. Sci.*, **18**:227.
- Rosenbaum, S., Mahon, H.I., Cotton, O. (1967), Permeation of H_2O and NaCl through Cellulose Acetate, *J. Appl. Polymer Sci.*, **11**:2041.
- Shatayeva, L.K., Samsonov, G.V., Vacik, J., Kopeček, J., Kalal, J. (1979), Permeability of Heterogeneous Membranes Based on Methacrylic Acid, *J. App. Polymer Sci.*, **23**:2245.
- Trostyanskaya, E.B., Belnik, A.R., Poimanov, A.M., Babaevskii, P.G. (1970), Adsorption and Diffusion of Water Vapor in Polymethylenephenols of Reticular Structure, *Vysokomol. Soyed.*, **A12**:1778.
- Vacik, J., Kopeček, J. (1975), Specific Resistances of Hydrophilic Membranes Containing Ionogenic Groups, *J. Appl. Poly. Sci.*, **19**:3029.
- Weiss, A.M., Grodzinsky, A.J., Yarmush, M.L. (1986), Chemically and Electrically Controlled Membranes: Size Specific Transport of Fluorescent Solutes through PMAA Membranes, *AIChE Symp. Ser.*, **250(82)**:85-98.
- Weiss, A.M. (1986), Real Time Control of the Permeability of Crosslinked Polyelectrolyte Membranes to Fluorescent Solutes, Ph.D. Thesis (EECS), M.I.T., Cambridge, Mass.

- Wilkins, J.B., Long, F.A. (1957), *Trans. Faraday Soc.*, **53**:1146.
- Wisniewski, S., Kim, S.W. (1980), Permeation of Water-Soluble Solutes through PHEMA Crosslinked with Ethylene Glycol Dimethacrylate, *J. Mem. Sci.*, **6**:309.
- Wisniewski, S.J., Gregonis, D.E., Kim, S.W., Andrale, J.D. (1976), Diffusion through Hydrogel Matrices, in *Hydrogels for Medical and Related Applications*, Andrade, J.D. (ed.), ACS Symposium Series, Amer. Chem. Soc., Washington, D.C., Vol.13:80.
- Wood, J.M., Attwood, D., Collett, J.H. (1983), *Drug Devel. Ind. Pharm.*, **4**:93.
- Yasuda, H., Lamaze, C.E., Ikenberry, L.D. (1968), Permeability of Solutes through Hydrated Polymer Membranes. Part I. Diffusion of Sodium Chloride, *Makromol. Chem.*, **118**:19-35.
- Yasuda, H., Ikenberry, L.D., Lamaze, C.E. (1969), Permeability of Solutes through Hydrated Polymer Membranes Part II. Permeability of Water Soluble Organic Solutes, *Makromol. Chem.*, **125**:108-118.
- Yasuda, H., Peterlin, A., Colton, C.K., Smith, K.A., Merrill, E.W. (1969), Permeability of Solutes through Hydrated Polymer Membranes. Part III. Theoretical Background for the Selectivity of Dialysis Membranes, *Makromol. Chem.*, **126**:177-186.
- Zentner, G.M., Cardinal, J.R., Kim, S.W. (1978), *J. Pharm. Sci.*, **67**:1352.